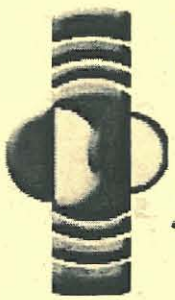

IMPACT CRATERING: BRIDGING THE GAP BETWEEN MODELING AND OBSERVATIONS

Houston, Texas — February 7-9, 2003

Abstract Volume

LPI Contribution No. 1155

Impact Cratering: Bridging the Gap Between Modeling and Observations

February 7–9, 2003

Houston, Texas

Sponsor
Lunar and Planetary Institute
National Aeronautics and Space Administration

Conveners
Robert Herrick, *Lunar and Planetary Institute*
Elisabetta Pierrazzo, *Planetary Science Institute*

Scientific Organizing Committee
Bevan French, *Natural History Museum*
Kevin Housen, *Boeing Corporation*
William McKinnon, *Washington University*
Jay Melosh, *University of Arizona*
Michael Zolensky, *NASA Johnson Space Center*

Lunar and Planetary Institute 3600 Bay Area Boulevard Houston TX 77058-1113

LPI Contribution No. 1155

Compiled in 2003 by
LUNAR AND PLANETARY INSTITUTE

The Institute is operated by the Universities Space Research Association under Agreement No. NCC5-679 issued through the Solar System Exploration Division of the National Aeronautics and Space Administration.

Abstracts in this volume may be cited as

Author A. B. (2003) Title of abstract. In *Impact Cratering: Bridging the Gap Between Modeling and Observations,* p. XX. LPI Contribution No. 1155, Lunar and Planetary Institute, Houston.

This volume is distributed by

ORDER DEPARTMENT
Lunar and Planetary Institute
3600 Bay Area Boulevard
Houston TX 77058-1113, USA
Phone: 281-486-2172
Fax: 281-486-2186
E-mail: order@lpi.usra.edu

Mail order requestors will be invoiced for the cost of shipping and handling.

ISSN No. 0161-5297

Preface

This volume contains abstracts that have been accepted for presentation at the workshop on Impact Cratering: Bridging the Gap Between Modeling and Observations, February 7–9, 2003, in Houston, Texas.

Logistics, onsite administration, and publications for this workshop were provided by the staff of the Publications and Program Services Department at the Lunar and Planetary Institute.

Contents

Program

Friday, February 7, 2003
OPENING SESSION
8:30 a.m. Lecture Hall

8:30 Welcoming Address and Introduction

8:40 Melosh H. J. * [INVITED]
Modeling Meteorite Impacts: What We Know and What We Would Like to Know

9:20 Grieve R. A. F. * [INVITED]
Observations of the Terrestrial Impact Cratering Record

10:00–10:15 BREAK

Friday, February 7, 2003
ROCK PROPERTIES THAT NEED TO BE KNOWN FOR THEORETICAL MODELING
10:15 a.m. Lecture Hall

10:15 Holsapple K. A. * [INVITED]
What Do We Need to Know to Model Impact Processes?

10:55 Spray J. G. * [INVITED]
Mechanisms of In Situ Rock Displacement During Hypervelocity Impact: Field and Microscopic Observations

11:35–12:15 PANEL DISCUSSION
Panel: K. Holsapple, J. Spray, T. Ahrens, E. Pierazzo

12:15–1:30 LUNCH

Friday, February 7, 2003
EFFECTS OF TARGET PROPERTIES ON THE CRATERING PROCESS
1:30 p.m. Lecture Hall

1:30 Housen K. R. * [INVITED]
Effects of Target Properties on the Cratering Process

2:10 Schenk P. M. * [INVITED]
Importance of Target Properties on Planetary Impact Craters, Both Simple and Complex

2:50 Ormö J. * [INVITED]
Next Step in Marine Impact Studies: Combining Geological Data with Numerical Simulations for Applications in Planetary Research

3:10–3:30 BREAK

* Denotes Speaker

3:30 Crawford D. A. * Barnouin-Jha O. S.
Application of Adaptive Mesh Refinement to the Simulation of Impacts in Complex Geometries and Heterogeneous Materials

3:45 Gisler G. * Weaver R. P. Mader C. L. Gittings M. L.
Two- and Three-Dimensional Simulations of Asteroid Ocean Impacts

4:00 Holsapple K. A. *
Does Melt Volume Give the Signature of the Impactor?

4:15 Osinski G. R. * Spray J. G. Grieve R. A. F.
Impact Melting in Sedimentary Target Rocks?

4:30–5:15 GENERAL DISCUSSION

Friday, February 7, 2003
POSTER SESSION AND RECEPTION
5:30–7:00 p.m. Great Room

Ai H. Ahrens T. J.
Dynamic Tensile Strength of Crustal Rocks and Applications to Impact Cratering

Cassidy W. A. Wright S. P.
Small Impact Craters in Argentine Loess: A Step Up from Modeling Experiments

Hagstrum J. T.
Antipodal Hotspots on Earth: Are Major Deep-Ocean Impacts the Cause?

Halekas J. S. Lin R. P.
Magnetic Fields of Lunar Impact Basins and Their Use in Constraining the Impact Process

Hargitai H. Kereszturi A.
Pyroclastic Flows and Surges: Possible Analogy for Crater Ejecta Deposition

Ivanov B. A.
Educational Experience in Numerical Modeling of Impact Cratering

Ivanov B. A.
Modification of ANEOS for Rocks in Compression

Karp T. Artemieva N. A. Milkereit B.
Seismic Investigation and Numerical Modeling of the Lake Bosumtwi Impact Crater

Kearsley A. T. Graham G. A. McDonnell J. A. M. Bland P. A. Hough R. M. Helps P. A.
Early Fracturing and Impact Residue Emplacement: Can Modeling Help to Predict Their Location in Major Craters?

Kereszturi A.
Crater Basin Rebound Above Plastic Layers: Model Based on Europa

Ohno S. Sugita S. Kadono T. Hasegawa S. Igarashi G.
Sulfur Chemistry in K/T-sized Impact Vapor Clouds

Onose N. Fujiwara A.
Velocity Distributions of Fragments and Its Time Dependence and Velocity Distributions of Fragments in Oblique Impact Cratering on Gypsum

Schmitt H. H.
Impact Crater Morphology as a Guide to Regolith Structure at Taurus-Littrow

Versh E. Jõeleht A. Kirsimäe K. Plado J.
Cooling of the Kärdla Impact Crater: I. The Mineral Parasequence Observations

Saturday, February 8, 2003
THERMODYNAMICS OF IMPACT CRATERING AND DETERMINING IMPACTOR CHARACTERISTICS
8:30 a.m. Lecture Hall

8:30 O'Keefe J. D. * Ahrens T. J. [INVITED]
Impact Induced Target Thermo-Mechanical States and Particle Motion Histories

9:10 Gibson R. L.. * Reimold W. U. [INVITED]
Thermal and Dynamic Consequences of Impact — Lessons from Large Impact Structures

9:50 Dence M. R. * [INVITED]
WIRGO in TIC's? [What (on Earth) is Really Going on in Terrestrial Impact Craters?]

10:10 Koeberl C. * [INVITED]
Using Geochemical Observations to Constrain Projectile Types in Impact Cratering

10:30–10:45 BREAK

10:45 Ahrens T. J. * O'Keefe J. D. Stewart S. T.
Calculation of Planetary Impact Cratering to Late Times

11:00 Sugita S. * Hamano K. Kadono T. Schultz P. H. Matsui T.
Toward a Complete Measurement of the Thermodynamic State of an Impact-induced Vapor Cloud

11:15 Gerasimov M. V. * Dikov Yu. P. Yakovlev O. I.
Experimental Modeling of Impact-induced High-Temperature Processing of Silicates

11:30 Jõeleht A. * Kirsimäe K. Versh E. Plado J. Ivanov B.
Cooling of the Kärdla Impact Crater: II. Impact and Geothermal Modelling

11:45 Newsom H. E. * Hagerty J. J.
Limits to the Presence of Impact-induced Hydrothermal Alteration in Small Impact Craters on the Earth: Implications for the Importance of Small Craters on Mars

12:00–12:30 GENERAL DISCUSSION

12:30–1:50 LUNCH

Saturday, February 8, 2003
EJECTA EMPLACEMENT AND OBLIQUE IMPACT EFFECTS
1:50 p.m. Lecture Hall

1:50 Artemieva N. A. * Pierazzo E. [INVITED]
Oblique Impact and Its Ejecta — Numerical Modeling

2:30 Schultz P. H. * [INVITED]
Atmospheric Effects and Oblique Impacts: Comparing Laboratory Experiments with Planetary Observations

3:10 Herrick R. R. * Hessen K.
Constraints on the Impact Process from Observations of Oblique Impacts on the Terrestrial Planets

3:25 Anderson J. L. B. * Schultz P. H. Heineck J. T.
The Evolution of Oblique Impact Flow Fields Using Maxwell's Z Model

3:40–4:00 BREAK

4:00 Haskin L. A. * McKinnon W. B.
Thicknesses of and Primary Ejecta Fractions in Basin Ejecta Deposits

4:15 Macdonald F. A. * Mitchell K.
Amelia Creek, Northern Territory: A 20 × 12 km Oblique Impact Structure with No Central Uplift

4:30–5:15 GENERAL DISCUSSION

Sunday, February 9, 2003
CREATION OF THE STRUCTURE OF COMPLEX CRATERS
8:30 a.m. Lecture Hall

8:30 Sharpton V. L. * Dressler B. O. [INVITED]
Excavation Flow and Central Peak Rings: Is There a Connection?

9:10 Collins G. S. * Turtle E. P. [INVITED]
Modeling Complex Crater Collapse

9:50 Ivanov B. A. *
Complex Crater Formation: Verification of Numerical Models

10:05 Osinski G. R. * Spray J. G.
Transient Crater Formation and Collapse: Observations at the Haughton Impact Structure, Arctic Canada

10:20–10:35 BREAK

10:35 McKinnon W. B. * Schenk P. M. Moore J. M.
Goldilocks and the Three Complex Crater Scaling Laws

10:50 Hildebrand A. R. *
Linking Experimental Modelling of Impact Craters to Structural Components of the Real Thing

11:05 Collins G. S. * Turtle E. P. Melosh H. J.
Numerical Simulations of Silverpit Crater Collapse: A Comparison of Tekton and SALES 2

11:20 Plescia J. B. *
Application of Gravity Data to Understanding Impact Mechanics

11:35–12:15 GENERAL DISCUSSION

12:15–1:30 LUNCH

Sunday, February 9, 2003
CRATERING ON LOW-GRAVITY BODIES
1:30 p.m. Lecture Hall

1:30 Chapman C. R. * [INVITED]
Cratering on Small Bodies: Lessons from Eros

2:10 Asphaug E. * [INVITED]
Formation of Impact Craters on Comets and Asteroids: How Little is Known

2:50 Yano H. * [INVITED]
Low-G Impact Experiments in Preparation for the Muses-C Mission

3:10 Onose N. * Fujiwara A.
Velocity Distributions of Fragments and Its Time Dependence and
Velocity Distributions of Fragments in Oblique Impact Cratering on Gypsum

3:25–3:40 BREAK

3:40–4:30 GENERAL DISCUSSION

4:30–4:45 BREAK

4:45–6:30 CLOSING DISCUSSION

CALCULATION OF PLANETARY IMPACT CRATERING TO LATE TIMES. Thomas J. Ahrens[1], John D. O'Keefe,[1] and Sarah T. Stewart[2], [1]Lindhurst Laboratory of Experimental Geophysics, California Institute of Technology, Pasadena, CA 91125, tja@caltech.edu, [2]Geophysical Laboratory, Carnegie Institution of Washington, Washington DC.

Simulation of impact cratering on planetary materials is crucially dependent on adequate description of shock processing of surface materials. Two recent examples of the importance of these processes is demonstrated by the simulation of impact induced flow from the impact of a ca. 10 km bolide at 20 km/sec onto the Earth. This has been inferred to have occurred along the Yucatan (Mexican) coast, 65 million years ago. This impact is inferred to have triggered global climatic change, induced by the impact devolatilization of the marine anhydrite ($CaSiO_4$) and gypsum ($CaSO_4 2H_2O$) deposits of the target rocks. These calculations conducted with Sandia's CTH code depend crucially upon utilizing a rock damage model which reduced crustal rock strength from 100 MPa to 1 MPa over a volume some 10^2 times that of the bolide in about 1 minute and gives rise to a 100 km diameter central peak, flat-floored crater with overturned target flap some 8 minutes after impact. Comparison of calculated post-impact deformation compares favorably with seismic profiling and drill-core data.

A second example is the formation of ejecta blankets giving rise to rampart Martian craters by fluidization with liquid water by a new impact cratering simulation and recent shock wave data on H_2O ice. We demonstrate that ground ice is melted by the impact shock within a hemisphere of radius equal to the final crater radius, resulting in excavation of a mixture of liquid water and brecciated rock into the continuous ejecta blanket. Our shock wave experiments demonstrate that ice at Mars temperature, 150 to 275 K, will begin to melt when shocked above 2.2 to 0.6 GPa, respectively, lower than previously expected. Hence, the presence of liquid water near the pre-impacted surface is not required to form fluidized ejecta. The amount of ice melted and incorporated into the ejecta blanket debris flow is within a factor of two of the subsurface ice content; therefore, debris flow modeling of fluidized ejecta morphologies may be used to quantify the amount of near-surface ground ice on Mars.

DYNAMIC TENSILE STRENGTH OF CRUSTAL ROCKS AND APPLICATION TO IMPACT CRATERING. H. Ai[1] and T. J. Ahrens[2], [1]Caltech, 100-23, Pasadena, CA, 91125, USA. ahr@gps.caltech.edu. [2]Caltech, 252-21, Pasadena, CA, 91125, USA. tja@gps.caltech.edu.

Dynamic tensile strengths of two crustal rocks, San Marcos gabbro and Coconino sandstone (Meteor Crater, Arizona), were determined by carrying out flat plate impact experiments. Porosity of San Marcos gabbro is very low,[1] and the reported porosity for Coconino sandstone is ~25%.[2] Aluminum flyer plates were used for gabbro with impact velocities of 13 to 50 m/s, which produce tensile stresses in the range of 120 to 450 MPa. PMMA flyer plates were used for sandstone with impact velocities of 5 to 25 m/s, resulting tensile stresses in the range of ~13 to 55 MPa. Impact was normal to the bedding of sandstone. Tensile duration times for two cases were ~1 and ~2.3 μs, respectively. Pre-shot and post-shot ultrasonic P and S wave velocities were measured for the targets.

Velocity reduction for gabbro occurred at ~150 MPa (Fig. 1a), very close to the earlier result determined by microscopic examination.[1] The reduction of S wave is slightly higher than that of P wave. This indicates that the impact-induced cracks were either aligned,[3] or there were residual fluids within cracks,[4] or both. Data for sandstone velocity reduction was few and scattered caused by its high porosity (Fig. 1b). The range of dynamic tensile strength of Coconino sandstone is within 25 and 30 MPa (Fig. 1b). Obvious radial cracks at certain stresses indicate that deformation was not restricted to one dimensional strain as being assumed. Spall fragmentation occurred above 40 MPa (Fig. 1b).

The combination of impact velocities, U (km/s), and impactor radii, a_0 (m), are constrained by Meteor Crater fracture depth, ~850 m,[5] and the dynamic tensile fracture strength from our experiments, 40 MPa (Fig. 2). Volume of the crater for each impact was calculated using $V = 0.009mU^{1.65}$,[6] where V is crater volume (m^3), m is the mass of the impactor (kg). Volume of impact with U = 28 km/s, a_0 = 10 m is close to the real Meteor Crater volume, 7.6e7 m^3.[7] Impact energy for this case is 3.08 Mt., which agrees well with theoretical calculation (3.3 to 7.4 Mt.).[10] (1 Mt.=4.18e15 J)

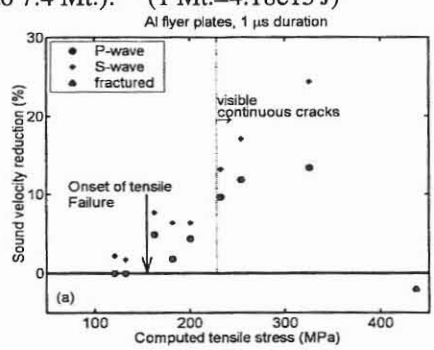

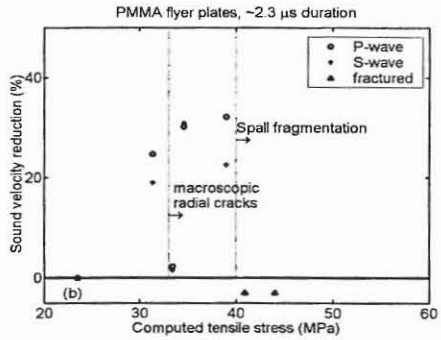

Figure 1: Velocity measurements for *(a)* gabbro and *(b)* sandstone experiments. Dashed line in (a) indicates pressure above which visible continuous cracks occurred. Dashed lines in (b) indicate pressures above which macroscopic radial cracks and spall fragmentation occurred.

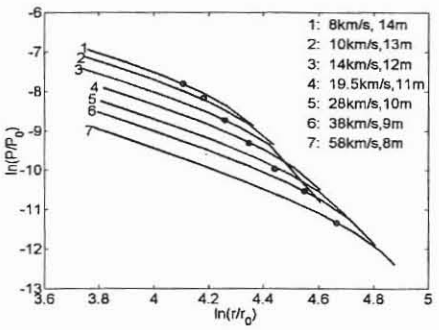

Figure 2: Normalized tensile pressure P at different depths, r, for sets of impact velocity U (km/s), and impactor radius r_0 (m) constrained by fracture depth of Meteor Crater and dynamic tensile fracture strength of Coconino Sandstone. P_0 is initial impact pressure, $P=P_r-P_z$, where $P_r=P_0(r/r_0)^{-n}$,[8] n is function of U[9] and P_z is the lithostatic pressure. Circles represent r = 850 m and P = 40 MPa.

References: [1] Lange, M. A. et al. (1984) *Icarus, 58*, 383-395. [2] Shipman, F. H. et al. (1971) *NASA report, MSL-7-14, 46*. [3] Anderson, D. L., Minster, B., and Cole, D. (1974) *JGR, 79*, 4011–4015. [4] O'Connell, R. J., and Budiansky, B. (1974) *JGR, 79*, 5412–5426. [5] Ackermann, H. D. et al. (1975) *JGR, 80*, 765–775. [6] Holsapple, K. A. (1993) *Annu. Rev. Earth Planet. Sci. 21*, 333-373. [7] Roddy, D. J. et al. (1980) *Proc. Lunar Planet. Sci. Conf. 11th*, 2275-2308. [8] Ahrens, T. J. and O'Keefe, J. D. (1977) in *Impact and Explosion Cratering*, Roddy, D. J., et al. (eds.) Perganon, New York, 639–656. [9] Ahrens, T. J. and O'Keefe, J. D. (1987) *Int. J. Impact Engng., 5*, 13–32. [10] Schmidt, R. M. and Housen, K. R. (1987) *Int. J. Impact Eng., 5*, 543-560.

THE EVOLUTION OF OBLIQUE IMPACT FLOW FIELDS USING MAXWELL'S Z MODEL. J. L. B. Anderson[1], P. H. Schultz[1] and J. T. Heineck[2], [1]Geological Sciences, Box 1846, Brown University; Providence, RI 02912 (Jennifer_Anderson@Brown.edu), [2]NASA Ames Research Center; Moffett Field, CA 94035.

Introduction: Oblique impacts are the norm rather than the exception for impact craters on planetary surfaces. This work focuses on the excavation of experimental oblique impact craters using the NASA Ames Vertical Gun Range (AVGR). Three-dimensional particle image velocimetry (3D PIV) [1, 2] is used to obtain quantitative data on ejection positions, three-dimensional velocities and angles. These data are then used to constrain Maxwell's Z Model and follow the subsurface evolution of the excavation-stage flow-field center during oblique impacts.

Three-Dimensional Particle Image Velocimetry: A laser sheet is projected horizontally above the target surface during impacts at the AVGR. A ring of particles within the ejecta curtain are illuminated and imaged twice in rapid succession by two cameras above the target surface. Processing software tracks the movement of ejecta particles between time frames and combines the data from the two cameras to obtain three-dimensional velocities of ejecta particles within the laser plane. Entire ballistic trajectories are reconstructed for ejecta in all directions around the impact point, leading to ejection positions, vector velocities and angles. These quantitative data can be compared directly to numerical models and predictions from empirical models such as Maxwell's Z Model.

Maxwell's Z Model: Maxwell's Z Model [3, 4] is based on three main assumptions: (1) subsurface material flow is incompressible, (2) material moves along independent, ballistic trajectories after spallation at the surface plane and (3) the subsurface radial component of velocity is given by $u_R=\alpha(t)/R^Z$.

The Z Model, an empirical model based on explosion cratering data, places the flow-field center at the target surface. However, the flow-field centers of vertical impacts best match a moving source located at some depth below the target surface [5, 6, 7]. Croft [8] generalized the Z Model to include a term for the depth to the flow-field center.

3D PIV measures the ejection position and ejection angle directly. With inverse modeling, it is possible to determine the values for the depth to the flow-field center. The model presented here allows one flow-field center to migrate from an initial depth along a subsurface trajectory that is parallel to the projectile trajectory (assuming that there is no lateral movement of the flow field center during oblique impacts, only uprange or downrange movement). The angle of the subsurface trajectory is also allowed to vary. In this way, the flow field center is allowed to move along a subsurface trajectory that rotates from vertical motion only (for 90°) to an angle that reflects the initial impact angle.

A combination of two superimposed flow field centers may explain the observed ejection angle variation with azimuth, as illustrated in figure 1. The uprange (0°/360° azimuth) ejection angles for this 30° impact are very high, while the downrange (180° azimuth) ejection angles are low. The Z Model suggests that high ejection angles, such as those observed in the uprange curtain, imply a deeper flow-field center, while low ejection angles (such as those downrange) imply a shallower flow-field center. As time progresses, the ejection angles increase downrange and decrease uprange. This indicates that the depth to the flow-field center is changing. These data will be modeled using two Z Models, each with their own evolution of the flow-field center depth and subsurface trajectory. The superposition of these two models will be required to fit the measured ejection angle and position data.

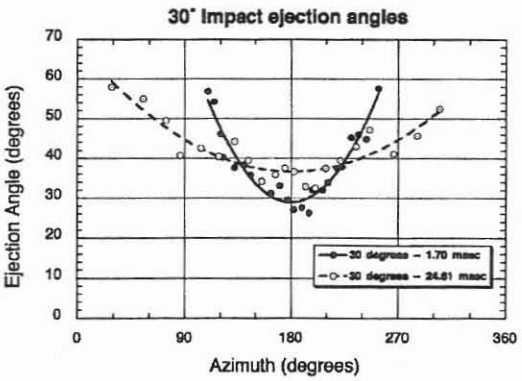

Figure 1. Ejection angles as a function of azimuth around the crater center for 30° impacts. Times represent the time after impact that the data was obtained.

Implications: Ejection angle data derived using 3D PIV is combined with Maxwell's Z Model, to determine a depth to the flow-field center for oblique impacts. The location of that flow-field center evolves as the crater grows. A superposition of flow fields defined by the Z Model may be able to better model the excavation flow of oblique impacts.

References: [1] Heineck J. T. et al (2001) *4th Intern. Symp. on PIV*, #R503. [2] Schultz P. H. et al. (2000) *LPSC 31*, #1902. [3] Maxwell D. E. (1977) *Impact & Explosion Cratering*, 1003-1008. [4] Orphal D. L. (1977) *Impact & Explosion Cratering*, 907-917. [5] Thomsen J. M. et al. (1979) *PLPSC 10*, 2741-2756. [6] Austin M. G. et al. (1980) *PLPSC 11*, 2325-2345. [7] Austin M. G. et al. (1981) *Multi-ring Basins*, 197-205. [8] Croft S. K. (1980) *PLPSC 11*, 2347-2378.

OBLIQUE IMPACT AND ITS EJECTA- NUMERICAL MODELING. N. Artemieva[1] and E. Pierazzo[2], [1]Institute for Dynamics of Geospheres, Leninsky pr., 38, bldg.6, Moscow, 119779, Russia; nata_art@mtu-net.ru, [2]Planetary Science Institute, 620 N. Sixth Ave, Tucson, AZ 85705; betty@psi.edu

Introduction: It is well known that impact events strike planetary surfaces at an angle from the surface. Assuming an isotropic flux of projectiles, probability theory indicates that the most likely angle of impact is 45° regardless of the body's gravitational field [1 -2]. While crater rims appear circular down to low impact angles, the distribution of ejecta around the crater is sensitive to the angle of impact and currently serves as the best guide to obliquity of impacts. A fair amount of numerical modeling of vertical impacts has been carried out from the early 60-s [3] to the present time [e.g., 4-5 and references herein]. In vertical impacts, the axial symmetry of the process allows the simplification of the model to two dimensions (2D). Oblique impact modeling requires 3D hydrocodes and, hence, much more powerful computers. The first documented detailed oblique impact studies were carried out at Sandia National Labs' supercomputers less than 10 years ago to describe the 1994 collision of comet SL9 with Jupiter [6-7]. Since then, substantial progress in computer science has made 3D modeling a reachable objective for the scientific community.

Hydrocodes The hydrocodes that are mostly used by the planetary impact cratering community for modeling oblique impacts are CTH [8], and SOVA [9]. Both are two-step Eulerian codes that can model multidimensional, multimaterial, large deformation, and strong shock wave physics. Both can be coupled with sophisticated equations of state models, and both have distinctive features: CTH allows for a sophisticated treatment of strength; SOVA contains a procedure to describe particle motion in an evolving ejecta-gas plume.

Melt productionis a strong function of angle of impact. However, scaling laws for oblique impacts are still not well constrained. Pierazzo & Melosh [10] found that for typical rocks the amount of impact melt produced decreases with impact angle. For impacts from 90° to 45° the decrease is less than 20%, whereas for impacts at 30° the volume of melt drops to about 50% of the vertical case, declining to less than 10% for a 15° impact. In this study, the projectile volume was kept constant. For geological studies, however, it may be more useful to focus on crater volume. Ivanov and Artemieva [12] found that for relatively high impact velocities (>20 km/s) the efficiency of the cratering excavation, based on the maximum volume of the transient cavity, for a 45° impact appears to be comparable with that of a vertical impact. Early on, the application of standard scaling laws for crater size to oblique impacts [11] suggested that for impact angles between 30° and 90° the melt ratio is more or less constant, with deviations within 20% of the average. Published laboratory data [13, 14] show that cratering efficiency in an oblique impact varies with impact velocity and projectile-target materials.

Complex targets must be treated with care. While the overall target melting seems to follow the general behavior described above, Stoffler et al [15] found that the amount of melting of finite thickness layers scales with the projectile's cross section (D^2), not its volume (D^3), as is the case for the overall melting. Furthermore, melting of near surface layers increases with impact angle decrease.

Fate of the projectile Oblique impacts show a downrange focusing of projectile material, becoming predominant at low impact angles [16]. Furthermore, most of the projectile is ejected from the opening crater in the early stages of the impact, and a significant amount of projectile material carries a downrange/upward velocity larger than escape velocity. Shock melting and vaporization in the projectile also decreases with impact angle [16,17].

Distal ejecta– tektites andmeteorites from other planets It is now widely accepted that both SNC-meteorites and tektites are produced by impact events. Geophysical and geochemical properties of tektites are consistent with an origin from high-temperature melt from the top few hundred meters of the Earth's surface that solidified in the upper atmosphere (low oxygen content) [18]. Martian meteorites originate from the upper layers of the youngest martian terrains [19, 20]. Different in their nature, both types of ejecta have a similar place of origin (upper target layers) and require high velocities (to travel distances of hundreds of km – tektites – or to escape Mars gravity – SNC meteorites). The main difference between them is in the degree of shock compression they must have experienced: melting must occur for tektites while, on the opposite end, meteorites must experience modest shocks. Since they are formed by the same mechanism, impact cratering, from the numerical modeling point of view both SNC and tektites may be treated in similar ways.

Transformation of continuum material into discrete particles is crucial for modeling ejecta during the late stages of impact cratering, when the properties of individual particles (i.e., mass, size, shape, individual velocity) become important. Modeling of ejecta as a

continuum is a reasonable assumption only in the early stages of impact cratering. The trajectories of discrete particles in the atmosphere should be defined by a two-phases hydrodynamics that includes the interaction of the particles with the post-impact gas flow. Various processes influence the size and shape of individual particles [e.g., 21,22,23]. The approach of representative tracer particles [9,24,25] is used to avoid limitations due to computer capacity. A simplified treatment models material disruption when the material is subject to tension. The hydrodynamic cell velocity defines the initial particle velocity, and the particle's initial position within the cell is randomly defined. An empirical size distribution for solid particles is adopted from experimental studies of high-energy chemical explosions, where particle sizes range from 1 mkm to 10 cm. The diameter of molten particles ranges from 1 to 3 cm, while particle size drops to 0.01 cm when produced by condensation from a two-phase mixture.

Tektites. Tektites (high-temperature, high-velocity melt from surface layers) are consistent with a production by relatively high-velocity (>20 km/s) impact into silica-rich, possibly porous and volatile-rich, targets with impact angles around 30° -50° [26]. In particular, very oblique impacts must be excluded, since they tend to produce target melt that is highly contaminated with projectile material. In [15] a numerical modeling study was performed to evaluate whether a single collisional event (a 30° impact) could have been responsible for the formation of the Ries and Steinheim craters and the moldavite tektite strewn field. The modeled spatial particle distribution shows promising similarities with the observed one (Fig.1), like the formation of a relatively narrow tektite distribution fan, symmetric with respect to the downrange direction, and a modeled mass of tektite-type material that is within a factor of two of that estimated for the Ries-related tektites.

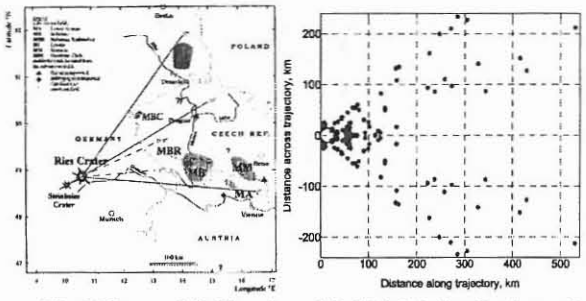

Fig.1 Observed (left) and modeled (right) distributions of moldavites.

Martian meteorites. The number of ejection events required to represent the known Martian meteorites (in the past 20 Ma) [19] combined with the known Martian cratering rate [27] suggest the need of parent craters of 1 to 3 km in diameter. Modeling studies [28] have shown that oblique impacts (15° to 60°) are much more efficient than vertical ones [29] at producing Martian meteorites. However, the modeled crater sizes are too large (>10 km) or particles should be larger than 20 cm in diameter to keep escaping velocity in upper atmosphere [28] (the idea of large pre-entry size of martian meteorites has been confirmed independently by measurements of ^{80}Kr produced by epithermal secondary cosmic-ray neutrons of 30-300 eV energy [30]). In our study, solid, modestly shocked material (6-7% of the projectile mass) is ejected to velocities >5 km/s from a thin surface layer (~1/10 of the projectile diameter), where the peak shock pressure is distinctly limited to about 9 to 45 GPa. This pressure range is essentially confirmed by the observations [31]. Thus, recent hypotheses [32, 33] that Martian rocks can reach the Earth without being intensely shocked and heated are incorrect or at least questionable.

References: [1] Gilbert G.K. (1893) *Bull. Philos. Cos. Wash. (D.C.) 12*, 241–292. [2] Shoemaker E.M. (1962) In *Physics and Astronomy of the Moon* (Z. Kopal, Ed.), pp. 283–359. [3] Bjork R. L. (1961) JGR 66, 3379-3387. [4] O'Keefe J.D. and Ahrens T.J. (1999) *JGR 104*, No. E11, 27,091. [5] Melosh H.J. and Ivanov B. (1999) *Annu. Rev. Earth Planet. Sci.*, 27:385–415 [6] Crawford et al. (1994) *Shock waves* 4, 47-50. [7] Boslough et al. (1994) *GeoRL* 21, 1555-1558. [8] McGlaun J.M.et al. (1990) *Int. J. Impact Eng. 10,* 351–360. [9] Shuvalov V.V. (1999) *Shock Waves 9*, 381-390. [10] Pierazzo E. and Melosh H.J. (2000) *Icarus 145,* 252–261. [11] Gault D.E. and Wedekind J.A. (1978) *Proc. Lunar Planet. Sci. Conf. 9th,* 3843–3875. [12] Ivanov B. and Artemieva N. (2002) *GSA Special paper 356*, 619-630. [13] Burchell M.J., and Mackay N.G.(1998) *JGR 103*, p. 22761–774. [14] Hayhurst C.J. et al. (1995) *Int. J. Impact Eng 17*, 375–386. [15] Stoffler et al. (2002) M&PS 37, in press. [16] Pierazzo E. and Melosh H.J. (2000b) M&PS 35, 117-130. [17] Artemieva, N.A. and Shuvalov V.V.(2001) in *Geological and biological effects of impact events,* Buffetaut & Koeberl Eds. (Springer-Verlag), 249-263. [18] Koeberl C. (1994) *GSA Special Paper 293,*133-151. [19] Warren P.H. (1994) *Icarus 111*, 338-363. [20] Nyquist L. E. et al (2001) *Space Science Reviews 96,* 105-164. [21] Melosh H.J. and Vickery A.M. (1991) *Nature 350*, 494-497. [22] Melosh H.J. (1984) *Icarus 59*, 234-260. [23] O'Kee fe J.D. and Ahrens T.J. (1986) *LPSC 17*, 1004-1005. [24] Teterev A.V. and Nemtchinov I.V. (1993) *LPSC 24*, 1415-1416. [25] Shuvalov V.V. (2001) *LPSC 32*, #1126. [26] Artemieva A.N. (2002) in Lecture Notes in Earth Physics. In press. [27] Hartmann W. K. and Neukum G. (2001) *Space Science Reviews 96,* 165-194. [28] Artemieva N. and Ivanov B. (2002) *LPSC 33*, #1113. [29] Head J. and Melosh H.J. (2002) *LPSC 31*, #1937. [30] Eugster O. et al. (2002) *LPSC 33*, #1096. [31] Fritz et al. (2002) *LPSC 33*, # 1504. [32] Weiss, B.P. et al. (2000), *Science, 290*, 791-795. [33] Mileikowsky. C. et al. (2000), *Icarus, 145*, 391-427

FORMATION OF IMPACT CRATERS ON COMETS AND ASTEROIDS: HOW LITTLE IS KNOWN.

Erik Asphaug, Earth Sciences Department, University of California, Santa Cruz CA 95064, asphaug@es.ucsc.edu

Impact phenomena shaped our solar system. From the accretion of planetesimals 4.6 billion years ago to the spallation of meteorites from their parent bodies, this process has left no bit of matter untouched. The study of impact craters on small bodies therefore provides a foundation for understanding accretion and the delivery of meteorites – topics central to the origin of planets. Moreover, geologic-scale impact craters forming in low gravity reveal details of the cratering process that are hidden on high-gravity worlds like the Earth and Moon.

The detailed study of small body cratering began with efforts by Housen et al. (1979), Veverka and Thomas (1979) and others, together with efforts related to catastrophic disruption of small bodies (Chapman and Davis 1975; Fujiwara et al. 1979; Farinella et al. 1982). But the discovery of Stickney (the ~10 km diameter crater on the ~20 km diameter Martian satellite Phobos) and comparably huge divots imaged by Voyager on satellites of Jupiter and Saturn made it clear that small bodies can sustain huge wallops despite the conclusion of scaling models, notably that the impactor responsible for Stickney would have catastrophically disrupted Phobos.

While large impact structures on bodies with significant gravity are much better understood today than they were originally, for small bodies this is not the case. We appear almost to be back-pedaling towards an earlier vision of the asteroid impact process, pioneered by Art Clokey (without much guidance from geologists) in his 1957 *Gumby* claymation adventure "The Small Planets". Although nobody today confesses to expect clear gravity signatures around ~10 m craters on ~100 m asteroids (we have yet to obtain clear images of anything much smaller than ten kilometers), few expected copious regolith on bodies the size of Eros (33×13 km) either. Surprise is the norm.

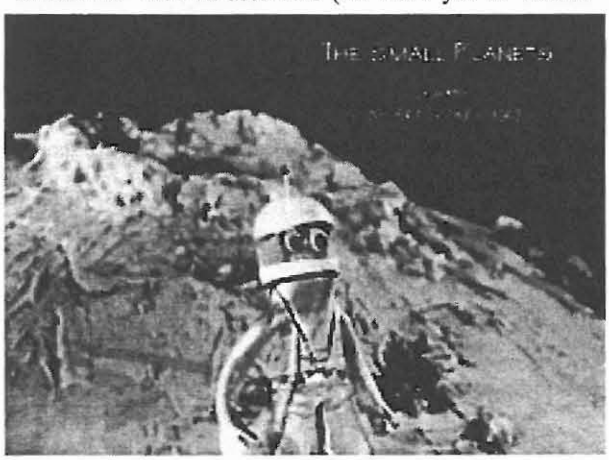

Fifteen years ago, bodies that size were widely believed to be capable of sustaining a few centimeters of regolith at best (e.g. Veverka et al. 1986). Instead, NEAR Shoemaker confirmed what had been hinted during less clearly resolved Galileo flybys of asteroids Gaspra and Ida: that Eros-sized asteroids can be awash in gravitationally bound debris (collisional or original is anybody's guess) ranging in size from ~100 m blocks (Chapman et al. 2001) to submicron grains accumulating in "ponds" (Robinson et al. 2002). Global regolith deposits on Eros range from 100's of m to undeterminable depth, and surface geophysics may even be dominated by quasi-aeolean processes such as electrostatic levitation (Lee 1996) and seismic shaking (Cheng et al. 2002; Asphaug et al. 2001).

Even on the smallest bodies yet observed, there is evidence for gravity dominance. Asteroid Ida's tiny (1.6 km) satellite Dactyl exhibits a spheroidal shape, as one would expected under self-gravitational control, and its major craters display rims and maybe central peaks[1].

But to contrast Dactyl, Phobos, Deimos and other gravity regime Lilliputians (e.g. Thomas 1998), one finds 60 km Mathilde, a body which trashes every established theory of impact cratering, and which is from impact cratering's point of view one of the most astonishing bodies. Here one sees huge craters devoid of any gravity signature, and devoid of any signature of overprinting, on a pitted spheroid lacking visible fractures or other strength-related de-

[1] Crater rims are not unique to the gravity regime, and can form by shear bulking during plastic deformation. Bulking requires weakly cohesive granular media on the smallest bodies since plastic deformation otherwise involves impact stresses that would result in material escape. In either case an asteroid is not monolithic if one sees rimmed craters.

formation. Nothing is here but the huge crater bowls themselves. Ejecta has either all entirely escaped (Asphaug et al. 2002) or was never ejected at all (Housen et al. 1999), evidently in a target sufficiently porous to not communicate each blow globally, yet sufficiently cohesive for its crater rims not to collapse into softer shapes.

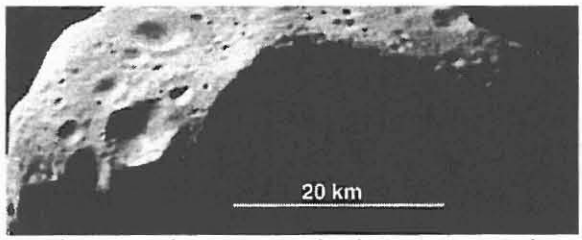

Clues to impact geophysics are everywhere. Shown below is pathological example (NEAR Image 0136819148) where four ~100 m fragments of an ejecta block appear to rest in the ~700 m diameter secondary crater they created. If this is not a chance association (the odds are small), it is the record of an impact involving geologic masses at known speed (v_{orb}^{max}~10 m/s) and mass (~2.e10 kg). Pi-group scaling predicts a crater about half as large, perhaps because low velocity coupling is more efficient than hypervelocity coupling.

While secondary craters on asteroids may seem oddities of cratering mechanics, they have potential significance for helping us understand accretion collisions in the solar nebula which took place at similar speeds and involved similar materials, and which are a problematic theoretical bottleneck (Benz 2000).

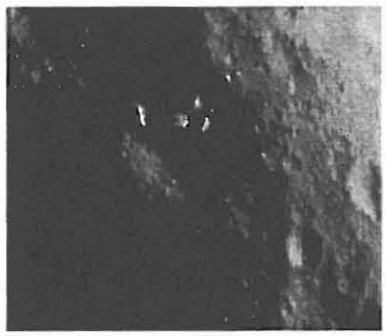

Another kind of comparative geology can be conducted by studying the largest craters on asteroids, which span the transition from the strength to gravity regimes and exhibit whole-body effects (e.g. Stickney on Phobos; Asphaug and Melosh 1993, Thomas 1998) or the lack thereof (Mathilde, as discussed above). From these, key impact aspects can be independently derived, and exhibit a unique geologic record of the planetary impact process masked in the enormous gravity of terrestrial planets. The mechanics of cratering is preserved like nowhere on Earth.

Conclusion: Two decades of experimental, theoretical, and numerical modeling (Holsapple et al. 2002; Asphaug et al. 2002) together with spacecraft reconnaissance of asteroids has forced us to revisit pretty much everything we think we know about how asteroids collisionally evolve. Geologists have had to get used to landscapes where sunlight may be as important a force as gravity, where cohesion less than that of dry snow can sustain cliff walls and monolithic structures, where puffballs can masquerade as rocks and vice-versa. Impact theorists have had to take a big step back in their view of the process, especially for oddities like Mathilde. But Mathilde is perhaps the norm, and we await an appropriate geophysical understanding of these objects, and how craters form when gravity and strength – the fundamental forces of geology – compete for dominance.

Asphaug, E. and Melosh, H.J. 1993. The Stickney impact of Phobos: A dynamical model, *Icarus* **101**, 144-164

Asphaug, E., Ryan, E.V, and Zuber, M.T. 2002. Asteroid Interiors. In *Asteroids III*, Univ. Arizona Press.

Benz, W. 2000. Low Velocity Collisions and the Growth of Planetesimals. *Space Science Reviews* **92**, 279-294

Chapman, C.R. and Davis, D.R. 1975, Asteroid collisional evolution - Evidence for a much larger early population, Science, 190, 553

Chapman, C.R. 2001. Eros at Very High Resolution: Meteoritical Implications. *Meteoritics & Planetary Science Supplement* **36**, A39.

Cheng, A.F., Izenberg, N., Chapman, C.R. & Zuber, M.T. 2002. Ponded deposits on asteroid 433 Eros. *MAPS* **37**, 1095-1105.

Clokey, A. 1957. The Small Planets. Clokey Productions, National Broadcasting Company

Farinella, P., P. Paolicchi and V. Zappala 1982. The asteroids as outcomes of catastrophic collisions. *Icarus* **52**, 409-433.

Fujiwara, A, Cerroni, P, Davis, DR, Ryan, EV, Di Martino, M, Holsapple, K, and Housen, K. 1989. Experiments and scaling laws for catastrophic collisions, in *Asteroids II*, edited by T.G. (R.P. Binzel, and M.S. Matthews, Eds.), pp. 240-265, Univ. of Arizona Press, Tucson

Holsapple, K.A. *et al.* 2002. Asteroid impacts: laboratory experiments and scaling laws. In *Asteroids III.*

Housen, K.R., K.A. Holsapple and M.E. Voss 1999. Compaction as the origin of the unusual craters on the asteroid Mathilde. *Nature* **402**, 155-157

Housen, K.R., L.L. Wilkening, C.R. Chapman and R. Greenberg 1979. Asteroidal Regoliths. *Icarus* 39, 317-351.

Housen, K.R., R.M. Schmidt and K.A. Holsapple 1983. Crater Ejecta Scaling Laws: Fundamental Forms Based on Dimensional Analysis. *J. Geophys. Res.* **88**, 2485-2499.

Lee, P.C. 1996. Dust Levitation on Asteroids. *Icarus* **124**, 181-194

Robinson, M.S., Thomas, P.C., Veverka, J., Murchie, S. and Carcich, B. 2001, *Nature* **413**, 396-400.

Thomas, P.C. 1998. Ejecta Emplacement on the Martian Satellites. *Icarus* **131**, 78-106

Veverka, J. and Thomas, P. 1979. Phobos and Deimos - A preview of what asteroids are like? In *Asteroids*, 628-651

Veverka, J., P. Thomas, T.V. Johnson, D. Matson, and K. Housen 1986. The Physical Characteristics of Satellite Surfaces. In *Satellites* (J.A. Burns and M.S. Matthews, Eds.), University of Arizona Press, Tucson, pp. 342-402.

SMALL IMPACT CRATERS IN ARGENTINE LOESS: A STEP UP FROM MODELING EXPERIMENTS.

W. A. Cassidy[1], S. P. Wright[1], [1]Department of Geology and Planetary Science, 200 SRCC Building, University of Pittsburgh, Pittsburgh, PA 15260 (ansmet@pitt.edu, spw3@pitt.edu)

Introduction: The Campo del Cielo crater field [1] in northern Argentina was formed about 4000 years ago by a shower of iron meteorites. The crater field contains at least twenty small impact craters, so there is a degree of redundancy here that is not often enjoyed in field work on impact craters. The target material is a very uniform, unconsolidated loess, and we could think of this as the same impact experiment repeated twenty times into the same target by projectiles of different mass, at nearly the same impact velocities, and over some range of impact angles. At least one, and possibly several of the larger craters are explosion-type features. The others were formed by shock-wave excavation and still contain the crater-causing masses within them. Most of the craters are small enough so that their original dimensions can be determined by trenching. The dimensions of each crater can be used to estimate the impact angle of the projectile and the energy of formation of the crater. When the mass of the crater-forming projectile has been determined, its velocity of impact can be calculated.

Characterization of Crater 10: See Table 1.

As shown in Fig. 1, after creating a crater by shock-wave excavation, the projectile came to rest at the end of a long penetration funnel. Presumably, shock-wave excavation ceased when the meteorite's velocity dropped below the speed of sound in the target material. Calculation of impact velocity based on the dimensions of the crater will be low by an amount equal to the speed of sound in the target material.

Impact velocity of the Crater 10 meteorite: Older estimates of impact velocity attributable to Baldwin [2] and Moore [3] are seen in Figure 2 to be much less precise than that derived by dimensionless-ratio gravity scaling [4,5]. All of these estimates, however, are not inconsistent with an impact velocity of 3.7 km/s. While the dimensionless-ratio gravity scaling value of 3.7 km/s is quite precise, it may be inaccurate for the following reasons: (1) we assumed the velocity of sound in loess to be 0.5 km/s; (2) the calculation was based on scaling factors determined for dry quartz sand, not loess; (3) the assumed density of the target material was 2100 kg/m^3; (4) the assumed diameter of the meteorite was that of an equivalent sphere; and (5) the mass of the Crater 10 meteorite was earlier believed to be 33,400 kg, but later information suggests it is closer to 36,000 kg. Problems (1, 3 and 5) could be mitigated by measurements in the field, and (2), the scaling factor for Argentine loess, could be determined by laboratory experiment. This would allow a much more accurate estimate of impact energy. Field studies should also include the excavation of more impact craters.

Discussion: There is some reason to believe there may be many more impact craters in this crater field, and modern methods of remote sensing may be instrumental in helping to discover them. Campo del Cielo is a good location for linking model studies and impact craters. Further accumulation of a body of data on Campo del Cielo can lead to better interpretations of small-scale cratering on other planetary bodies. Direct analogies may be made, in general, to elongated fields of small craters on planetary surfaces, and also, specifically, to secondary crater fields around major impacts, which tend to be low-angle impacts occurring at relatively low velocities.

References: [1] Cassidy, W. A. and Renard, M. L. (1996) *Meteoritics and Planet. Sci.,31,* 433-448. [2] Baldwin, R. B. (1963) *The Measure of the Moon,* 488 pp. [3] Moore, H. J. (1968) *Science, 159,* 333-334. [4] Holsapple, K. A. (1993) *Ann. Rev. Earth Planet. Sci.,21,* 333-373. [5] Melosh, H. J. (1989) *Impact Cratering: A Geologic Process,* 245 pp.

Table 1. The shock-wave-excavated cavity

$Depth_{max}$	4.6 m
Length	24 m
$Diameter_{max}$	16.4 m
Mass of Projectile	33400 – 36000 kg
Impact Angle	9° with the horizontal
Azimuth of infall	N75.5°E (geog.)

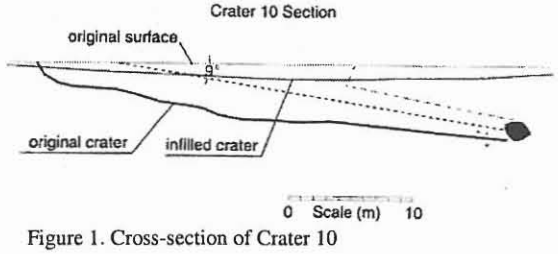

Figure 1. Cross-section of Crater 10

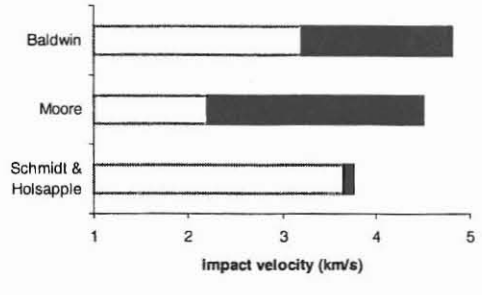

Figure 2. Impact velocity estimates for Crater 10.

CRATERING ON SMALL BODIES: LESSONS FROM EROS. C. R. Chapman[1], [1]Southwest Research Institute, Suite 400, 1050 Walnut St., Boulder CO 80302; cchapman@boulder.swri.edu.

Introduction. Cratering and regolith processes on small bodies happen continuously as interplanetary debris rains down on asteroids, comets, and planetary satellites. Butthey are very poorly observed and not well understood. On the one hand, we have laboratory experimentation at small scales and we have examination of large impact craters (e.g. Meteor Crater on Earth and imaging of abundant craters on terrestrial planets and outer planet moons). Understanding cratering on bodies of intermediate scales, tens of meters to hundreds of km in size, involves either extrapolation from our understanding of cratering phenomena at very different scales or reliance on very preliminary, incomplete examination of the observational data we now have for a few small bodies. I review the latter information here.

It has been generally understood that the role of gravity is greatly diminished for smaller bodies, so a lot of cratering phenomena studied for larger bodies is less applicable. But it would be a mistake to imagine that laboratory experiments on gravitationless rocks (usually at 1 g) are directly applicable, except perhaps to those monolithic Near Earth Asteroids (NEAs) some tens of meters in size that spin very rapidly and can be assumed to be "large bare rocks" with "negative gravity". Whereas it had once been assumed that asteroids smaller than some tens of km diameter would retain little regolith, it is increasingly apparent that regolith and megoregolith processes extend down to bodies only hundreds of meters in size, perhaps smaller. Yet these processes are very different from those that pertain to the Moon, which is our chief prototype of regolith processes. The NEAR Shoemaker spacecraft's studies of Eros provide the best evidence to date about small-body cratering processes, as well as a warning that our theoretical understanding requires anchoring by direct observations.

Eros: "Ponds", Paucity of Small Craters, and Other Mysteries. Although Eros is currently largely detached from interactions with main-belt asteroids in its Earth-approaching orbit, almost all of its cratering history must have occurred in the main belt, where it almost certainly lived for a long time and where the impact rate is orders-of-magnitude greater than in its present environment. Thus NEAR Shoemaker's year-long orbital studies of Eros should be representative of asteroidal cratering processes for medium-small (tens of km) asteroids generally – with the caveat that small bodies are made of many different materials, ranging from metal to whatever comets are made of, and we already have indications from NEAR Shoemaker's flyby of Mathilde that responses to impacts on such bodies may be very different from what is observed on rocky Eros.

As viewed from a distance, the saturated crater fields on Eros look similar to those on Ida and, indeed, on the Moon itself. It is at smaller scales, never before studied for asteroids, where Eros' appearance diverted dramatically from expectations based on modest extrapolations from our lunar experience. Flat, level "ponds" are common on Eros and were certainly not expected. Most striking, however, is the virtual absence of small-scale (cm to meters) craters and the dominance of rocks and boulders on the surface. Apparently many of the larger boulders were distributed about Eros by the comparatively recent impact that produced the Shoemaker crater, providing insight to ejecta processes on small bodies. But, assuming that Shoemaker didn't form practically "yesterday", the dearth of small craters is extremely puzzling. Some researchers have attempted to explain the shortage by traditional geological processes; I will explain why these fail and we are being forced to turn to explanations involving shortages of small projectiles in the asteroid belt (e.g. due to the Yarkovsky Effect).

Even if projectile shortages help to explain the data, other non-lunar processes must be at work, as well. Mass-wasting processes are evident on large crater walls and the ponds reflect a still-not-understood deposition or sedimentation process. The boulder-strewn surfrace itself also serves to "armour" the surface against impacts. The role of seismic shaking on small bodies also must play a major role, relatively unfamiliar for larger bodies. I will summarize the observations of Eros that shed light on these various processes.

Even Smaller Bodies. An interest in sub-km scale bodies has developed in the context of imagining how a potentially dangerous NEA might be diverted. Meanwhile, observational evidence concerning their general geophysical configurations has grown rapidly. A significant proportion of these bodies (~20%) appear to have satellites or be binary in nature, and most of the remainder exhibit properties consistent with being "rubble piles" of one form or another.

Eros, with less than a millionth the mass of the Moon, turned out to be extremely non-lunar-like in its small-scale responses to impact cratering. NEAs of the size being analyzed as prototypes for deflection are a millionth the mass of Eros. We should not expect our insights from Eros, therefore, to be directly applicable to them. And as we learn more about small asteroids and comets, we must expect to be surprised.

MODELING COMPLEX CRATER COLLAPSE. G. S. Collins and E. P. Turtle, Lunar and Planetary Laboratory, University of Arizona, Tucson, AZ 85721, (Contact: gareth@lpl.arizona.edu, or turtle@lpl.arizona.edu).

Introduction: Impact crater collapse is the gravitationally driven modification of the cavity generated during the early stages of an impact event. It is the last major stage in the formation of an impact crater and has the most profound influence on the final morphology of the crater. The aim of this paper is to summarize the robust conclusions drawn from modeling crater collapse and highlight the questions that remain unanswered, particularly those that will require the collaboration of modelers and observers to answer.

Why do modeling? Abstract computer simulations provide one of the only feasible methods for studying complex crater collapse. There has been no direct observation of complex crater collapse in recorded history; large impact events are, perhaps fortunately, too infrequent. In addition, the scale of experimental studies is somewhat inappropriate for drawing conclusions about the collapse of the largest craters in the Solar System. The dominance of gravity in influencing the collapse stage of crater formation implies that the results of the small-scale laboratory collapse experiments cannot be extrapolated meaningfully to the scale of complex craters. Similarly, underground nuclear explosions, although extremely valuable in elucidating the principal features of the excavation stage, are also not of an applicable scale.

Modeling complex crater collapse: The fundamental procedure behind all numerical models of complex crater collapse is the same. First, the physical situation being simulated is simplified and divided into manageable portions, in which all properties are constant. In other words, a grid (mesh) of points and cells is defined to represent the geometry and material properties of the target. Next, the effect of external and internal forces on each of these points and cells is determined, assuming that these forces are constant during a very short interval of time, known as the time step. The mesh is then adjusted to account for the displacements induced by the net effect of the calculated forces for the duration of the time step. Repeating this process of calculating the forces acting on each cell and then adjusting the mesh allows the solution to be advanced in time until the end of the simulation.

Impact crater collapse is controlled by the competition between the gravitational forces tending to close the excavated cavity and the inherent material strength properties of the post-shock target. Thus, to simulate crater collapse, a detailed knowledge of the strength and rheologic behavior of the collapsing material is required. This is the fundamental difficulty in simulating complex crater collapse: numerous studies [for example, 1-7] have concluded that crater collapse controlled by the well-understood standard strength models for rock materials does not involve any uplift of material from beneath the crater floor, which precludes the formation of a central peak, peak ring, or external rings; or the slumping of the transient crater walls, which precludes formation of terraces and significant widening of the crater. In other words, to reproduce the observed morphologies of complex craters, collapse requires significant, but temporary, weakening of the target material beneath the crater floor.

Several processes act during an impact event that might help explain the transient weakening associated with crater collapse. These include wholesale fracturing of the target, bulking (the decrease in density associated with the fracturing of a material and the movement of broken rock debris), acoustic fluidization (the reduction in ambient overburden pressure due to the presence of high-frequency vibrations remnant from the initial impact), melt production, thermal softening (the reduction in strength of material close to its melting temperature) and shear melting in regions of strain localization (pseudotachylite formation). Most, if not all, of these processes have been implemented and tested in numerical models of complex crater collapse; however, the relative importance of each mechanism is still poorly constrained. Thus, there is little agreement on the nature of this weakening.

Results: The impact modeling community is in strong consensus about the need for increased mobility of the target rocks surrounding large craters. Recent modeling work has constrained the required effects of the target weakening mechanism associated with complex crater collapse [6,7,8,9]. The weakening mechanism must: (1) Reduce the strength of the target material surrounding the crater by an order of magnitude or more; (2) weaken the target material surrounding the crater sufficiently for a volume of material at least equal to the crater volume to flow during collapse; and (3) in the case of peak-ring craters, mobilize this material enough such that during collapse the central uplift may overshoot the target surface, which implies an effective viscosity for the collapsing material less than $\sim 10^9$ Pa s for craters less than ~200 km in diameter.

There is also close agreement between the different modeling groups on the details of the collapse flow. Figure 1 illustrates the current paradigm for complex crater formation derived from recent modeling work [6,7,8,9]. Regardless of the weakening mechanism, simulation results support the observation that central peaks are the result of uplift of material originally well

below the crater floor, and that peak-rings are the result of uplift and collapse of the central region. Figure 2 illustrates the subsurface structure of a generic peak ring crater, as inferred from various numerical simulations of complex crater collapse [7].

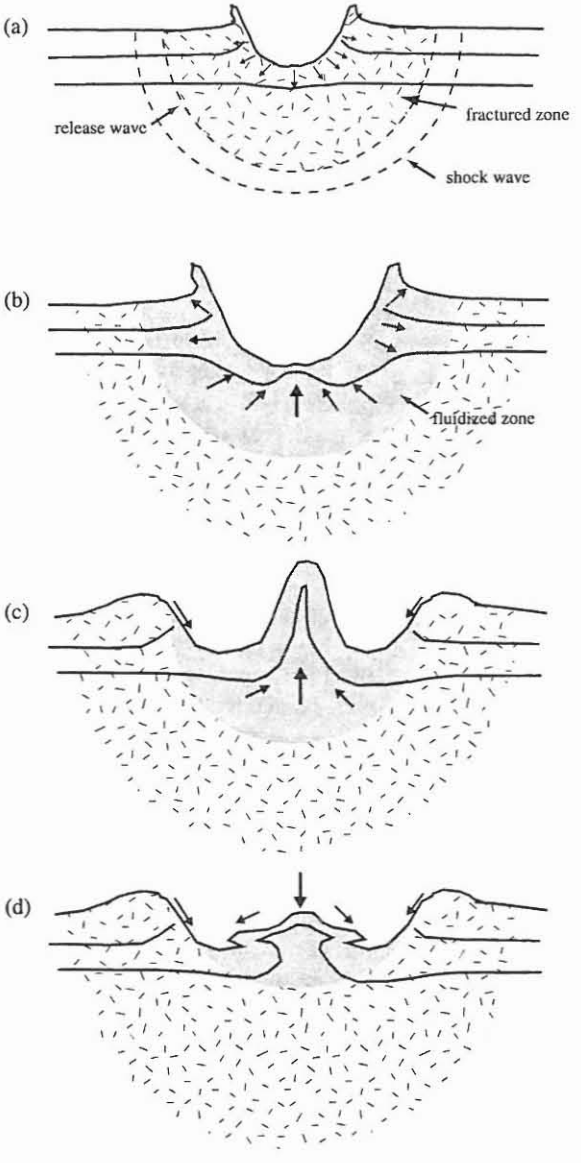

Figure 1 Illustration depicting the current paradigm for how a complex crater collapses to produce its final morphology. (a) During the early stages of the impact the outward propagation of the shock wave and subsequent release wave comprehensively fractures a large region of the target (stippled) and initiates the excavation of the crater. (b) A weakened, mobile region of the target surrounding the crater (grey) enables the onset of collapse, in the form of uplift below the crater and slumping of the walls. The extent of this fluidized region decays with time, effectively freezing the crater morphology in place. In small craters the collapse is frozen before the central uplift gets too high: a central peak crater is formed. (c and d) In large impacts, however, the uplift overshoots the target surface before collapsing back down and out to generate a peak ring.

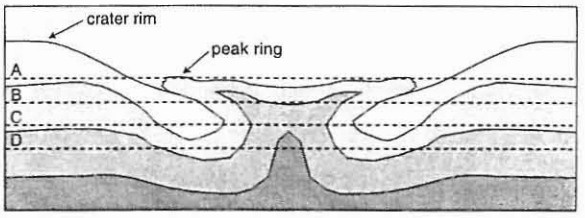

Figure 2 Illustration depicting the subsurface structure of a generic peak ring crater as derived from our simulation results. The dashed lines labeled A-D refer to possible stages in the erosion of an initially fresh crater. Note that the vertical scale has been exaggerated; the illustration has an aspect ratio of 1:2. Thus, the pre-impact thickness of the stratigraphic layers is on the order of D/20, where D is the final crater diameter.

Models of crater collapse have also elucidated the mechanism responsible for the formation of multiple concentric scarps around large impact structures [9]. Simulations based on the ring-tectonic theory [10] have demonstrated that inward flow of a low-viscosity layer (with effective viscosities comparable to that of the weakened material within the transient crater) is an effective way of forming rings around large craters. The mechanism responsible for this low-viscosity behavior and the degree to which it is controlled by the target structure and composition, or the impact process itself, are still not well understood.

Conclusion: Impact modeling has produced a robust paradigm for how complex craters must collapse. However, current models do not provide a complete explanation for why large impact craters collapse in this manner. Developing a complete model for the collapse of large impact craters will, therefore, require close collaboration between impact modelers, and observers. More work needs to be done to: (1) understand better each potential target weakening mechanism; and (2) establish under what conditions each mechanism may be important—does field evidence support one or more weakening mechanism? Collaboration should also concentrate on the testing and refining of numerical models of peak-ring and external-ring formation based on geological observation, geophysical data and drill cores.

References: [1] Dent, B. (1973), *EOS, 54*, 1207. [2] Melosh, H. J. (1977) *Impact and explosion cratering*. 1245-1260. [3] McKinnon, W. B. (1978) *Proc. LPSC IX*, 3965-3973. [4] Melosh, H. J. (1989), *Impact cratering*. [5] O'Keefe, J. D. & Ahrens, T. J. (1993) *JGR, 98*, 17001-17028. [6] Melosh, H. J. and Ivanov, B. A. (1999) *Ann. Rev. Earth Planet. Sci., 27*, 385-415. [7] Collins, G. S., et al. (2002) *Icarus, 157*, 24-33. [8] O'Keefe, J. D. & Ahrens, T. J. (1999) *JGR, 104*, E11, 27091-27104 [9] Turtle, E.P., (1998) *Ph.D. Thesis, Univ. of Arizona*. [10] Melosh, H. J. & McKinnon, W. B. (1978) *Geophys. Res. Lett. 5*, 985-988.

NUMERICAL SIMULATIONS OF SILVERPIT CRATER COLLAPSE: A COMPARISON OF TEKTON AND SALES 2. G. S. Collins, E. P. Turtle and H. J. Melosh, Lunar and Planetary Laboratory, University of Arizona, Tucson, AZ 85721 (Email: gareth@lpl.arizona.edu or turtle@lpl.arizona.edu).

Introduction: SALES 2 and Tekton are two numerical tools that have been used to simulate complex crater collapse [1,2]. SALES 2 is a hydrocode capable of modeling the dynamic collapse of large impact craters. It has been successfully applied to the problem of central peak and peak-ring formation [1]. Tekton is a finite-element code designed to be applied to a wide range of tectonic problems, where displacements are relatively small and the dynamics are less important. It has been used extensively to simulate the relaxation of large craters and the formation of exterior rings in multi-ring basins [2]. Here we apply both techniques to the collapse of the Silverpit crater, to compare and contrast their capabilities.

Silverpit crater: The Silverpit crater is a recently discovered, 60-65 Myr old complex crater, which lies buried beneath the North Sea, about 150 km east of Britain [3]. High-resolution images of Silverpit's subsurface structure, provided by three-dimensional seismic reflection data, reveal an inner-crater morphology similar to that expected for a 5-8 km diameter terrestrial crater. The crater walls show evidence of terrace-style slumping and there is a distinct central uplift, which may have produced a central peak in the pristine crater morphology. However, Silverpit is not a typical 5-km diameter terrestrial crater, because it exhibits multiple, concentric rings outside the main cavity. External concentric rings are normally associated with much larger impact structures, for example Chicxulub on Earth, or Orientale on the Moon. Furthermore, external rings associated with large impacts on the terrestrial planets and moons are widely-spaced, predominantly inwardly-facing, asymmetric scarps. However, the seismic data show that the external rings at Silverpit represent closely-spaced, concentric fault-bound graben, with both inwardly and outwardly facing fault-scarps [3]. This type of multi-ring structure is directly analogous to the Valhalla-type multi-ring basins found on the icy satellites. Thus, the presence and style of the multiple rings at Silverpit is surprising given both the size of the crater and its planetary setting.

The mechanics of Valhalla-type multi-ring basin formation: Theoretical and numerical modeling of multi-ring craters [2,4] suggests that external ring formation is a consequence of the basal drag exerted on a brittle, elastic surface layer by a more mobile substrate as it flows inwards to compensate for the absence of mass in the excavated crater. This model has been further constrained for Valhalla-type multi-ring basins. The formation of closely-spaced, concentric fault-bound graben, appears to require that the elastic upper layer be thin and that the mobile substrate be confined to a relatively thin layer [5,6,7]. This rheologic situation is easily explained in the context of the icy satellites; however, the presence of a thin highly mobile layer just below the surface is not a common occurrence on rocky bodies in the Solar System. In the case of the apparently unique Silverpit structure, it has been suggested that the mobile subsurface layer was caused by the presence of overpressured chalk layers at depth that acted as detachments and expedited bulk inward flow of a thin subsurface layer [3].

Numerical Simulations: We have begun to test the proposed model for the formation of the Silverpit crater using two contrasting yet complementary numerical tools: SALES 2 and Tekton. In both cases, we simulate the gravity-driven collapse of a bowl-shaped transient crater, 1-km deep and 3-km in diameter. We model the target to a radial distance of 20 km and a vertical depth of 10 km to avoid boundary effects. Our models consist of three, originally-horizontal layers, deformed using the Z-model approximation of the excavation flow. The top two layers are assigned appropriate rheologic parameters to represent the brittle upper chalk layer and the lower mobile chalk layer at Silverpit. The bottom layer occupies the remainder of the mesh. We simulate the inner-crater collapse using the acoustic fluidization model for complex crater collapse, where a fluidized region surrounding the transient crater facilitates slumping of the crater wall and uplift of the crater floor [for example 1,2]. We define the viscosity of the acoustically fluidized region to be the same as the viscosity of the mobile chalk layer.

Results: Results from our preliminary simulations suggest that the brittle upper layer must be ~1-km thick in order to reproduce the observed fault patterns and the central uplift. We will present the results of our models and the implications for both Silverpit and the two modeling methods.

References: [1] Collins, G. S., et al. (2002) *Icarus, 157*, 24-33. [2] Turtle, E.P., (1998) *Ph.D. Thesis, University of Arizona*. [3] Stewart, S. A. and Allen, P. J. (2002) *Nature 418*, 520-523. [4] Melosh, H. J. and McKinnon, W. B. (1978) *Geophys. Res. Lett. 5*, 985-988. [5] McKinnon, W. B. and Melosh, H. J. (1980) *Icarus 44*, 454-471. [6] Melosh, H. J. (1982) *JGR 87*, 1880-1890. [7] Allemand, P and Thomas, P. (1999) *JGR E 104*, 16501-16514.

APPLICATION OF ADAPTIVE MESH REFINEMENT TO THE SIMULATION OF IMPACTS IN COMPLEX GEOMETRIES AND HETEROGEOUS MATERIALS. D. A. Crawford[1] and O. S. Barnouin-Jha[2], [1]Sandia National Laboratories, MS 0836, P. O. Box 5800, Albuquerque, NM 87185 (dacrawf@sandia.gov), [2]The Johns Hopkins University Applied Physics Laboratory, Johns Hopkins Rd., Laurel, MD 20723.

Introduction: Adaptive mesh refinement (AMR) has been used for improving computational resolution on hyperbolic problems when resources are limited [1-2]. For a mature Eulerian multi-material shock-physics code like CTH [3], adaptivity is considered a natural next step in code development [4]. Recent work has demonstrated the utility of AMR for studying shock processes in 2-D heterogeneous targets for planetary impact applications [5]. In this study, even more complex targets such as a pre-fractured 433 Eros are being simulated with 3-D AMR (Fig. 1).

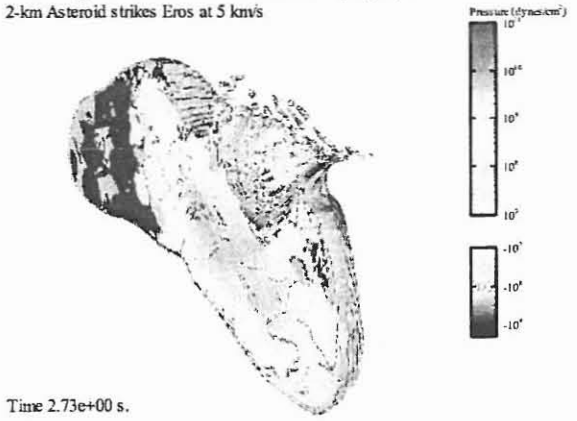

FIGURE 1. AMR CTH simulation of a 2-km dunite asteroid striking Eros at 5 km/s. Eros was constructed of thousands of random dunite spheres and tetrahedra (ρ=3.32 g/cc, C_s=6.65 km/s) with a tuff matrix and surface regolith (ρ=1.83, C_s=1.6 km/s. The density of dunite is comparable to an ordinary chondrite, the best meteoritic candidate for Eros [6]. The final density of the asteroid is 2.7g/cc similar to that measured by the NEAR spacecraft [e.g., 7]. The shape of Eros shown was obtained from data acquired by the NEAR Laser Rangefinder (shape model No. 393) [8]. In this cutaway view, color represents pressure.

Discussion: Adaptive mesh refinement allows us to maintain sufficient resolution across important features, such as the projectile or target grains, yet maintain computational efficiency. A minimum of 20-40 zones across the projectile or target grains is a requirement that has been demonstrated in many studies [e.g., 9]. Prior to AMR, such resolution has only been available for 3-D problems running on the largest parallel computers. With AMR, these calculations can be run on a small cluster of workstations. On large parallel computers, extraordinary resolution and dramatic improvements in problem scaling can be achieved (Fig. 2).

Putting together a good AMR calculation requires an artistry beyond that normally required for traditional "flat mesh" simulations. Indicators for determining regions of the mesh to target for refinement and unrefinement must be developed. CTH allows up to 20 refinement indicators constructed of operators (such as gradient magnitude) and database variables (such as pressure, density or material volume

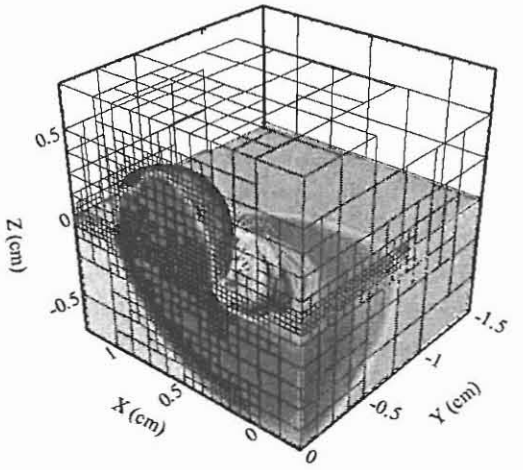

FIGURE 2. Highly oblique impact of ¼" spherical aluminum projectile onto aluminum half-space target. Level 7 adaptive mesh (equal to 160 cells across the projectile diameter) is shown. Block outlines are shown. Color represents pressure. This calculation ran 15 times faster than a comparable resolution non-AMR run.

fraction). In this presentation, we will demonstrate adaptive mesh refinement strategies for several planetary impact applications with an emphasis on understanding shock processes in heterogeneous materials.

We believe that the use of AMR should significantly improve our understanding of the cratering process because one-to-one realistic simulations of laboratory impacts are now possible even on relatively small workstations. Where once it was difficult to run a laboratory scale simulation to completion, AMR puts it within reach. AMR allows more parameter studies that can be run for much longer periods of time than was previously possible. By comparing such investigations with, for example, topographic information on the shape of craters seen on planets and asteroids, additional insights into the cratering process are within reach.

References: [1] Berger, M. J. and J. Oliger (1984), *J. Comp. Phys*, **54**, 484-512. [2] Berger, M. J. and P. Colella (1989) *J. Comp. Phys*, **82**, 64-84. [3] McGlaun, J.M., S.L. Thompson and M.G. Elrick (1990) Int. J. Impact Eng., 10, 351-360. [4] Crawford, D. A., *et al.*, *New Models and Hydrocodes for Shock Wave Processes in Cond. Matter,* Edinburgh, U.K., May 19-24, 2002, (in press). [5] Barnouin-Jha, O.S., M.J. Cintala and D. A. Crawford (2002), *LPS XXXIII*, 1738-1739.[6] Veverka, J. et al., (2000) *Science*, 289, 2088-2097. [7] Yeomans *et al.* (2000), *Science 289*, 2085-2088. [8] Zuber, M. et al., 2000, *Science*, 289, 2097-2101. [9] Pierazzo *et al.* (1997), *Icarus* 127, 408-423.

Acknowledgements: Sandia is a multi-program laboratory operated by Sandia Corporation, a Lockheed Martin Company, for the United States Department of Energy under Contract DE-AC04-94AL85000.

WIRGO in TIC's?
[What (on Earth) is *Really* Going On in Terrestrial Impact Craters?]

Michael R. Dence, 824 Nesbitt Place, Ottawa, Ontario, Canada, K2C 0K1;
(613) 225-3737; Fax (613) 991-6996; e-mail: mrdence@rsc.ca

Abstract

Canada is well endowed with impact craters formed in crystalline rocks with relatively homogeneous physical properties. They exhibit all the main morphological-structural variations with crater size seen in craters on other rocky planets, from small simple bowl to large peak and ring forms. Lacking stratigraphy, analysis is based on the imprint of shock melting and metamorphism, the position of the GPL (limit of initial Grady-Kipp fracturing due to shock wave reverberations) relative to shock level, the geometry of late stage shears and breccias and the volume of shocked material beyond the GPL.

Simple craters, exemplified by Brent (D=3.7km) allow direct comparison with models and experimental data. Results of interest include:

- The central pool of impact melt and underlying breccia at the base of the crater fill is interpreted as the remnant of the transient crater lining;
- the overlying main mass of breccias filling the final apparent crater results from late-stage slumping of large slabs bounded by a primary shear surface that conforms to a sphere segment of radius, $r_s \approx 2d_{tc}$, where d_{tc} is the transient crater depth;
- The foot of the primary shear intersects *above* the GPL at the centre of the melt pool and the rapid emplacement of slumped slabs produces further brecciation while suppressing any tendency for the centre to rise.

In the autochthonous breccias below the melt and in the underlying para-allochthone below the GPL, shock metamorphism weakens with depth. The apparent attenuation of the shock pulse can be compared with experimentally derived rates of attenuation to give a measure of displacements down axis and estimates of the size of a nominal bolide of given velocity, the volume of impact melt and the energy released on impact. In larger complex craters (e.g. Charlevoix, D=52km) apparent shock attenuation is low near the centre but is higher towards the margin. The inflection point marks the change from uplift of deep material in the centre to subsidence of near-surface material at the margins.

From the observed general relationship $P_{GPL} = 3.5\ D^{0.5}$, where P_{GPL} (in GPa) is the estimated level of shock metamorphism at the Grady-Kipp fracture limit, it is apparent that the differential stress due to shock wave reflections weakens at about twice the attenuation rate of the initial shock pulse. Thus, with increasing size, compression of the para-authochthone below the GPL plays an increasingly larger role in controlling the depth of the transient crater and hence the radius of the primary shear. It follows that, where the rate of relaxation of the para-authochthone is more rapid than the propagation of the primary shear from the rim towards the centre, the shear surface intersects *below* the GPL and central uplift occurs.

EXPERIMENTAL MODELING OF IMPACT-INDUCED HIGH-TEMPERATURE PROCESSING OF SILICATES. M.V.Gerasimov[1], Yu.P.Dikov[2], and O.I.Yakovlev[3]. [1]Space Research Institute, RAS, Moscow 117997, Profsoyuznaya st., 84/32, mgerasim@mx.iki.rssi.ru, [2]Institute of Ore Deposits, Petrography, Mineralogy and Geochemistry, RAS, Moscow 109017, Staromonetny per., 35, dikov@igem.ru, [3]Vernadsky Institute of Geochemistry and Analytical Chemistry, RAS, Moscow 117975, GSP-1, Kosygin st., 19, yakovlev@geokhi.ru.

Introduction: Large scale impacts of asteroids and meteorites play an important role in the evolution of planets and their satellites. Pulse input of huge energy during an impact results in noticeable changes in both mechanical and geochemical state of colliding material. The complexity of geochemical processes during an impact suggests experimental modeling as the main tool of its investigation rather than computing approach. On the other side, the modeling of mechanical issues of large scale impacts is mainly a success of computations. We need to have a good cooperation between both computer modeling of mechanical issues of an impact and experimental investigations of geochemical processes to build up a more or less realistic picture of a large-scale impact.

Experimental investigation of high-temperature modification of silicates. Experiments were done by use of hypervelocity gun facilities and laser pulse installation [1]. Some principal effects of high-temperature processing of silicates are:

Formation of clusters during vaporization. Volatilization of elements during impact-induced vaporization proceeds not only as classical volatilization of atoms and oxides but by formation of molecular clusters which can assemble a number of elements with different individual volatility. Experiments prove the formation of "enstatite", "netheline", and "wollastonite" clusters [2,3]. The formation of clusters provides less specific energy of vaporization of silicates compared to that calculated in assumption of total dissociation of materials and must be accounted for in computations.

Noticeable redox processes. The main element of silicates is oxygen which is also mobile during high-temperature processes and provide noticeable redox processes in the system. Experiments indicate simultaneous formation of mainly all possible redox states of elements [4]. Highly oxidized states of elements coexist with their reduced states. Phases of reduced carbon, iron, and other elements can be formed during impacts despite of oxidizing conditions.

Abnormal volatility of refractory elements. Experiments show a rather high mobility of elements which are usually considered as refractory and are accounted for as indicators of parts of different materials during mixing [5]. Among such elements are REE, highly siderophile elements (HSE), and other. The mechanism of abnormal volatility need more investigation but it can be a result of formation of specific clusters. HSE can be mobilized into forming and dispersing metallic iron droplets [6].

Problem of mixing of colliding materials. Chemical composition of forming objects during an impact is the result of mixing of parts from naturally heterogeneous projectile and target materials and also due to selective mobility of elements. The mixing of projectile and target materials does not have sufficient coverage by computing modeling and the estimation of the volume and degree of mixing is still uncertain. Usually, the input of projectile material is considered by an account for of the increase of HSE in impactites and by isotopical considerations. None of methods is strict and can be applied only to individual samples. There is a reasonable deficit of impactites which represents a pure projectile material. Mixing seems to be a valuable factor of modification of projectile material and it should be considered using computing methods. The mechanism of mixing of projectile and target materials probably can be simulated involving Kelvin-Helmholtz and/or Reyley-Taylor instability mechanisms.

Experimental investigation of the possibility of impact-induced formation of so called "pristine" lunar glasses shows that they could be formed by an impact of a chondritic projectile into lunar basalts. The mixing of basaltic and chondritic materials together with high-temperature processing develop impact glasses with the composition similar to lunar "pristine" glasses, which is characterized by: high Mg/Mg+Fe ratio, high Al/Mg ratio, homogeneity, surface correlated volatiles, etc. [7]. The formation of metallic iron drops and their dispersion from high-temperature melts is an important mechanism for depletion of silicate melts in siderophile elements and for formation of agglutinitic glasses.

Acknowledgment. The research was supported by RFBR grant No 01-05-64564.

References: [1] Gerasimov M.V. et al. (1998) *Earth, Moon, and Planets*, *80*, 209-259. [2] Dikov Yu.P., et al. (1994) *LPSCXXV*, 329-330. [3] Yakovlev O.I., et al. (1996) *Geochem. Intern.*, *34*, No. 8, 706-713. [4] Yakovlev O.I., et al. (1993) *Geochem. Intern.*, *30*, No. 7, 1-10. [5] Dikov Yu.P., et al. (1992) *Geokhimiya*, № 2, 291-296 (Rus.). [6] Yakovlev O.I., et al. (2002) *LPSCXXXIII*, #1271 (CD-ROM). [7] Yu.P. Dikov et al. (2001) *LPSCXXXII*, #1559 (CD-ROM).

THERMAL AND DYNAMIC CONSEQUENCES OF IMPACT – LESSONS FROM LARGE IMPACT STRUCTURES. Roger L. Gibson and W. Uwe Reimold, Impact Cratering Research Group, School of Geosciences, University of the Witwatersrand, Private Bag 3, P.O. Wits 2050, Johannesburg, South Africa (E-mail: 065rlg@cosmos.wits.ac.za, reimoldw@geosciences.wits.ac.za).

Introduction: In the early years following the recognition of meteorite impact cratering as an important geological process within the Solar System, impact researchers were largely confined to inferring cratering mechanics from studies of surface crater morphologies and small-scale experiments. With the advent of sophisticated computer-based numerical simulations and high-resolution geophysics, however, researchers have begun to explore more fully the detailed 3-D structure of craters and the processes that give rise to them. This paper examines some of the issues raised by the model simulations from the perspective of the field evidence presented in impact structures, with particular reference to the Vredefort structure in South Africa.

Reality vs simulation: Impact is a short-term catastrophic process driven by the transfer of the kinetic energy of a hypervelocity projectile into a target. At a first-order approximation, the cratering process varies as a function of energy released by the impact – small impacts create simple craters whereas larger events create complex craters with central uplifts, peak rings or multiple rings. Projectiles of varying sizes, densities and velocities can effectively release similar amounts of energy and, thus, create similar structures. Additional levels of complexity can be added by varying, inter alia, the shape of the impactor, the angle of impact, and the structure and composition of the target. To a large extent, numerical simulations have allowed researchers to experiment with a wide range of input parameters and to examine the consequences of changing these variables (e.g. [1], [2]). The question remaining, however, is whether direct observation of impact structures in the field and laboratory-based experimental work can facilitate further refinement of such simulations.

The Vredefort impact structure: The 2.02 Ga Vredefort impact structure in South Africa is the world's oldest impact structure. It may lay claim to being the largest as well, however, substantial erosion (by between 7 and 10 km) has obliterated the original crater rim and impact breccias. Like the similarly large 1.85 Ga Sudbury structure, Vredefort has attracted the attention of numerical modelers (e.g. [3], [4]) in part because the high levels of erosion require indirect estimation of the size of the respective impact events and craters. In the Vredefort structure, the root zone of the central uplift – the ~90-km-wide Vredefort dome – is the best-preserved part, although impact-related structural and hydrothermal effects are evident up to radial distances of at least 100 km from the center, and possibly further afield as well. Shock effects (shatter cones, planar deformation features, high pressure quartz polymorphs and textures suggestive of diaplectic glass and mineral melt formation) are confined to the dome, and display a distribution consistent with a broad increase in maximum shock pressure radially inwards ([5], [6]). A similar broad increase in the grade of shock-induced thermal metamorphism is observed towards the center of the dome ([6]-[8]). In addition, dykes of impact melt and voluminous pseudotachylitic breccias are present in the rocks. Therriault et al. [9] estimated an original crater diameter of 270 to 300 km based on the distribution of the shock features. Henkel and Reimold [10] obtained a similar estimate from geophysical modeling. Numerical simulations by Turtle and Pierazzo [4, 11], however, have suggested a diameter as small as 120-160 km. These scaling simulations used the distribution of common shock effects such as PDFs in quartz, and the distribution of post-shock isotherms, respectively, as a basis for reconstructing the impact crater. Clearly, such a wide discrepancy requires further scrutiny. A critique of the modeling parameters and assumptions is beyond the scope of this paper. Instead, we wish to focus on the geological evidence within impact structures such as Vredefort that can assist in understanding the cratering process.

The problem with impact structures: The fundamental problem with impact structures is that their large-scale order and symmetry disguises the chaotic nature of their constituent features at smaller scales. The heterogeneous nature of shock wave interaction with rocks at the grain scale has long been known from experimental and field studies, yet the principal aim of integrating observational data from partially eroded structures such as Vredefort and Sudbury with simulation results is to obtain a match between the large-scale morphology and the spatial distribution of peak shock isobars and post-shock isotherms, on the one side, and the model results on the other. Model predictions for complex impact structures (e.g., [3], [12]) are that the shock effects are largely confined to the central uplift and that the radial inward movements that accompany central uplift formation modify the original hemispherical pattern of shock isobars into an elongate bulbous shape with a vertical long axis. As post-shock temperatures are directly proportional to the magnitude of the shock, they will display a similar elongate bulbous pattern, enhanced by interaction between the shock heating and the heat already present in the rocks

due to the pre-impact geotherm [3]. At the large scale, results from the Vredefort dome have confirmed the simulation predictions. In fact, Melosh and Ivanov's [12] and Ivanov and Deutsch's [3] results were instrumental in directing geological investigations to the central parts of the dome where the models predicted shock pressures as high as 60 GPa and post-shock temperatures in excess of 1000 °C. Whereas a previous study based on quartz PDFs in the dome by Grieve et al. [13] had been unable to confirm shock pressures of more than 10-15 GPa in these rocks, but had speculated that pressures may have been as high as 25 GPa, these studies confirmed widespread shock metamorphism of feldspars and hydrous ferromagnesian silicates at pressures in excess of 30 GPa and possibly as high as 50 GPa ([5], [6]), and post-shock temperatures of between 1000 and 1350 °C ([6], [8]). These results confirmed Grieve et al.'s [13] original contention that post-shock annealing in the core of the dome had selectively annealed PDFs, rendering the pressure estimation technique useless.

Whilst the modeling predictions and direct observations concur on the broad scale, it is important to note that Ivanov and Deutsch's [3] models are for a 200-250 km diameter structure whereas [4, 11] maintain that they have achieved good agreement with a 120-160 km diameter structure. Apart from the heterogeneous grain-scale response to shock noted from experimental studies and many other impact structures, our group has recently established larger-scale heterogeneity in the formation of pseudotachylite veins in the dome that suggests that shock pressures varied by as much as a factor of 2-3 on scales ranging from millimeters to tens of meters. This finding, which is attributed to complex reflection and refraction of the impact shock wave through the target rocks as a result of preexisting heterogeneities, not only makes the immediate geological context in which samples for "average" peak pressure calculations are chosen of extreme importance, but also questions whether such an "average" pressure approach is realistic. The link between peak shock pressure and post-shock temperature means that this also has implications for "average" post-shock isotherms. Gibson [8] has noted highly variable post-shock metamorphic textures in rocks in the dome and widespread evidence of disequilibrium that confirm localized thermal heterogeneity. A similar conclusion was drawn by [14] from the deep borehole through the Puchezh-Katunki central uplift.

A further issue with estimation of peak shock pressures in impact structures relates to the reliability of shock experimental data in constraining peak shock pressures in natural events. [15] have recently reviewed the problems in extrapolating data from experiments to natural rocks. They caution that, because of the short duration of experiments relative to natural events, and even the design of some of these experiments, threshold pressures for the formation of certain shock effects may be considerable overestimates. Such a breakdown in basic knowledge would have fundamental implications when attempting to use shock isobar patterns to refine numerical simulations.

In addition to the shock and thermal patterns generated by an impact cratering event, numerical simulations are attempting to explain how, on a gross scale, a well-ordered structure evolves. The Vredefort dome provides a rare opportunity to access large areas of rock from deep levels within the central uplift and to test whether models such as acoustic fluidization [12] or the block model [3] can explain central uplift formation. Preliminary data from the dome by our group have failed to identify pervasive block rotation, even where substantial pseudotachylitic melts are likely to have existed during central uplift formation. Most movements appear to reflect late-stage extensional collapse of the structure along faults at a variety of scales. Further from the central uplift, impact-related deformation involves brittle-ductile folding and extensional faulting on scales of tens of meters to kilometers that also appears to be related to the latter stages of central uplift formation.

Summary: At present, numerical modeling of large impact events provides a good first-order indication of the distribution of impact-related features. However, the low spatial resolution of the models (typically of the order of kilometers) hampers full integration of the modeling results with the observed geological features and does not allow the latter to be used to refine model parameters. More work is needed to understand the local-scale interaction between a shock wave and its target rocks to assist resolution of this problem.

References: [1] Pierazzo E. and Melosh H.J. (1999) *EPSL, 165,* 163-176. [2] Ivanov B.A. and Artemieva N.A. (2002) *GSA Spec. Pap., 356,* 619-630. [3] Ivanov B.A. and Deutsch A. (1999) *GSA Spec. Pap., 339,* 389-397. [4] Turtle E.P. and Pierazzo E. (1998) *MAPS, 33,*483-490. [5] Gibson R.L. et al. (2001) *LPS XXXII,* Abstract #1012. [6] Gibson R.L. et al. (2002) *Geology, 30,* 475-478. [7] Gibson R.L. et al. (1998) *Geology, 26,* 787-790. [8] Gibson R.L. (2002) *JMG, 20,* 57-70. [9] Therriault A.M. et al. (1997) *MAPS, 32,* 71-77. [10] Henkel H. and Reimold W.U. (1998) *Tectonophys., 287,* 1-20. [11] Turtle E.P. and Pierazzo E. *Geology,* submitted. [12] Melosh H.J. and Ivanov B.A. (1999) *Ann. Rev. EPS, 27,*385-415. [13] Grieve R.F. et al. (1990) *Tectonophys., 171,* 185-200. [14] Masaitis V. (1999) *MAPS, 34,* 691-711. [15] DeCarli P.S. et al. (2002) *GSA Spec. Pap. 356,* 595-605.

TWO- AND THREE-DIMENSIONAL SIMULATIONS OF ASTEROID OCEAN IMPACTS. G. Gisler, R. P. Weaver, C. L. Mader[1] and M. L. Gittings[2], [1]Los Alamos National Laboratory, MS T087, Los Alamos NM 87545 USA, [2]Science Applications International MS T087, Los Alamos NM 87545 USA

We have performed a series of two-dimensional and three-dimensional simulations of asteroid impacts into an ocean using the SAGE code from Los Alamos National Laboratory and Science Applications International Corporation. The SAGE code is a compressible Eulerian hydrodynamics code using continuous adaptive mesh refinement for following discontinuities with a fine grid while treating the bulk of the simulation more coarsely. We have used tabular equations of state for the atmosphere, water, the oceanic crust, and the mantle. In two dimensions, we simulated asteroid impactors moving at 20 km/s vertically through an exponential atmosphere into a 5 km deep ocean. The impactors were composed of mantle material (3.32 g/cc) or iron (7.8 g/cc) with diameters from 250m to 10 km. In our three-dimensional runs we simulated asteroids of 1 km diameter composed of iron moving at 20 km/s at angles of 45 and 60 degrees from the vertical. All impacts, including the oblique ones, produce large underwater cavities with nearly vertical walls followed by a collapse starting from the bottom and subsequent vertical jetting. Substantial amounts of water are vaporized and lofted high into the atmosphere. In the larger impacts, significant amounts of crustal and even mantle material are lofted as well. Tsunamis up to a kilometer in initial height are generated by the collapse of the vertical jet. These waves are initially complex in form, and interact strongly with shocks propagating through the water and the crust. The tsunami waves are followed out to 100 km from the point of impact. Their periods and wavelengths show them to be intermediate type waves, and not (in general) shallow-water waves. At great distances, the waves decay faster than the inverse of the distance from the impact point, ignoring sea-floor topography. For all impactors smaller than about 2 km diameter, the impacting body is highly fragmented and its remains lofted into the stratosphere with the water vapor and crustal material, hence very little trace of the impacting body should be found for most oceanic impacts. In the oblique impacts, the initial asymmetry of the transient crater and crown does not persist beyond a tsunami propagation length of 50 km.

OBSERVATIONS OF THE TERRESTRIAL IMPACT CRATERING RECORD

R.A.F. Grieve, Earth Sciences Sector, NRCan, 588 Booth Street, Ottawa, ON K1A 0Y7, CANADA. (rgrieve@nrcan.gc.ca)

Introduction: The currently known terrestrial record of impact cratering stands at over 160 impact structures and several new examples are identified each year (1). The record, however, is a biased sample of an originally much larger population, favoring younger, larger structures in geologically stable areas of the Earth's continental crust. The largest and oldest known structures are limited to diameters of ~ 250-300 km and ages of < 2 Ga. Care must be taken, therefore, in making generalised statements regarding the record with respect to such time-integrated effects as variations in cratering rate, periodicities, etc. (e.g., 2). The terrestrial record, however, does provide cumulative observations of aspects of the cratering process and is the only available source of ground truth with respect to the structural and lithological results of large-scale natural impact events.

Some critical observations: Although attribution is often open to dispute, it is clear that detailed studies at a select number of terrestrial impact structures have provided important boundary constraints on aspects of cratering processes. Impact craters are three-dimensional structures and the ability to drill and recover core, to conduct multi-parameter geophysical surveys and to observe impact craters of similar size and morphology at different erosional levels is the ultimate strength of the terrestrial record. Concepts such as transient cavities formed by excavation and displacement and the collapse of transient cavity walls in simple craters have resulted (e.g., 3). Similarly, the confinement of significant excavation to only the central volume, with the structural preservation of near-surface lithologies exterior to this volume and the structural uplift of originally deeper-seated lithologies in the center of complex structures can be traced, in large part, to detailed and repeated observations of terrestrial impact craters (e.g., 4). Similarly, effects associated with shock metamorphism of various rock types and how its manifestation can differ (e.g., in porous targets) preceded and moved in parallel with shock-recovery experimentation. Observations have been particularly useful in understanding the effects of shock loading in the upper range of experimentally generated shock stresses, such as those leading to impact melting (e.g., 5).

Some less certain observations: Morphometric relations for terrestrial structures have been defined but are subject to considerable uncertainty, due to the effects of erosion and the statistics of small numbers (4). While it is only the more pristine terrestrial examples that can be used to define morphometries, the situation is exacerbated by the fact that many terrestrial impact craters have been studied in insufficient detail or without modern understanding of impact processes. In some cases, the literature is confined essentially to the "discovery" publication or dates from pre-Apollo to periods between Apollo missions, which were a major driver for the study of terrestrial impact structures. The impetus provided by the Apollo program has been replaced to some degree by economic and biosphere drivers. In the

U.S., government funding for studies at terrestrial impact structures appears to fall between the responsibilities of both NASA and NSF. This has tended to favor modelling studies at the expense of field work. It is clearly less costly to engage in modelling studies, but how can we, as a community, evaluate the veracity of the models without observational data from the field? (e.g., 6,7). Experimental data will not suffice to fill this gap, as there are problems with scale and understanding of the physical properties of the relevant materials, despite innovative procedures to compensate for them (e.g., 8). It is true, however, it is easier to connect observational data to later-time cratering processes because that is what they more closely reflect, representing as they do the end of the cratering process. Conversely, modeling has traditionally focussed on more early time processes in cratering events. Clearly, there are opportunities for closer partnerships of observational and modeling studies. The probem, however, is often that no one wants to be the bridesmaid!

Some closing thoughts on observations: We are very much prejudiced by the appearance of fresh lunar craters. It is the database with which we are most familiar regarding crater morphology. It is a fact, however, that some of the younger (fresher) complex craters on Earth (e.g., Ries, Haughton, Zhamanshin) do not have an emergent central peak, yet other, albeit buried, structures do (e.g., Boltysh, Moljnir). This begs a very fundamental question: Why? At first glance, it would appear to be a target effect, with the latter formed in crystalline targets and the former in mixed targets. There is also the question of the occurrence of ring or multi-ring basins on Earth (e.g., 9). Several structures have been "proposed" as ringed basins — Manicouagan, for instance. The question is, however, are these rings erosional artefacts? Among the larger structures is Chicxulub – again proposed as a ring structure — but it is buried and inferences rely upon (sometimes conflicting) interpretations of geophysical data (e.g., 10). Drilling at Chicxulub to date has served little to address this problem. Sudbury is also often portrayed as a terrestrial example of a multi-ring basin. There are rings of pseudotachylite, or so the limited pattern of exposed outcrops suggests (e.g., 11). If these do, in fact, exist, what is their relation to the megascarps in lunar basins? Model calculations, albeit simplistic, suggest that the high-gravity environment of Earth will not necessarily produce basins in the same size range as the large multi-ring basins of the moon, due to the increased relative proportion of impact melt to cavity volume on Earth.

References: (1) www.unb.ca/passc/ImpactDatabase. (2) R. Grieve (2001) In *Accretion of Extraterrestrial Material throughout Earth's History*, Kluwer, 379-399. (3) M. Dence *et al.* (1977) In *Impact and Explosion Cratering*, 247-276, Pergamon. (4) R. Grieve & M. Pilkington (1996) *Jour. Aust. Geol. Geophy.* **16**, 399-420. (5) J. Whitehead *et al.* (2002) *MAPS* **37**, 623-647. (6) A. Therriault *et al.* (1997) *MAPS* **32**, 71-77. (7) E. Turtle and E. Pierazzo (1998) *MAPS* **33**, 483-490. (8) K. Housen *et al.* (1999) *Nature* **402**, 155. (9) R. Grieve & A. Therriault (2000) *Ann. Rev. Earth Planet. Sci* **28**, 305-338. (10) J. Morgan *et al.* (2002) GSA Sp. Pap. 356, 39-46. (11) J. Spray & L. Thompson (1995) *Nature* **373**, 130-132.

ANTIPODAL HOTSPOTS ON EARTH: ARE MAJOR DEEP-OCEAN IMACTS THE CAUSE? J. T. Hagstrum, U. S. Geological Survey, 345 Middlefield Road, MS 937, Menlo Park, CA 94025, jhag@usgs.gov.

Introduction: Hotspot volcanism on Earth is restricted to relatively small areas, on the order of 100 km in diameter, and is generally believed to result from narrow upwellings of hot mantle material called 'plumes'. At first glance, hotspots appear randomly distributed. General associations with geoid highs and divergent plate margins have been noted [1], and hotspots tend to occur in provinces separated by spotless areas [2]. Matyska [3] investigated angular symmetries of hotspot distributions, and showed that the highest maxima were obtained with 180° rotations. Rampino and Caldeira [4] also conducted a statistical analysis of large and small data sets and found that more hotspots occur as nearly antipodal pairs than would be expected from random distributions.

The rise of antipodal plumes from the core-mantle boundary through a convecting mantle seems unlikely, but axial focusing of an impact's energy by the spherical Earth might underlie the antipodal pairing of hotspots. Such a focusing mechanism has been proposed to explain seismically disrupted terrains antipodal to major impact basins on the Moon and Mercury [5], and to have formed fractured crust on Mars opposite the Hellas basin—perhaps later exploited as a conduit for volcanism at Alba Patera [6]. First-order problems with this model for Earth, however, include the expected low seismic efficiency of impacts [5] and the lack of any volcanic features opposite large continental impact structures (e.g. Chicxulub).

Antipodal Hotspots: Although as many as 122 hotspots have been proposed [7], the number most commonly discussed is between 40-50. In a compilation of hotspots totaling 57 from 3 different published lists [8-10], 30 form antipodal pairs (~53%) with angular distances ranging from 167° to 178°. Deviations from 180° might be explained by an observed drift rate between hotspots of ~10-20 mm/yr [11].

One test of antipodal formation due to impact and focusing of seismic waves is to determine whether hotspots of a given pair began simultaneously. Tectonic recycling of oceanic crust, however, has made this impossible for most of the older pairs. For a few younger pairs, the initiation ages are basically contemporaneous. Both Roratonga and Tibesti (177°) are Quaternary in age; Kerguelen and the Columbia River basalts (Yellowstone; 175°) are early Miocene in age; the Marquesas hotspot track and Ethiopian flood basalts (Afar; 178°) are ~30 Ma in age; and the Balleny track indicates an age >40 Ma consistent with Iceland's (177°) age of ~50 Ma.

The hotspot pairs can be uniformly divided between those associated with flood basalts and rifting (e.g., Afar), and those having oceanic affinities which are not (e.g., Maquesas). It is hypothesized that oceanic hotspots might represent impact sites and those associated with more voluminous volcanism the antipodal sites. Moreover, the geographic distribution of a large (122) hotspot compilation [7] shows that hotspot provinces are generally opposite oceans and that spotless areas are opposite continents [2].

Deep-Ocean Impacts: If these observations are correct, what process would cause oceanic impacts to form hotspot pairs, and continents to apparently shield their formation? A signigicant distinction between continenal and oceanic impacts is the formation of a high-pressure steam cloud above the oceanic impact site [12]. The pressure of the steam cloud might 'cap' the explosive release of energy from the seafloor impact, causing significantly more energy to be directed downwards—ultimately becoming seismic waves focussed at the antipode.

A simple analogy is the surface blasting technique for secondary rock breaking known as 'mudcapping'. Mudcapping works due to the impulse action of explosives, which is proportional to the detonation pressure and its time of application on a rock burden [13]. A mudcap maintains the impulse pressure over a longer period of time, and the coupling effect depends partly on the amount of mudcap being used. In contrast, most of the energy released in a continental impact would be directed upward and away from the land surface resulting in a much lower seismic efficiency.

Conclusions: Although few impacts in the deep oceans are known, these events might have important consequences in the formation of hotspots, flood basalt provinces, and the breaking up of continents on Earth. Moreover, oceanic impacts and continental flood basalts could be the cause of global mass extinctions. Few models of deep-ocean impacts have been made, and it is suggested that a needed modification is the consideration of pressure effects from the steam cloud above on energy release from the seafloor impact below.

References: [1] Jurdy D.M. and Stefanick M. (1990) *GRL, 17*, 1965-1968. [2] Vogt P.R. (1981) *JGR, 86*, 950-960. [3] Matyska C. (1989) *EPSL, 95*, 334-340. [4] Rampino M.R. and Caldeira K. (1992) *GRL, 19*, 2011-2014. [5] Schultz P.H. and Gault D.E. (1975) *The Moon, 12*, 159-177.[6] Williams D.A. and Greeley R. (1994) *Icarus, 110*, 196-202. [7] Burke K.C. and Wilson J.T. (1976) *Sci. Am., 235*, 46-57. [8] Duncan R.A. Richards M.A. (1991) *Rev. Geophys., 29*, 31-50. [9] Crough S.T. and Jurdy D.M. (1980) *EPSL, 48*, 15-22. [10] Richards M.A. et al. (1988) *JGR, 92*, 7690-7708. [11] Molnar P. and Stock J. (1987) *Nature, 327*, 587-591. [12] Melosh HJ. (1982) *GSA Spec. Pap. 190*, 121-127. [13] Cook M.A. (1958) *Am. Chem. Soc. Monogr., 139*, 278-279.

MAGNETIC FIELDS OF LUNAR IMPACT BASINS AND THEIR USE IN CONSTRAINING THE IMPACT PROCESS.
J.S. Halekas, R.P. Lin, *Space Sciences Laboratory, University of California, Berkeley CA 94720 (email: jazzman@ssl.berkeley.edu).*

Measurements by the Magnetometer/Electron Reflectometer instrument on the Lunar Prospector spacecraft, which completed its mapping mission in 1999, have been used to construct the first completely global maps of lunar crustal magnetic fields. Now, for the first time, we have a data set with global coverage and a sensitivity and resolution which allow us to investigate the magnetic fields of lunar impact basins and craters. As on the Earth, impact sites have a variety of magnetic signatures associated with them, ranging from nearly complete demagnetization to strong central magnetic anomalies. Observations of the magnetic fields of terrestrial basins have been used to make inferences about the impact process, and we wish to show that lunar observations can also provide valuable constraints.

It is clear that we can not achieve the same kind of magnetic field data coverage of lunar basins with measurements from orbit that we can for terrestrial basins using ground magnetometer or aeromagnetic data. Furthermore, lunar missions have only returned a limited number of samples of actual magnetized crustal rocks, while on the Earth we can study as many samples as one could wish. Therefore, one might wonder why lunar data should be used at all, when terrestrial data has these clear advantages. However, the Moon has several key advantages over the Earth for this type of study. First and foremost, the Moon currently has no global magnetic field. This means that we do not have to subtract off a huge global field when measuring local crustal fields, nor do we need to deal with induced magnetic fields. Instead, we can be sure that the signal we measure is purely due to remanent magnetization in the local crustal rocks. Furthermore, on the Earth impact basins formed in the presence of a strong ambient magnetic field. On the Moon, on the other hand, at least the younger basins and craters appear to have formed with no significant ambient magnetic field present. This means that we can more easily determine the demagnetization effects of these impacts.

Studies of terrestrial impact basins have revealed many basin-associated magnetic anomalies [1]. These range from short-wavelength anomalies with a radial extent of a fraction of the transient cavity radius (e.g. Manicougan [2]), to larger groups of anomalies which fill most of the transient cavity region (e.g. the outer ring of anomalies in the Chicxulub basin [3]). The more localized anomalies have generally been ascribed to shock remanence (SRM) or other processes in the central uplift region, while more extensive anomalies have been interpreted as thermal remanent magnetization (TRM) in impact melt rocks. Many lunar basins and craters also display central magnetic anomalies, with the older large (> 200 km in diameter) craters and basins having the most significant anomalies. These anomalies roughly fill the transient cavity region, and therefore by analogy with terrestrial basins, may be due to TRM in impact melts. If this is the case, these anomalies indicate the location of the most substantial amounts of impact melt in lunar basins. On the other hand, if they are instead due to SRM in uplifted materials, they could be used to delineate central uplift structures in multi-ring basins.

Earlier work has shown that many lunar impact craters and basins, especially the youngest ones, are demagnetized with respect to their surroundings [4]. This is also true of many smaller terrestrial craters [1,5]. However, for younger lunar impact sites, demagnetization is especially clear, probably because there were no strong ambient magnetic fields present at the time of these impacts. The demagnetization of lunar craters and basins has been found to extend well beyond the main rims of these structures, which provides strong evidence that impact-generated shock is mainly responsible for demagnetizing the crustal rocks [4].

The physical mechanism of shock demagnetization is still not particularly well understood. However, laboratory measurements of shock demagnetization of both lunar and terrestrial rocks have been performed [6,7,8]. The degree of demagnetization is, in general, dependent on the peak shock pressure and on the remanent coercivity of the crustal magnetization, and laboratory experiments have roughly quantized this relationship for terrestrial basalts [6]. The returned lunar samples show a wide variety of magnetic coercivity spectra. However, lunar breccias tend to carry the strongest remanence, and we have therefore constructed average coercivity spectra for various sets of breccias [9,10]. By combining coercivity spectra with impact demagnetization data and experimental shock demagnetization results, we have attempted to derive the radial peak shock pressure attenuation. Our preliminary results imply peak shock pressures at the transient cavity rim of 2 Gpa and power law attenuation with a power of -2 to -3. These results are consistent with modeling [11] and shock pressure reconstructions from terrestrial basins [12].

We believe that the magnetic fields of lunar impact craters and basins can provide important information about the impact process. Though performing this work with lunar rather than terrestrial data has some drawbacks, there are also clear advantages. So far, our results are encouragingly consistent with terrestrial observations and modeling.

REFERENCES: [1] Pilkington and Grieve, *Rev. Geophys., 30*, 161-81, 1992. [2] Coles and Clark, *J. Geophys. Res., 83*, 2805-8, 1978. [3] Pilkington and Hildebrand, *J. Geophys. Res., 99*, 13147-62, 1994. [4] Halekas *et al., Geophys. Res. Lett., 29, 10.1029/2001GL013924*, 2002. [5] Scott *et al., Meteorit. Planet. Sci., 32*, 293-308, 1997. [6] Pohl *et al., J. Geophys., 41*, 23-41, 1975. [7] Cisowski and Fuller, *J. Geophys. Res., 83*, 3441-58, 1978. [8] Cisowski *et al., Proc. Lunar Planet. Sci. Conf., 6*, 3123-41, 1975. [9] Gus'kova *et al., Cosmic Research, 12*, 680-8, 1974. [10] Fuller, *Rev. Geophys., 12*, 23-70, 1974. [11] Ahrens and O'Keefe, in *Impact and Explosion Cratering* ed. Roddy, Pepin, and Merrill, 639-56, 1977. [12] Robertson and Grieve, in *Imp. and Exp. Crat.*, 687-702.

PYROCLAST FLOWS AND SURGES: POSSIBLE ANALOGY FOR CRATER EJECTA DEPOSITION. H. Hargitai[1], A. Kereszturi ([1]Dept. of Physical Geogr., Email: hargitai@emc.elte.hu, Dept. of Physical and Historical Geol., Eötvös Loránd University of Sciences, H-1083 Budapest, Ludovika tér 2., Email: krub@freemail.hu)

Introduction: We analyse a possible modell of the crater ejecta development and deposition with pyroclastic flows and surges. Because several of their characteristics and depositional structures are known and observable on the Earth it is useful to try to find resembling phases of the crater ejecta formation.

The modell: We analyzed similarities and differences of physical parameters between pyroclastic flows and crater ejecta formation. At volcanic eruptions the p, T are lower than at the moment of impact. In the origin of the pyroclastic flows we can analyse the physical circumstances at really explosive eruptions like Krakatoa-type eruptions too. The 1st seconds of the impact – contact/compression stage (CC), the kinetic energy is transfered to the rock by schock waves. In our analogy we ignore this phase because the differences are too large. The original energy is lost fast because of the expanding shock front and the conversion of the energy to heat, rock deformation etc. When the pressure drops to 1-2 GPa it behaves like normal seismic waves. [1] Heat melts the projectile and target rock layers, which is mixed to partly melted and brecciated target rocks.

At the end of the excavation stage [E] the ejecta material (the near surface ejecta curtain) falls out of the rim of the crater and its material flows away and settles down. At pyroclastic flows and surges originally high central pressure formed the fragments which later was transported by gravity at slopes. At a crater formation the impact explosion gas schock waves, reflected waves drive the upward movement of the debris. We can use the analogy at that point where the effect of the central pressure is lower and gravity driven current movement is important. Our analougue is best in the modification [M] stage when the transient crater reached its final dimensions and no more material is ejected. The ejecta blanket is now "in the air" and starts falling down. From this point the physical parametrs of this material is more or less similar to the ones in a volcanic eruption. By this time, the crater rim is higher then the surroundings so there is a slope corresponding to a volcanic dome that makes the flow movement possible.

In pyroclastic structures several distinct layers are identifiable. A crater ejecta structures can be taken as one cycle of a pyroclastic structure. The cratering process is ended after the solid materials fell down, with the finer particles gravitational settleing and the fallout of the solidified materials that were vapourized during the impact. The resulting distal ejecta can be extended to a global scale. These later stages are also analogues to the volcanic eruptions.

Characteristics	Pyroclastic flows	Pyroclastic surges	Crater ejecta emplacement
Temperature	900-1100 K and lower	900-1100 K and lower	1000-2000 K and lower
Pressure	first in the order of Mpa, later near to the atmospheric	firstly in the order of MPa, later near to the atmospheric	first [CC] in the order of GPa, later [M] nearly near to the atmospheric
Fragments	Mostly solid with gas and very few liquid phase	large gas content with lower solid matter ration	Solid phase and gas, with more plastic components (melts) Melts from projectile/target, solid rocks from target area, vapourized gas from projectile/target
Depositional structures	Poorly sorted and bedded, graded basal zone, trains of large fragments, alternating coars to fine graded layers, oriented fragments, at pumice inverse grading	laminated, cross bedding, lenses of well-sorted-rounded pumice lapilli, better sorted, no very fine and very coarse fractions	Fallout partly influenced by flowing movements
Driving force	gravitational induced movement on slopes	gravitational induced movement on slopes	first the gas pressure of the explosion [E], later gravitational induced motion on slope
Topography	relative high slope angle	relative high slope angle	nearly no originally slope, only in the late phase of the deposition low slope angle (from the rim)
Origin	collapse of the ejecta containing (sometimes km high) gas column above the central vent	mostly explosion driven fallout of ejecta, and later the collapse of shorter gas driven explosion column	fallout (ejecta) from the central explosion
Duration of material upload	several hours/days?		Few seconds
Source of gas content	eruption column; outgassing of melt	eruption column; outgassing of melt; water of crater lake	vapourized projectile (if comet, more) or rock, in situ ground- or surface water or ice; outgassing of melt; On Venus: atmosphere
Speed	ejected material: 200-600 m/s; flow: 100-200 km/h	flow: 100-200 km/h	ejected material: 500 to several 1000 m/s

Comparison of flows, surges, crater ejecta

It is a question whether there is an eruption column at the impact site. In the case of volcanoes, the eruption column is supported by the continuos gas thrust from the crater which is not the case at impacts where the process takes place for few seconds. Observations of nuclear explosion tests show both eruptive coloumns and gasious flows just like surges too. [3] The ejecta blanket is partly fluidized by water.

The atmosphere is important with its pressure for the gas content inside the pyroclastic flow. At the crater ejecta in the depositional phase the difference between the atmospheric and the internal pressure is relative low – just like at a pyroclastic flow. Because pyroclastic structures are known from airless body our analogy can be used at the crater ejecta deposition on airless bodies, eg. on moons. Higher gas content cab make fluidization. On Venus, the long-run ejecta flows were spread in a fluid manner, extending beyond the continous ejecta, moving on a fluidized "bed" which are linked to impact melts, impact angle [2] and dense atmosphere.

Conclusion: In the late phase of the crater ejecta formation pyroclastic flows can be used as an analogy in the analysis of physical circumstances in the flow (flow regime, temperature, gas content, ration of liquid phases). The depositional structures can suggest to the density of the debris and fallout style/time.

References: [1] B.M. French: Traces of Catastrophe LPI Contribution No. 954. [2] W.B. McKinnon et al. (1997): Cratering on Venus: Models and Observations in Venus II. Geology, Geophysics, Atmosphere, and Solar Wind Environment. UAP. [3] J.G. Moore (1998): Base surge in recent volcanic eruptions. Bull. Volc. 30, 337-363, ref. in: D. Karátson: Volcanology. ELTE.

THICKNESSES OF AND PRIMARY EJECTA FRACTIONS IN BASIN EJECTA DEPOSITS. Larry A. Haskin and William B. McKinnon, Department of Earth and Planetary Sciences and McDonnell Center for the Space Sciences, Washington University, One Brookings Drive, St. Louis, MO 63130; lah@levee.wustl.edu, mckinnon@levee.wustl.edu

We have developed a model for production of basin ejecta deposits to address provenances of materials collected at the Apollo and Luna landing sites and for consideration in interpreting remote sensing data [1].

Model Steps: **1)** We take the cumulative mass (m) distribution of primary ejecta fragments ("PriFrags") to vary as $m^{-0.85}$ everywhere, with a maximum PriFrag mass (which can vary with ejection velocity) [e.g., 2, p. 91]. **2)** Ejecta mass is distributed according to [3]. We map their results, for a flat surface, onto a spherical one using ejecta velocities and an assumed launch angle. **3)** Given the surface density of PriFrags of each size falling in the vicinity of the site of interest, we use Schmidt-Holsapple scaling to obtain the sizes of secondary craters. We assume *excavated* volumes of those craters have a depth/diameter ratio of 0.1. **4)** We calculate the probable range of ejecta deposit thickness and % of PriFrags in the deposits, and express them as the fraction of the area at the site of interest. We define "Coverage Level" (CL) as the fraction of that area excavated by craters of a specific size *or larger*. **5)** Beginning with the cavity produced by the largest PriFrag to excavate at a location, we consider how much additional substrate is excavated by the smaller PriFrags that land on or near that spot. We calibrate to deposit thicknesses surrounding Orientale [4] and the Ries [5]. Results suggest that the total excavation by all secondary craters at a specific position corresponds roughly to a right cylinder with the same diameter and 3 times the depth of the largest crater to affect that position.

General Model Results: Ejecta deposit thickness decreases with distance to ~3500 km followed by a modest increase on the anti-basin hemisphere due to ejecta convergence. The fraction of PriFrags in the ejecta deposits shows a similar pattern. Differences due to varying ejection angle from 35° to 55° (to the horizontal) are not substantial.

Apollo 16 Landing Site: Fig. 1a shows the range of deposit thicknesses expected in the vicinity of the Apollo 16 site ~1600 km from the center of Imbrium. Thickest deposits are produced where the largest PriFrags excavate; at higher coverage levels, relatively smaller PriFrags have excavated. Locations where different deposit thicknesses occur are not known, as the impact points of all PriFrags are random. Thus, some half of the vicinity of the site has ejecta deposits ≥1 km or so. From Fig. 1b, the fraction of PriFrags in the deposits is not sensitive to coverage level.

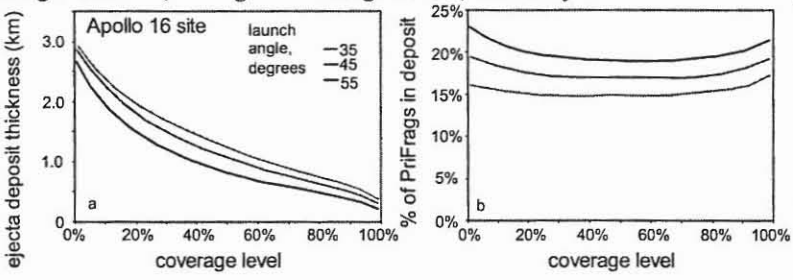

Estimated deposit thicknesses at the Apollo 16 site are reasonable as determined by criteria such as crater fill and fraction of Th-rich ejecta presumed delivered to the site by the Imbrium event from the Procellarum KREEP Terrane [6]. In contrast to conclusions of other studies [7,8], our modeling suggests that all materials sampled at the site, including North Ray Crater ejecta, are more likely part of the Imbrium deposit than part of a primary Nectaris deposit. The Imbrium deposit is estimated to consist of 18% Imbrium ejecta, 21% Serenitatis ejecta, 19% Nectaris ejecta, and 40% pre-Nectarian substrate, with only minor contributions from Humorum, Crisium, and later, Orientale. These materials may not be well mixed; large blocks from different provenances could presumably survive in some locations. The presence of significant Serenitatis materials at the Apollo 16 site has been discounted owing to lack of compelling photogeologic evidence [9, Fig. 10.39; 10, Fig. 10.25].

Concerns: Our model does not reproduce observed densities of secondary craters (it predicts too many) or the largest ones at Copernicus, Orientale, or Imbrium. Mutual obliteration and contributions from "spall" fragments may be responsible, respectively [cf. 11]. Nevertheless, thick deposits should have been produced at great distances from basin impact sites, and these deposits should consist of mixtures of primary ejecta and megaregolith produced by previous large impact events. How thick, however, depends on scaling parameters and factors that are still poorly known. These will be discussed. This work supported by NASA grant NAG5-10458.

References: [1] HASKIN ET AL. (2003) *MAPS*, in press; [2] MELOSH H.J. (1989) *Impact Cratering*, Oxford; [3] HOUSEN ET AL. (1983) *JGR* **88**, 2485–2499; [4] MOORE ET AL. (1974) *Proc. LPSC* **5th**, 71–100; [5] HÖRZ, F. ET AL. (1983) *Rev. Geophys. Space Phys.* **21**, 1667–1725; [6] JOLLIFF B. L. ET AL. (2000) *JGR* **105**, 4197–4216; [7] SPUDIS P. D. (1993) *The Geology of Multi-Ring Impact Basins*, Cambridge; [8] STÖFFLER D. ET AL. (1985) *JGR* **90**, suppl. C449–C506; [9] WILHELMS D. E. (1987) The Geologic History of the Moon, *USGS Prof. Paper* **1348**; [10] SPUDIS P. AND PIETERS C. (1991) in *Lunar Sourcebook*, G. Heiken et al. (eds.) Cambridge; [11] VICKERY A. M. (1987) *GRL* **14**, 726–729.

CONSTRAINTS ON THE IMPACT PROCESS FROM OBSERVATIONS OF OBLIQUE IMPACTS ON THE TERRESTRIAL PLANETS. R. R. Herrick and K. Hessen (Lunar and Planetary Institute, 3600 Bay Area Blvd., Houston, TX 77058; Herrick@lpi.usra.edu).

Introduction: Recently there have been significant advances in both experimental and numerical modeling techniques that hold promise for providing details on how the cratering process is affected by impact at a nonvertical angle [1,2]. Anectdotal observations of craters on the terrestrial planets validated initial experimental efforts [3,4]. Recent and ongoing systematic characterizations of craters reslting from oblique impact on the Moon, Mars, and Venus provide important constraints for the detailed modeling efforts currently being conducted [5,6,7].

Observations: Pertinent observations from surveys conducted to date are:

- The general variation in ejecta pattern and crater shape with decreasing impact angle on the moon matches well with experimental work conducted in a vacuum. On the moon the following transitions occur with decreasing impact angle with respect to horizontal: < ~50 degrees, the ejecta blanket becomes asymmetric; < ~30 degrees, a forbidden zone develops in the uprange portion of the ejecta blanket, and the crater rim is depressed in that direction; < ~20 degrees, the rim topography becomes saddle-shaped, or depressed in both uprange and downrange directions; < ~15 degrees, the rim becomes elongated in the direction of impact and the ejecta forms a "butterfly" pattern in the crossrange direction [5].
- In agreement with experimental work, the presence of an atmosphere significantly increases the onset angle of oblique impact phenomena in the ejecta pattern [5]. No downrange forbidden zone occurs at low impact angles [4].
- Our preliminary work with Martian craters shows that the change in ejecta pattern with decreasing impact angle closely resembles that of the moon, with the development of uprange and then downrange forbidden zones with decreasing impact angle. While the transition angles to different ejecta patterns are generally similar on the moon and Mars, the development of a forbidden zone in the uprange direction occurs at a significantly higher impact angle on Mars than the moon.
- The transition to elliptical craters and a butterfly ejecta pattern occurs at a higher angle on the planets than in early experimental work [3,5,6].
- Adequate data on crater wall topography of oblique impacts currently only exist for the moon. Unlike in experimental work, there is no strong evidence of uprange steepening of the crater wall for oblique impacts [5]. Internal slopes for lunar craters appear largely independent of impact angle. However, interior crater wall slopes approach the angle of repose, and post-impact slumping to a uniform slope cannot be ruled out.
- There is minimal evidence that central structures are offset in any direction relative to the crater rim [7], nor could we find observations in imagery that were indicative of the point of impact.

Constraints on the Impact Process: The observations suggest the following constraints on modeling efforts of the impact process:

- That the ejecta pattern is more affected by oblique impact than the final crater shape suggests near-field versus far-field effects; material ejected from near the point of impact "sees" the impact angle the most.
- Modeling of ejecta emplacement in an atmosphere must consider the disturbance of the atmosphere by the incoming projectile.
- Whatever causes the higher onset angle for elliptical craters and butterfly ejecta on the planets relative to past experimental work, those causes are only important at the lowest impact angles.
- The lack of variation for interior shape and slope suggests that the cross-section of stream tubes for late-stage excavation does not vary with impact angle.
- Mars is clearly below the threshold for the atmospheric disturbance caused by the incoming projectile to have a significant effect on ejecta emplacement.
- While subsurface features may reflect the initial point of impact, observable surface features do not. In other words, while the shock level of the rocks can be modeled as strongly direction-dependent, final crater shape must not be (with exception of rim elevation).

References: [1] Pierazzo E. and Melosh H. J. (2000) *Ann. Rev. Earth Plan. Sci., 28,* 141-167. [2] Schultz P. H. et al. (2000) *LPS XXXI,* Abs. #1902. [3] Gault D. E. and Wedekind J. A. (1978) *Proc. LPSC 9th,* 3843-3875. [4] Schultz P. H. (1992) *JGR, 97,* 16,183-16,248. [5] Herrick and Forsberg (2002) submitted to *Met. and Plan. Sci.* [6] Bottke W. F. et al. (2000) *Icarus, 145,* 108-121. [7] Ekholm A. G. and Melosh H. J. (2001) *GRL, 28,* 623-626.

LINKING EXPERIMENTAL MODELLING OF IMPACT CRATERS TO STRUCTURAL COMPONENTS OF THE REAL THING. A. R. Hildebrand[1], [1] Department of Geology and Geophysics, 2500 University Drive NW, University of Calgary, Calgary, AB T2N 1N4 (hildebra@geo.ucalgary.ca)

Introduction: Impact crater scaling relationships, such as for impact energy, are usually derived solely from experimental impact or explosion craters [e.g., 1]. Relating craters to a suite of possible source projectiles, and predicting what size crater a given impactor will produce in a surface of known composition, are basic requirements for reconstructing impactor populations from cratering records, comparing cratering rates derived from cratering records to those derived from observed impactor populations (known velocities), and assessing the hazard associated with a given impactor.

Impactor to Crater Size/Energy: Scaling from a given crater to impact energy is currently controversial even when the same energy scaling relationship [e.g. 2] is used. For example, energy estimates for the Chicxulub crater [3,4] vary by an order of magnitude due to interpretation differences, although agreement exists on the relevant internal crater structural element (the collapsed disruption cavity diameter; see Fig. 1). (Discussion indicates that confusion exists within the cratering community on terminology for the different crater elements illustrated in Fig. 1; agreement on a common terminology as discussed by [3] is desirable.) The difference stems from one calculation being based on the reconstructed size of D_d [4] and one being based on D_{at} [3]. The latter have been convinced by the argument (p.c., H. Melosh) that the apparent transient cavity diameter corresponds to that of the experimental craters produced by [2] on the grounds that no collapsed blanket of breccia or melt fills the craters.

Possible Link Through Ejecta Blankets: The appropriate cavity diameter to be used for energy scaling might be established by comparing the ejecta blanket thicknesses observed around Chicxulub to those around experimental craters. Figure 2 attempts this comparison (the ejecta thicknesses are plotted normalized to a D_{at} of 80 km [3]). However, sufficient observations are not yet available to make a clear distinction, and erosion by ballistic sedimentation proximal to Chicxulub has over thickened its ejecta blanket by nearly an order of magnitude (as also observed around other well preserved craters). Although the thickness of the proximal ejecta blanket has also been compromised by erosion of its top, comparison of the observed thickness to that predicted from experimental craters may be useful in predicting the proportion of the ejecta blanket that is derived from ballistic erosion. At >15 crater radii observed ejecta blanket thicknesses are greater than predicted by [1, Fig. 2], this range is beyond the thickness resolution of these experiments.

References: [1] Housen, K.R., Schmidt, R.M. and Holsapple, K.A. (1983) *JGR, 88,* 2485–2499. [2] Schmidt, R.M. and Housen, K.R. (1987) *Int. Jour. Imp. Eng., 5,* 543-560. [3] Hildebrand, A.R. et al. (1998) *Meteorites: Flux with Time and Impact Effects, Geol. Soc., London, Spec. Pub. 140* 155–176. [4] Morgan, J. et al. (1997) *Nature 390,* 472-476.

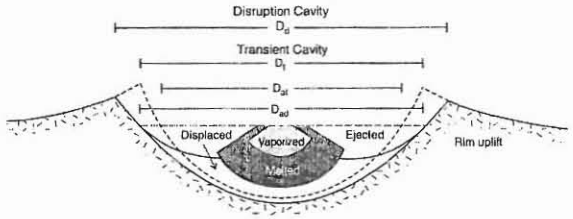

Figure 1: Schematic distinguishing a crater's transient (diameter D_t) and disruption (diameter D_d) cavities. At the pre-impact ground surface these diameters are D_{at} and D_{ad}, respectively. The horizontal dashed line indicates the position of the pre-impact surface within the crater. (from [3])

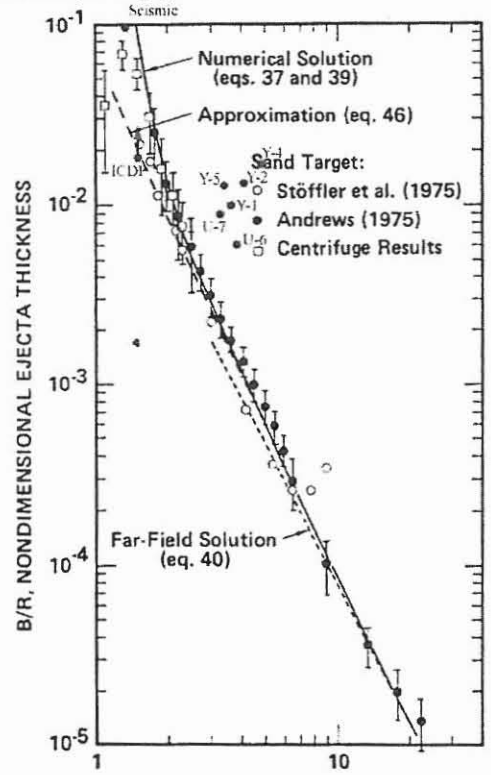

Figure 2: Ejecta-blanket profiles resulting from experimental impacts and explosions in sand compared to profiles predicted by the ejecta model of Housen et al. [1] and the ejecta blanket thicknesses observed at the Chicxulub crater. (Modified from [1])

DOES MELT VOLUME GIVE THE SIGNATURE OF THE IMPACTOR?

K.A. Holsapple, University of Washington, 352400, Seattle, WA 98195. holsapple@aa.washington.edu.

1. Introduction. Many analyses of impact events attempt to solve an inverse problem: Given the result, what was the impactor? One common example is the use of careful measurements of impact melt with the hope of deducing the impactor size and velocity.

The approach is as follows. Suppose the amount of impact melt is, for a given geological site and assuming a given impactor material, known (for example by code calculation) as a function of impactor mass m, velocity U. (I shall ignore complexities of oblique impacts here.) Then we have some known functional relationship

$$V_{melt} = F(m,U) \tag{1}$$

Then also we have some other known quantity, say the crater size given as

$$V_{crater} = G(m,U) \tag{2}$$

The goal is then to solve these two equations in two unknowns for the impactor mass m and the velocity U. Of course, that will fail if the two equations are not independent, and therein often lies the problem.

Equation (2) for the crater size is usually assumed to be of the form determined by the point-source approximation to impact problems, as given by the scaling relations of Holsapple, Schmidt and Housen (see, for example, the review in Holsapple 1993 [1]). The point-source approximation is expected to be valid for any measure of the cratering process that is large compared to the impactor size. Those relations have the form

$$V_{crater} = f(aU^{\mu}) \tag{3}$$

where the exponent m is assumed to be known, it is about 0.55-0.6 for non-porous materials. One must distinguish between the strength regime or the gravity regime for the function f. Assuming as a specific example a large terrestrial crater in a hard rock geology, then a specific form is given (Holsapple, 1993 [1]) as

$$V_{crater} = 0.48 m^{0.78} U^{1.3} \tag{4}$$

Thus, the measurement of the crater volume gives the numerical value for the product $mU^{1.67}$. (This is just the cube of the product aU^{μ} with some factors thrown in.)

We cannot perform laboratory experiments at impact velocities greater than 5-6 km/s, well below the minimum velocity for melt production. Therefore, code calculations must be used to determine the melt volume function of equation (1). Such calculations have been reported by O'Keefe and Ahrens [2], Orphal et al. [3] Bjorkman and Holsapple [4], Pierazzo et al. [5] and others.

O'Keefe and Ahrens [2] report that the melt volume for impact velocities greater than a threshold is proportional to the impactor kinetic energy:

$$V_{melt} = Ka^3U^2. \tag{5}$$

Later, Bjorkman and Holsapple [3] determined an importantly different result: that, for impact velocities greater than about 50 km/sec the melt volume scaled in the same way as the crater volume, namely that

$$V_{melt} = Km^{0.78}U^{1.3}. \tag{6}$$

although energy scaling does hold for lower velocities where the majority of melt is produced close to the impactor. The problem then arises for the larger velocities: if the melt and crater volumes scale in exactly the same way, both are determined by the same combination $mU^{1.67}$. Then there is no way to determine separately the mass and velocity.

Much more recently Pierazzo et al. [5] revisited the question of melt production. Their conclusion returns to that of O'Keefe and Ahrens: that the melt volume scales linearly with the energy of the impactor. They attribute the Bjorkman and Holsapple [3] result to be a consequence of insufficient grid resolution in the calculations.

I shall reevaluate the reevaluation of Pierazzo et al. Specifically, I shall show calculations and argue that, not only does energy scaling not hold for the higher velocities, it does not hold about 30 km/s. The consequence is that melt volume cannot be used to separate the effects of size and velocity for any impact velocity greater than that value.

In fact though, the different interpretations are really somewhat moot. Numerical examples will be presented that show, that even if energy scaling for melt volume is adopted down to lower velocities, the inverse problem is highly non-robust: Factors of uncertainty of only 2 in the melt or crater volume functions result in factors of uncertainty of several decades in impact velocity.

References:

[1] Holsapple, K.A., "The Scaling of Impact Processes in Planetary Sciences", *Annual Reviews of Earth and Planetary Sciences* **21** pp333-373, 1993.

[2] O'Keefe J.D. and Ahrens T.J. "Impact induced energy partitioning, melting, and vaporization on terrestrial planets." *Proc. Lunar Planet. Sci. Conf, 8th*, 1977.

[3] Orphal D.L., Borden W.F. Larson S. A. and Shultz P.H., Impoact melt generation and transport. *Proc. Lunar Planet. Sci. Conf. 11th*, 1980.

[4] Bjorkmann M.D and Holsapple K.A. Velocity scaling impact melt volume. *Int. J. Impact Engr.* 5, 155-163, 1987.

[5] Pierazzo E.,Vickery A.M., and Melosh H.J. A reevaluation of impact melt production. *Icarus* 127, 408-423, 1997.

WHAT DO WE NEED TO KNOW TO MODEL IMPACT PROCESSES?

K. A. Holsapple, University of Washington, 352400, Seattle, WA 98195. holsapple@aa.washington.edu.

Introduction. The computer modeling of hypervelocity impacts into planetary bodies is one of the most challenging computer tasks we attempt. The physical states encountered in impact events can begin with pressures measured in gigabars and temperatures measured in hundreds of electron-volts, and then proceed all the way down to the ordinary partial bars of pressure and few degrees of temperature as in our common experience in terrestrial soils and rocks. The interest in planetary science applications spans not only those common terrestrial soils and rocks, but also gases, ices at extreme low temperatures, and very loose, rubble-pile materials that could not even withstand the pressures of the Earth's gravity without crumbling.

The extreme range of physical conditions and materials makes the job of a modeler extremely difficult, especially for descriptions of the models for the material behavior. While, in principle, current computer power would seem to allow the detailed calculation of any specific impact event of interest by integrating the known physical laws, that view is specious. The cold, cruel facts are that, first, we do not yet know how to mathematically model the extreme range of conditions of importance, and second, even if we develop meaningful models, we do not have sufficient physical tests to measure the material properties needed for those models.

This state of affairs means that the community must be aware of the shortcomings, and must spend much more time and effort on the development of models of material behavior, on the laboratory and field measurements to calibrate those models, on calculations to determine the sensitivity of the results on the models, on actual physical experiments of impacts, and, finally, on calculations of those physical laboratory results and large scale field events with known impact conditions. The computer tools must prove their reliability and robustness for calculations when both the initial and final conditions are well known before they can be used with any meaning to determine unknown impact conditions.

This presentation is to review what we know and what we do not know; what needs to be known, and what remains to be discovered about material modeling for impacts.

The EOS. The evolution of the pressure and temperature states from extremely large to very small leads to a parallel separation of the required material models into two distinct but intertwined parts. First are the models for the high-pressure behavior in the early stages of the process. Those pressures are commonly much larger that the material stress scales: the compressibility modulus and various material strengths, so the stress deviators can be ignored. The state is then measured by five state variables: the pressure p, mass density ρ, internal energy e temperature T and entropy η. Any pair can be chosen as independent, and the other three are then given in terms of those two by the "equations of state" which are material property functions. However, insofar as the solution for the motion is concerned, it is only the relation between e, p and ρ that matters.

Since impact problems encounter the same extreme conditions as nuclear events, it is not surprising that we borrow the knowledge and tools of the national weapons laboratories for those equations of state, which they have been studying for over half a century.

There are a variety of EOS models: simple algebraic models that relate pressure and density with no dependence on temperature (e.g. linear elasticity or Murnaghan); simple analytical models for single solid phases (Mie-Gruneisen and Tillotson); complex analytical models including phase changes such as melt and vapor (ANEOS); and complete tabular databases such as the SESAME and SESLAN libraries from the DOE laboratories. Those latter two are often developed from complex solid-state physics theories using the PANDA computer code [1]. The EOS equations govern the early-time response and determine a number of significant aspects of the energy coupling, including the initial pressure and velocity, and the decay of the pressure and velocity as a shock propagates through the target.

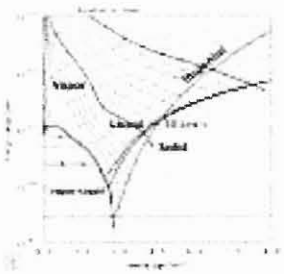

A typical EOS is as shown at the left. The important elements include the Hugoniot, which relates the conditions at the shock, and the "release adiabat" the path followed during the unloading behind the shock.

These paths determine a measure of an equivalent point source input, which in term determines most of the scaling of the final cratering or disruption results.

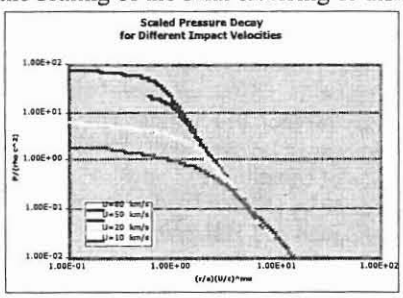

The left figure illustrates the commonality of different impact problems arising from the simplicity of the point-source measure. (See [2] and many prior references of the author

and his colleagues.)

These EOS descriptions are quite well developed and understood, a consequence of the fact that they are needed for calculations and development of nuclear weapons. For impact calculations, it is necessary to choose the model and its constants. However, for any particular geological material, that can often be a difficult task, so that the resulting model is usually quite uncertain.

Strength. When the shocks decay into the kilobar pressure range, material strength dominates the target response and subsequent cratering or disruption. Here we borrow from the civil engineering soil-mechanics and rock-mechanics communities.

Strength models include none (hydrodynamic), constant strength in tensile or compression, constant strength in shear (Tresca), maximum deviator invariant J_2 (VonMises), pressure-dependent shear strength (Mohr-Coloumb), pressure-dependent J_2 (Drucker-Prager), rate-dependent tensile (e.g. Grady-Kipp), and complex damage models (e.g. Johnson-Cook). This description of the fracture, flow or yielding (generically called "failure") is the most difficult part of impact calculations into geological materials.

A common starting point is to describe how the initial failure depends on the stress or strain tensors, which have six independent components; or, equally well, three invariants and three directions. Assuming isotropy, directions are of no consequence and the stress tensor can be measured by the three invariants. It is common to further suppose that only two are necessary, taken as the pressure or mean stress (essentially the first invariant), and what is commonly denoted by J_2, the second invariant of the deviator stress. Then the ranges of stress for which flow or fracture does not occur are described by defining an enveloping curve in pressure-J_2 space. (Changes to this envelope such as hardening or softening are described below).

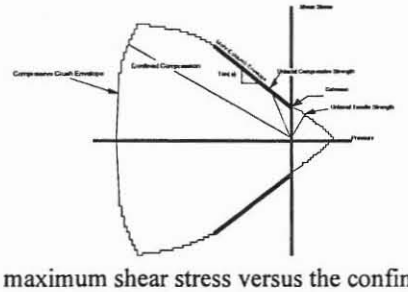

The figure at the left indicates the general nature of an initial failure envelope for a geological material, as a plot of the maximum shear stress versus the confining pressure. Various different measures of "strength" exist and are indicated on this envelope. There is a curve of limit shear stress that depends on pressure, commonly modeled as a Mohr-Coloumb (shear strength versus pressure) or a Drucker-Prager envelope (J_2 versus pressure). Often those curves are assumed to be linear, but that assumption is not essential. Then since failure can also occur at sufficiently high pure compressive pressure, a "cap" is constructed to model that compressive pressure crushing; that is the termination of the envelope at the left of this figure.

For uniaxial tension loading, the loading path as shown intercepts the failure envelope at a uniaxial stress limit known as the tensile strength. In pure uniaxial compression, the path as indicated intercepts the shear envelope at a higher stress, called the compressive strength. In pure shear, the maximum is at the intersection of the shear envelope with the vertical axis, the shear strength or "cohesion". Biaxial or triaxial loading can proceed along different paths until they intersect these limit curves, those define biaxial and triaxial strengths. A confined compression curve is shown sloped to the left and intersecting the compression cap.

The next part of the modeling concerns the question of the change of this envelope as failure proceeds. These questions involve the features of ductility (plastic flow) versus brittle (fracture or flaw growth). Commonly, brittle failure occurs at low values of confining pressure, especially tensile states; while ductile failure occurs at high values of confining pressure in compressive states. Ductile failure is modeled by describing how the material develops plastic strain (the "flow rule") and by how that flow affects the failure envelope (hardening or softening). Common metal-plasticity models include those effects. Brittle failure is commonly modeled using a "damage" parameter, which measures the internal damage of the material in a macroscopic way. It typically ranges from zero at no damage, to unity at complete damage. An equation describing its evolution as a function of the current stress or strain state is required to track its values at material points. The Grady-Kipp model is an example of a damage model for brittle tensile failure. All of these aspects can also depend on the temperature.

When failure occurs, a granular material also has a tendency to "bulk": an increase in volume and decrease in density at constant pressure. That can be suppressed by the pressure state, but then adds a component of pressure. Equally well, bulking is included if an associated flow rule is used with a pressure-dependent shear strength, since that flow rule has a component of dilation. The relative amounts of deviator and dilation can be adjusted by using a non-associated flow rule.

I will review various material property data and different models used in the community, and relate their features and failures to this overview picture.

References:

[1] Kerley G. I., "Users Manual for PANDA II: A Computer Code for Calculating Equations of State", Sandia Report SAND88-2291, 1991.

[2]Holsapple, K. A., "The Scaling of Impact Processes in Planetary Sciences", *Annual Reviews of Earth and Planetary Sciences* **21** pp333-373, 1993.

EFFECTS OF TARGET PROPERTIES ON THE CRATERING PROCESS. K.R Housen, Shock Physics, MS 2T-50, The Boeing Co., P.O. Box 3999, Seattle WA 98124. kevin.r.housen@boeing.com.

Impact events in the solar system occur in a variety of materials, ranging from the rocky surfaces of the terrestrial planets to the icy mantles of the satellites of the outer planets to the undoubtedly highly fractured and porous materials that make up many asteroids and comets. A major challenge to impact modelers has been to understand how the composition and mechanical properties of these varied target materials dictate the outcome of an impact event. Four sources of information have historically been used to study this problem.

Scaling theory provides guidelines as to when specific material properties may have a significant effect on the outcome of an impact event. The initial work in scaling separated cratering events into the strength and gravity regimes. In the former, crater size is determined by the mechanical strength properties of the target while, in the latter, strength is unimportant compared to the effects of the lithostatic overburden. The transition between the two regimes is determined by the condition $Y/\rho gh$ = constant, where Y is a measure of target strength, ρ is the density, g is gravity and h is crater depth. This simplistic picture has now been modified in two ways. First, Gaffney and Holsapple [1] noted that the strength of many geological materials depends on the rate at which they are loaded and that loading rates depend on the size scale of the event. As a result, mechanical strength of the target decreases with increasing event size, so the transition into the gravity-dominated regime occurs at smaller crater sizes than the simple constant-strength model would predict. Second, numerical simulations by Nolan *et al.* [2] indicate that passage of the shock ahead of the expanding crater bowl pre-fractures rocky target materials, which allows the crater to form in an essentially cohesionless (but not strengthless) material. In essence, an impact event can alter the mechanical properties of the material in which the crater forms.

Scaling considerations have also been applied to impacts in highly porous targets [3, 4], which may be representative of comets and many asteroids. In this case, craters are formed mostly by compaction of pore spaces. Crater size is therefore determined by the crushing strength of the target. Impacts in these materials may not experience a gravity regime because at large size scales (where gravity would be expected to dominate), the material crushes to a point where the lithostatic compressive stress is comparable to the crushing strength. Hence, a situation is never attained in which gravitational stresses are large compared to the important strength measure.

In addition to mechanical strength, scaling analysis has been used to identify conditions under which target viscosity is the most important property in determining crater size. Cratering in a viscosity-dominated regime has been applied to studies of Martian rampart craters [5] and craters on icy satellites [6].

Scaling theory is essential to identify the conditions under which various target material properties might be important in determining crater size and morphology. However, scaling laws by themselves cannot establish the relation between crater size and material properties. Instead, experiments and code calculations must be used to determine those dependences.

Field explosion experiments are a second source of information on the effects of material properties. Field tests are especially useful in that they can be conducted at size scales much larger than laboratory experiments. The largest conventional explosion test conducted in the U.S. involved 4.36×10^9 g of explosive and produced a crater 88.4 m in diameter [7]. While still small by planetary standards, these craters are more than 100 times larger than those that can be studied in the lab. Additionally, field tests have been performed in various geologic settings and can be used to illustrate the dramatic effects of material properties. For example, Figure 1 compares the crater profiles produced in two tests involving hemispheres of high explosives with a mass of 4.5×10^8 g, one in basalt and one in unconsolidated alluvium.

Laboratory experiments have of course been the main source of information for cratering studies. An advantage of laboratory experiments is that they can be conducted under controlled conditions, whereas field tests are at the mercy of the natural settings under which they are conducted. That is, it would be difficult to determine the influence of material properties from field tests alone because a multitude of important properties may vary from one test site to the next. As an example, Figure 2 uses the results of impact experiments to addresses the dependence of crater size on target density. Cratering efficiency (target density * crater volume/impactor mass) is shown for three cohesionless granular materials whose bulk densities vary by a factor of 2.6. The results show that cratering efficiency in nearly independent of target density for this particular type of target material

A limitation of laboratory studies is that they are, by definition, conducted at small size scales. Therefore, if any important material properties are scale dependent (e.g. the strength of rock), then the experimental results will not be directly applicable to larger events and must consider the scaling issues involved with extrapolation to larger sizes.

Numerical simulations have become a popular method for studying crater formation and offer the potential benefit of being able to study the separate effects of material properties on crater size and morphology. While this benefit is alluring, a considerable drawback to code calculations is that the results are

only as good as the physical models that they incorporate. The constitutive models used in present codes such as CTH are reasonably accurate for some materials (e.g. metals), but are not well-developed for others, notably rock or highly porous soils. As a result, code results should be viewed with skepticism until validated extensively against laboratory and field tests [9]. Nevertheless, when such validations are accomplished, numerical simulations can provide tremendous insight into the effects of material properties.

Figure 3 presents an example. It was noted above that impact shock in rocky targets pre-fractures the material ahead of the expanding crater. This phenomenon has been used at times to assume that this preprocessing reduces the material strength to zero. While pre-fracturing should eliminate cohesion, the fractured rock will still have considerable strength in shear due to the effective friction angle associated with the interlocking of the rock fragments. The effect of friction angle is addressed in Figure 3, which shows the result of two CTH calculations of the Sailor Hat explosion event. Crater profiles are shown at an intermediate time during crater growth. The two simulations were identical except that the one on the left assumed a friction angle of 0° (equivalent to assuming a strengthless material), while that on the right shows a more realistic value of ~30°. These results show the significant effect that the material shear strength has on crater formation; an effect that is ignored in many calculations reported in the literature.

Additional calculations are underway. These results, along with those from scaling, field tests and laboratory experiments will be summarized to identify what is and is not known about the effects of material properties on crater formation.

References: [1] Gaffney E.S. and Holsapple K.A. (1983) Crater scaling relations for strain-rate dependent materials, (Unpublished report). [2] Nolan M.C. *et al.* (1996) *Icarus* 124, 359-371. [3] Housen K.R. *et al.* (1999) *Nature* 402, 155-157. [4] Housen K.R. and Holsapple K.A. (2002) Submitted to *Icarus*. [5] Gault D.E. and Greeley R. (1978) *Icarus* 34, 486-495. [6] Fink J. *et al.* (1984) *J. Geophys. Res.* 89, 417-423. [7] Lee C.K.B. and Mazzola T.A. *J. Geophys. Res.* 94, 17,595-17,605. [8] Holsapple K.A. and Housen K.R. (2002). *LPSC* Abstract.

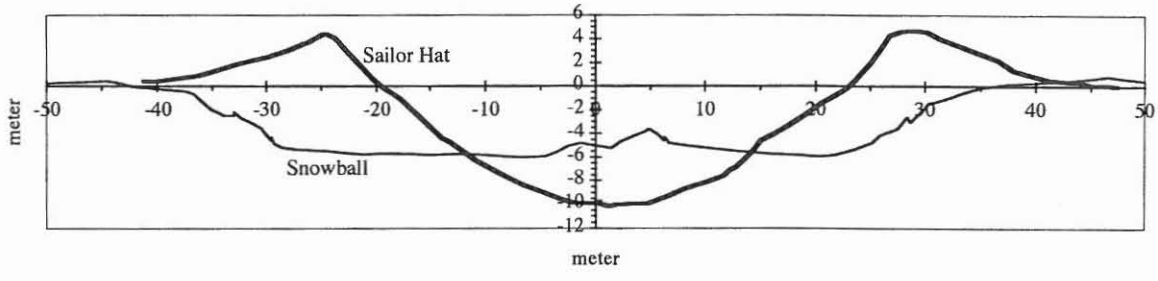

Figure 1. Comparison of crater profiles from two explosive field tests. Both tests used hemispherical charges of TNT (4.5×10^8 g) situated at the target surface. The Sailor Hat event was conducted in basalt, whereas Snowball was conducted in unconsolidated alluvium with the water table at a depth of approximately 7 m.

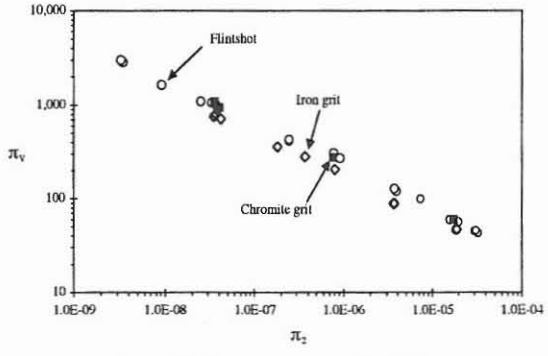

Figure 2. Cratering efficiency, π_v, vs π_2 for 1.8 km/s impacts into three granular cohesionless materials of density 1.8 (Flintshot sand), 3.1 (Chromite sand) and 4.6 gm/cm^3 (Iron sand). These data show that cratering efficiency is nearly independent of target density.

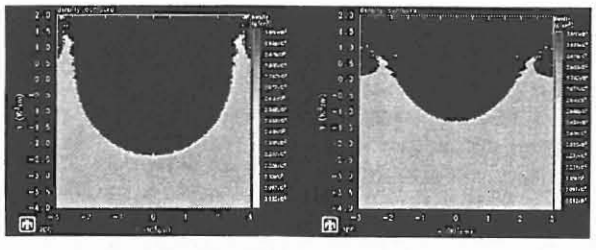

Figure 3. Comparison of two numerical simulations (CTH) of the formation of the Sailor hat explosion crater. The crater profiles are shown at an intermediate time of 0.18 s. Both models assume a Mohr-Coulomb behavior. The Profile on the left is for a case where the angle of internal friction is zero, while the case on the right is for approx. 30°. The formation time of the crater is ~0.5 s.

COMPLEX CRATER FORMATION: VERIFICATION OF NUMERICAL MODELS. B. A. Ivanov, Institute for Dynamics of Geospheres, Russian Academy of Sciences., Leninsky prospect., 38-6, Moscow, 117334, Russia (baivanov@onlime.ru, ivanov@lpl.arizona.edu).

Introduction: The growing capability of modern computers offers increased possibilities for numerical modeling of impact crater formation. However, complex crater formation include various particular models of rock massifs dynamical behavior in a wide range of thermodynamic parameters and strain rates. At the same time geological and geophysical investigations of impact craters give only the final structure of craters and geophysical fields around. The verification of numerical models should take into account comparison of computed results with maximum possible set of observational data.

Ground truth: The list of parameters one should compare includes crater morphology and morphometry, deformation of stratigraphic layers and their structural uplift; impact melt volume; shock wave decay; geometry and size of fractured zone, and individual specific features available for some terrestrial craters (presence of tektites, evidences of underwater formation etc.).

Primary experience: The list of recent publication gives an impression about strong and weak topics in the current state of model's verification.

Crater morphology and morphometry.. Models for many craters has been published, however rare papers deals with a systematic investigation of a crater shape in a wide range of crater diameters with the *same model.* A good example is done in [1] where the depth/diameter relation bend is reproduced qualitatively for the moon, Earth and Venus. However, quantitative fit of models to measurements is still an open question.

Deformation of stratigraphic layers and their structural uplift. First attempts to compare models for specific craters has been published for Chicxulub [2] and Puchezh-Katunki [3]. Again, qualitative fit of models is obtained with many quantitative misfits.

Impact melt volume is the best-studied model value [4] ready to be compared with observational data [5]. One can state the good fit of models to field data. The fit demonstrate that current scaling laws allow us to estimate impact energy for a given crater with the accuracy of factor of 2. However, the melt production in oblique impacts is still under investigation [6, 7].

Shock wave decay is easy to get in a numerical model and is very hard to compare with observations: due to a structural uplift formation the final position of shocked rocks are very far from their initial position in a target. Hence only full model of a complex crater modification allow us to verify models with a shock wave decay [3] (Fig. 1).

Geometry and size of fractured zone are just began to be used in model/nature comparisons. Rare papers for several craters has been published (eg. [8]). At the same time namely modeling of a fracture zone allow to compare code results with available gravity and seismic survey. This direction looks like a promising way for future modeling evolution.

Individual specific features for several terrestrial craters allow to verify a complex interaction with layered targets. One can refer for recent estimates of a tektite origin [9] and underwater crater modeling [10]. The modeling of individual specific features is also fast evolving approach to verify numerical models of impact cratering.

Conclusion: Numerical models of complex impact crater formation can be and should be verified by comparison with field geological and geophysical data.

References: [1] Wünnemann, K.. et al. (2002) *LPS XXXIII,* Abstract #1277.. [2] Collins, G. S. et al. (2002) *Icarus 157*, 24-33. [3] Ivanov, B. A. (2002) *LPS XXXIII,* Abstract #1286. [4] Pierazzo E. et. al. (1997) *Icarus 127* 408-423.. [5] Grieve R. A. F. and Cintala M. J. (1992) *Meteoritics 27*, 526–538. [6] Pierazzo E. and Melosh H. J. (2000) *Icarus 145*, 252-261.[7] Ivanov B.A. and Artemieva N. A. (2002) *GSA Spec Paper 356*, 619-630. [8] O'Keefe, J. D.and Ahrens, T. J.(1999) LPS XXX, Abstract #1304. [9] Artemieva N.A. (2002) In *Impact studies*, Springer Verlag, Berlin, pp. 257-276. [10] Ormö, J. et al. (2001) MAPS 36, Suppl. p.A154.

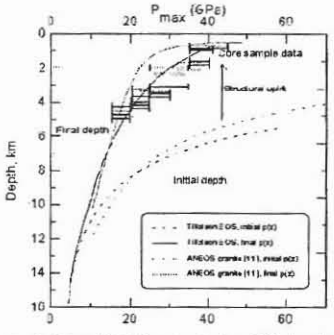

Fig. 1. The apparent shock wave decay with depth along the deep drill hole in the center of the Puchezh-Katunki crater, diameter D~40 km Maximum shock pressures recorded in minerals are shown as error bars. All EOS's used show that the central uplift top is constructed of rocks uplifted from ~6 km depth [3].

EDUCATIONAL EXPERIENCE IN NUMERICAL MODELING OF IMPACT CRATERING. B. A. Ivanov, Institute for Dynamics of Geospheres, Russian Academy of Sciences., Leninsky prospect., 38-6, Moscow, 119334, Russia (baivanov@online.ru, ivanov@lpl.arizona.edu).

Introduction: The growing capability of the impact crater numerical modeling makes actual questions how to attract young students to the research and how to educate students specialized in general geology and geophysics. An experience in this direction has been accumulated in September 2002 during the ESF IMPACT Short Course "Numerical Modeling of Impact Crater Formation ".

Scope: The goal of the short course was to introduce basics of the numerical modeling techniques to non-professionals. "Non-professional" in this context means that the course was oriented to students and post-docs without a special background in computer science, shock wave physics and rock mechanics. However, most of students have an experience in impact crater related researches. Hence, all of them was highly motivated by their previous education and current research activity.

Attendance: 10 students from 6 European countries attended the short course (Germany - 3, France -2, Estonia - 2, Spain - 1, the Netherland -1, Finland -1). The general information about the ESF IMPACT program is available at http://www.esf.org WEB site.

Support and organization: The living and housing expenses have been covered by the ESF IMPACT program. The lecture room and the computer class have been offered by Vienna University (Prof. C. Koeberl was an excellent course manager). The computer class gives an opportunity for which student to work with a personal networked computer (PC under Windows 2000). The main lecturer (B. Ivanov) has used a beamer as for lecturing and for the demonstration of the practical work at the large screen. It was very important during the installation of the software and practice - students has seen simultaneously the output of each operation at their personal terminals and at the big ("master") screen repeated the "master" computer of the lecturer.

Short course program includes 5 main lectures and 5 practical lessons (totally 5 days with lectures before lunch and a practice in the computer class after lunch). Lecture topics include:

1. "What and how can be modeled for impact cratering. Shock waves, excavation and modification of a transient cavity".
2. "SALE hydrocode, general logic, input file, outputs"
3. "Equation of state (EOS). Ideal gas, Murnaghan, Mie-Gruneisen, ANEOS"
4. "Rock strength. Basics (elasticity, placticity, fragmentation/damage, dry friction). Implementation into hydrocodes. Acoustic fluidization"
5. "Examples of numerical modeling implementation in a geoscience research projects: Puchezh-Katunki deep drill core analysis, trigger volcanism, penetration of the Europa ice crust".

Practice includes software (Fortran compiler and a hydrocode) installation, the code compiling with a graphic package PGPLOT [1].

Numerical code used for the short course is based on the SALE code [2], enhanced with options to compute multimaterial problems (2 materials plus vacuum) in the Eulerian mode with a simplified description of rock's elastic-plastic behavior. The code with a working name "SALEB" is armored with 2 kinds of EOS's: Tillotson's EOS [3] with an addition for the real temperature estimates [4], and tabulated ANEOS [5] for several types of rocks.

Practice includes the solution of 3 problems: shock recovery container (calcite in the iron container), vertical crater-forming impact, oblique 2D (planar) impact. Students have been asked to compute several variants changing the input file parameters to get an impression about sensitivity of results. Naturally, only initial stages has been modeled during the class hours.

Handouts included a CD ROM with the source code and a set of publications relevant to the topic. In addition, each lecture, prepared in PowerPoint has been printed out as handouts.

Conclusion. The experience with the short course shows that it is possible to organize a "quick entry" to the topic in a relatively short time for highly motivated students. Post-course correspondence shows that at least 4 students continue to work with the code. It is early to say is the course enough to begin a real numerical research. However, one can hope that the course will help all students to understand better publications about numerical modeling.

References: [1] http://astro.caltech.edu/~tjp/pgplot/. [2] Amsden A. et al.. (1980). *Los Alamos National Laboratory Report LA-8095*, Los Alamos, NM, 101pp. [3] Tillotson J. H. (1962) *Gen. At. GA-3216*, 140 pp. [4] Ivanov B. A. et al. (2002) *GSA Spec. Pap. 356*, 587-594. [5] Thompson, S. L., Lauson, H. S. (1972) Sandia National Laboratory Report SC-RR-71 0714.

MODIFICATION OF ANEOS FOR ROCKS IN COMPRESSION. B. A. Ivanov, Institute for Dynamics of Geospheres, Russian Academy of Sciences., Leninsky prospect., 38-6, Moscow, 119334, Russia (baivanov@online.ru, ivanov@lpl.arizona.edu).

Introduction: The Analytical Equation of State (ANEOS) [1] is a useful computer code to generate equations of state (EOS) for rocks and minerals. An accurate EOS is one of essential points necessary for the numerical modeling of impact events. We analyze here a possibility to use a "standard" ANEOS in a "non-standard" way to make more flexible the procedure of an EOS construction.

ANEOS: The ANEOS Fortran package gives an opportunity to construct EOS for geomaterials, needed for the numerical modeling of planetary impact cratering. In comparison with the widely used Tillotson's EOS [2, 3], ANEOS has many advantages in respect to more accurate and self-consistent description of melting and vaporization. The practical convenience is that ANEOS gives the temperature of a material as an explicit output parameter. The calculation of temperature with the Tillotson EOS is possible (at least in compression) but needs an additional thorough treatment [4].

The original version of ANEOS [1] has several limitations which complicate its usage for rocks and minerals. The first one - monoatomic vaporization (good for metals and wrong for main minerals) - has been partially released by J. Melosh [5]. The second one - a simplified description of the solid-solid phase transition is the matter of the presented work.

Solid-solid phase transitions is a typical feature of shock (and static) compression for most of main rock-forming minerals (quartz, plagioclase, olivine etc.). ANEOS treats this phase transition via the modification of the "cold compression" curve. It is an elegant way to reproduce the complexity of the Hugoniot curve at a transition area. However, the simplicity of the approach has a high price: the thermal part of the EOS use the same parameters for the high pressure phase (hpp) and for low-pressure phase (lpp). For main rocks (granite, dunite) it leads to the artificially large heat expansion close to the normal pressure. Due to enlarged heat expansion an attempt to construct the Earth-like target with a typical geothermal gradient results in density decreasing with depth. for 10 to 100 km depth. Another disadvantage is that to use the solid-solid phase transition option one needs to switch out the melt curve construction.

HPP as a second material. We investigate here a possibility to "improve" ANEOS using it separately for hpp and lpp phase areas. A similar approach is used in the other "analytical" equation of state, PANDA [6, 7]. For each rock material we build the ANEOS input file as for 2 materials: hpp material and lpp material. The hpp material has a proper "shift" for energy and entropy to use the same reference level both for lpp and hpp. A relatively simple Fortran routine is added to compute the phase equilibrium between lpp and hpp. The parameter fit is conducted, as usual, via the comparison with available thermodynamic and Higoniot data for materials under investigation. The output for the following usage in hydrocodes is assumed to be in the form of tables.

Preliminary results. Currently we have tested two materials of interest - granite and olivine. For these rocks some experimental data on shock and released temperatures are available (eg. [8, 9]). Fig. 1 illustrates the output of the updated ANEOS for olivine showing the dependence of complete (*cm*) and incipient (*im*) meting pressure for the preheated target. The preliminary estimate for the *im* shock pressure of a pre-heated peridotite is shown for a comparison. Further testing would show is it a plausible way to "improve" ANEOS for rocks and minerals.

References: [1] Thompson, S. L., Lauson, H. S. (1972) *Sandia National Laboratory Report* SC-RR-71 0714. [2] Tillotson J. H. (1962) *Gen. At. GA-3216*, 140 pp. [3] Allen RT (1967) *Spec. Nuclear Eff. Lab. - Defense Atomic Support Agency:* DA49-146-XZ-462 16 p [4] Ivanov B. A. et al. (2002) *GSA Spec. Pap. 356*, 587-594. [5] Melosh H. J. (200) *LPS XXI*, Abstract # 1903. [6] Kerley G. I. (1989.) *High Pressure Res. 2*, 29–47. [7] Kerley, G. I. (1991) *Sandia Report SAND88-2291*, Albuquerque, NM,. 176 pp. [8] Holland K. G. and Ahrens T. J. (1997) *Science 275*, 1623-1625. [9] Lyzenga G. A. et al. (1983) *J. Geophys. Res.* 88, 2431-2444.

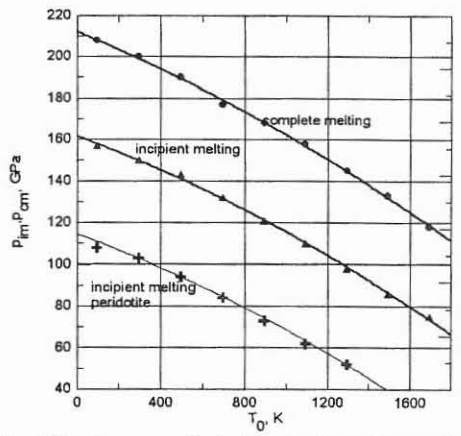

Fig. 1. Shock pressure for incipient and complete melting after a release for olivine and peridotite estimated with ANEOS.

COOLING OF THE KÄRDLA IMPACT CRATER: II. IMPACT AND GEOTHERMAL MODELLING. A. Jõeleht[1], K. Kirsimäe[2], E. Versh[3], J. Plado[4] and B. Ivanov[5], [1,2,3,4]Institute of Geology, University of Tartu, Vanemuise 46, 51014 Tartu, Estonia; [1]ajoeleht@ut.ee, [2]arps@ut.ee, [3]desty@ut.ee, [4]jplado@ut.ee; [5]Institute for Dynamics of Geospheres, Russian Academy of Sciences, Leninsky Prospect 38-6, Moscow 117979, Russia, baivanov@idg.chph.ras.ru.

Introduction: Hydrothermal mineralization has occurred in many impact craters including also a 4-km marine complex crater in Kärdla, Estonia. Mineralogical and fluid inclusion data [1,2] provide temperature ranges for different mineralization events and, thus, giving a starting point for modelling. Modelling includes both (1) impact modelling to get the structure and temperature distribution in crater rocks right after the impact, and (2) geothermal modelling to get information on heat transfer processes and time-scale of post-impact cooling.

Impact Modelling: The target in Kärdla was about 150 m thick sedimentary layer on top of crystalline basement [3]. The impact took place in a ~100 m deep epicontinental Ordovician sea. SALE hydrocode was used to simulate formation, modification, and impact-induced heating in Kärdla crater. Both Tillotson equation of state and ANEOS algorithm were tested.

Modelling results suggest that usage of Tillotson equation of state gives very poor estimate of impact heating effect. It gives a temperature rise of ~100 K only, which contradicts with temperature of at least 300°C proven by PDF studies, quartz fluid inclusion homogenization temperatures, and chloritization geothermometry [1]. Maximum temperature estimate of 450°C [1] relies on formation of K-feldspar prior chloritization and maximum fluid inclusion homogenization temperature estimates. Results obtained using ANEOS algorithm are in better agreement with observations and suggest maximum temperatures of 300-350°C.

The crater is filled with resurge deposits which are at least 170 m thick. Unfortunately we were not able to simulate resurge flow and formation of resurge gullies with 2-D software in axisymmetric coordinates.

Geothermal Modelling: Post-modificational temperature distribution in crater rocks was one of the input parameters for transient fluid flow and heat transfer simulations for 2-D axisymmetric case. Fluid and rock properties were temperature-dependent. Effects due to fluid phase changes and associated latent heat effects were also implemented in the software.

The phase change of water has a double effect on heat transfer. First, when water vaporizes, its density decreases by more than one order of magnitude resulting in high buoyancy and rapid upward flow. Second, vaporization requires additional (latent) heat, which is absorbed from surrounding rocks resulting in their effective cooling at the high water vaporization rates.

The preliminary results suggest that vaporization of upward flowing fluid contributes significantly to cooling, decreasing the maximum temperature below boiling point (~ 250°C in case of Kärdla) in a few tens to hundreds of years. Heat transfer by liquid fluid is not as powerful as in vapor phase. The radiative heat transfer would start to contribute noticeably at temperatures above 600 °C, but is insignificant in Kärdla-size crater because of too low temperatures even immediately after the impact.

In the early stage of cooling, convective heat transfer prevails whereas at later stage conduction dominates. The ratio of convection over conduction (Peclet number) depends largely on assumed permeability structure. Direct measurements give information only about present day permeability, therefore, detailed investigations are needed to estimate the decrease of permeability due to closure of pores by hydrothermal mineralization.

It should be noted that the same hydrothermal mineral precipitated at a different time at different location inside the structure. Because different parts of the crater cooled at different rate the lifetime of hydrothermal mineralization varied. For example, at comparable depths the rocks in central uplift are not cooling as fast as rocks near the ring depression because, in respect to groundwater convective system, they are located at discharge and recharge areas, respectively. Rocks at rim might have got additional heat by upward flowing fluid.

Cooling to ambient temperatures in the central part of the crater lasts for thousands of years. Despite of relatively rapid cooling, the thermal perturbations in the deeper part of the central uplift should be observable with geothermal tools even a few tens of thousands of years after the impact.

References: [1] Versh et al (2003) in this volume. [2] Kirsimäe et al. (2002) *Meteoritics & Planet. Sci., 37,* 449–457. [3] Puura & Suuroja (1992) *Tectonophysics,* 216, 143-156.

SEISMIC INVESTIGATION AND NUMERICAL MODELING OF THE LAKE BOSUMTWI IMPACT CRATER. T. Karp[1], N. A. Artemieva[2] and B. Milkereit[3], [1]Institute for Geosciences, Dept. of Geophysics, Kiel University, Otto-Hahn-Platz 1, 24118 Kiel, Germany, tkarp@geophysik.uni-kiel.de; [2]Institute for Dynamics of Geospheres, Leninsky pr., 38, bldg.6, 119334, Moscow, Russia, nata_art@mta-net.ru; [3]Dept. of Physics, University of Toronto, 60 St. George Street, Toronto, Ontario M5S1A7, Canada, bernd@core.physics.utoronto.ca

Introduction: The Lake Bosumtwi impact crater, Ghana, (age 1.07 Ma, diameter 10.5 km) is one of the youngest and best-preserved complex terrestrial impact structures. It was excavated from hard crystalline target rock and is the source of the Ivory Coast tektite strewn field. It is almost entirely filled by the Lake Bosumtwi.

Seismic investigations of the Bosumtwi crater identify the proposed central uplift [1] and indicate a low-velocity breccia-layer below the lake and the post-impact sediments [2]. Recent evaluation of a longer seismic refraction line extends information on velocity-depth distribution down to ~1.7 km (Fig. 1). The structure is characterized by a vertical velocity gradient. Lateral velocity variations also occur. Higher seismic velocities are observed right below the central uplift, north and south of it velocities are lower. The area of higher velocity is interpreted to consist of uplifted basement originally situated at greater depth. The area of lower velocity is interpreted to be an allochthonous breccia cover surrounding the uplift. A distinct interface between the breccia layer and brecciated crater floor cannot be resolved. Lateral velocity changes occur down to a depth of 1.6 km below the lake indicating that rocks are brecciated down to at least this depth. The structural uplift is estimated by the 3.9 km/s-isoline to be at least 800 m. The apparent depth of the crater is 550 m.

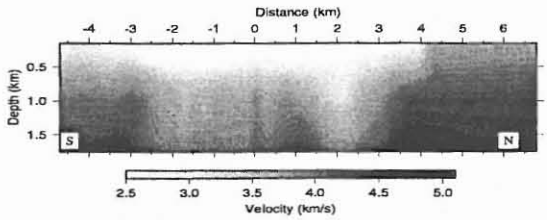

Fig. 1: Seismic velocity distribution of the Bosumtwi crater. Vertical reference is the estimated original target surface (150 m above lake surface). White area corresponds to water and post-impact sediments.

Numerical modeling of the crater is performed (1) with the SALE code to receive final crater shape after a vertical impact, and (2) with the SOVA code to model an oblique impact and tektites production. Projectile size estimates with scaling laws [3] vary in the range 400 - 1600 m, depending on impact angle and velocity. ANEOS equation of state for granite is used to describe both the target and the projectile.

Vertical impact and final crater shape. To simulate the temporal decrease of friction in rocks around a growing crater the "block model" (a version of the general acoustic fluidization model) is used [4]. Projectile velocity is 12 km/s, diameter is 750 m. The "block model" parameters for Bosumtwi have been published in [5]. The modeled rock mechanics include the gradual shear failure, an instant tension failure, the decrease of strength and internal friction close to the melt temperature, and the pressure dependence on the melt temperature. Variations of friction for damaged materials (0.2 - 0.5) and decay time for block oscillations (9 - 15 s) will produce a ~10 km in diameter crater, 200-300 m deeper than seismic data reconstruction (Fig. 2). Reasons for this discrepancy may be: (1) dilatancy of damaged rocks (not yet included); (2) deposition of fallout ejecta (suevite) inside the crater (in 2D models the ejected material is deposited outside the crater); (3) an oblique impact produces a shallower crater, but no strength model for 3D modeling is currently available.

Oblique impact and tektites. Most suitable conditions for tektite origin arise in the case of high-velocity impact (>20 km/s) with impact angle 30°-50°. 3D modeling shows that the fallout ejecta thickness inside the crater does not exceed 30-40 m. This is too thin to fill the gap between modeled and observed profiles.

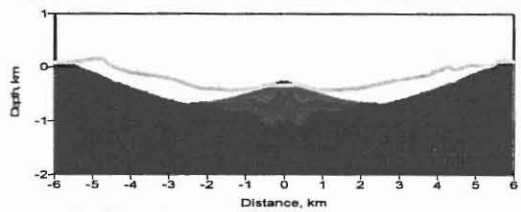

Fig.2: Density distribution after 100 s represents final crater shape obtained with the SALE modeling. Seismic-topographic profile is shown as grey line.

Discussion: Numerical modeling allows partial reconstruction (diameter, central uplift) of the Bosumtwi crater. Dilatancy and obliquity have to be included. Results from gravity and magnetic surveys and future scientific drilling (ICDP) will refine structural information of the crater and improve modeling results.

Acknowledgements. This work was financially supported by DFG grant Ja 290/15-2. We thank Boris Ivanov for the help with the SALE-modeling and useful discussions.

References: [1] Scholz et al. (2002) *Geology 30 (10)*, 939-942. [2] Karp et al. (2002) *Planetary and Space Science 50 (7-8)*, 735-743. [3] Schmidt R.M. and Housen K.R. (1987) *Int. J. Impact Engn 5*, 543-560. [4] Melosh H.J. and Ivanov B. (1999) *Ann. Rev. Earth and Plan. Sci. 27*, 385-415. [5] Ivanov B. and Artemieva N. (2002). *GSA Spec. Paper 356*, 619-630.

EARLY FRACTURING AND IMPACT RESIDUE EMPLACEMENT: CAN MODELING HELP TO PREDICT THEIR LOCATION IN MAJOR CRATERS? A. T. Kearsley[1], G. A. Graham[2], J. A. M. McDonnell[2], P. A. Bland[3], R. M. Hough[4] and P. A. Helps[5]. [1]BMS, Oxford Brookes University, Oxford, OX3 0BP, UK, atkearsley@brookes.ac.uk, [2]Planetary and Space Sciences Research Institute, The Open University, Walton Hall, Milton Keynes, MK7 6AA, UK, [3]Geology (Earth Sciences and Engineering), Imperial College of Science Technology and Medicine, London, UK, [4]Museum of Western Australia, Francis St, Perth, WA 6000, Australia, [5]School of Earth Sciences and Geography, Kingston University, Kingston-upon-Thames, Surrey, KT1 2EE, UK.

Introduction: The nature of the extraterrestrial bodies that created some terrestrial impact craters has been determined by collection of disrupted and shocked impactor fragments (e.g. the well-known iron meteorite Canyon Diablo from the vicinity of Barringer Crater, Arizona). In other cases, finding sufficient chemical residue from the bolide for diagnostic analysis has proven more difficult, yet modern trace-element and particularly isotopic analyses have been successfully employed, e.g. [1]. The big question is often: "In a limited field investigation, where should we look?"

Locations of Residue Preservation: If a major melt sheet is still preserved (e.g. Ries, Germany or Popigai, Siberia) materials may be relatively easy to collect for analysis and recognition of extraterrestrial signature, especially as there can be remarkably widespread dissemination of impactor residue. Many large impact structures are exposed only as deep remnants (e.g. Vredefort, South Africa and Sierra Madera, Texas). These may show characteristic large-scale structure (e.g. central uplifts and ring-synclinoria) and diagnostic shock indicators (e.g. shatter cones, planar deformation fabrics and high pressure mineral polymorphs), yet have lost the high-level crater morphology, ejecta-blanket and melt sheet.

Fractures: Intriguingly, some eroded structures have been shown to retain extraterrestrial residues and debris from high structural levels, within fractures into the basement and rim rocks, e.g. Vredefort [1] and Roter Kamm [2]. We have found distinctive, fine-scale siderophile element segregations in breccias from the Rieskrater, akin but not identical to those of impact glasses from Barringer, Lonar, Wabar and Monturaqui craters. In some craters there is also evidence of substantial outward motion of target debris along major radial fracture systems, such as in the 'Offset Dykes' at Sudbury [3]. Outward compressive motion along early brittle structures has been seen in the reverse faults of the Chicxulub [4] and Silverpit [5] craters.

Modeling: Numerical modeling has proven remarkably successful in simulation of the larger scale features of crater development. The significance of small-scale brittle structures has also become apparent from both modeling and field studies [6]. Important questions that have not yet been fully addressed by simulations of large crater formation include timing and location of major fractures in relation to the availability of bolide material, and also the role of early-formed fractures in outward transport, thickening, and subsequent inward crater collapse.

Evidence from small craters: We have studied millimeter-scale impact craters on brittle, laminated glass solar cells exposed to hypervelocity collision during exposure in low Earth orbit on the Hubble Space Telescope [7]. Craters may contain particulate impactor residue in fractures, as well as in a thin melt sheet. The fractures have been considered late-stage features, due to extensional failure close to the glass surface, following passage of a shock wave through the laminate structure. Our laboratory experiments, utilising a light gas gun, also reveal delicate, volatile-rich residues in fractures. Such small craters show outward directed thrusts, but do not undergo significant gravitational shape modification.

Numerical modeling: Modeling of analogous small impacts, utilising Century Dynamics Autodyn version 4.1.09 [8], has revealed that extensive fractures are generated early in the impact process, prior to rebound of the crater floor and ejection of the remnants of the impacting body. The model fractures correspond in position and orientation to locations in which we have observed residue in space-exposed and laboratory craters.

Conclusions: Although we do not suggest that the results of simulation from a mm-size should be scaled to km-size craters, our intriguing results suggest that modeling the early brittle responses of geological materials in lithified stratified target sequences may help to explain the distribution of fracturing and residue emplacement in and around major craters.

References:

[1] Koeberl C. et al. (1996) *Geology, 24*, 913-916. [2] Degenhardt J. J. et al. (1994) *Geological Society of America Special Paper 293,* 197-208. [3] Spray J. G. (2001) pers. comm. [4] Morgan J. and Warner M. (1999) *Nature, 390,* 472-476. [5] Stewart S. A. and Allen P. J. (2002) *Nature, 418,* 520-523. [6] Kenkmann T. and Ivanov B. A. (1999) *LPS XXX*, Abstract #1544. [7] Graham G. A. et al. (2000) *Adv. Space Research, 25*, 303-307. [8] McDonnell J. A. M. et al. (2001) *Int. Journal of Impact Engineering, 26*, 487-496.

CRATER BASIN REBOUND ABOVE PLASTIC LAYERS: MODEL BASED ON EUROPA. Akos Kereszturi (Department of Physical and Historical Geology, Eötvös Loránd University of Sciences, H-1083 Budapest, Ludovika tér 2., Hungary, E-mail: krub@freemail.hu)

Introduction: Isostatic rebound and mega-slumpings are important processes in the modification of large craters. Beside the exmaples for these on Mercury, Moon, Earth, Callisto (possibly Venus and Mars) we have good images from Europa. Analysis of internal rings and benches of great (usually greater than 100 km) craters and palimpsests help in the reconstruction of formation. The its young, pristine and tectonically homogene surfaced Europa can improve our knowledge in the reconstruction of crater basin formation.

The modell: Based on our up to date knowledge, the origin of the circular – and not central – ring structures are the follows (Fig. 1.) [1]: 1. Outcrops of isostatically uplifted internally layered matter [2],

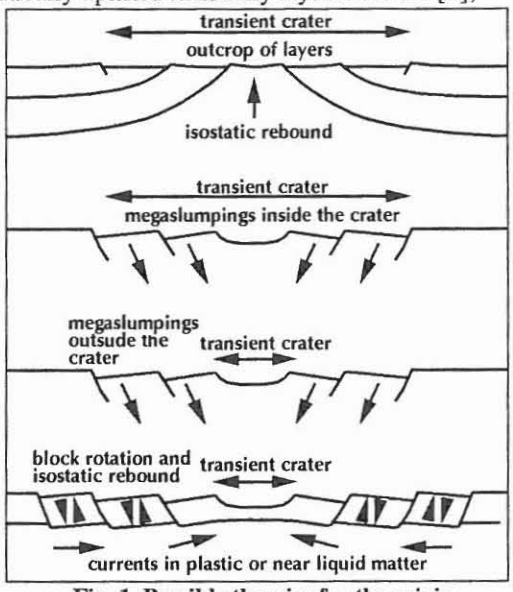

Fig. 1. Possible theories for the origin

2. Mega-slumpings inside the crater. 3. Mega-slumpings outside the crater. 4. Block rotation and isostatic lifting [3]. With the analysis of the great craters of Europa we can nearly rule out the internal layering and slumping theories in the formation. Because of the thin ice crust Europa can serve as a unique modell for the crater formation on terrains with small lithospheric thickness, and it gives the possibility for the analysis of ancient craters on the Earth and current craters on Venus with relative thin litospheres.

Results: We analysed 32 relative great craters on icy moons, the best examples of them are on Europa (Fig. 2.). We make a somewhat similar analysis for the greatest basins on rocky bodies (eg. Caloris, Orientale, Argyre). We measured the diameters of the structures, the topography, the distribution of certain structures according to the crater diameter/the possible thickness of the lithosphere/cryosphere, distance from the center. The greatest problem is the definition of the original crater rim or the transient crater and to devide the internal rings from the outer narrow tectonic structures. We suggests: 1. Structures are originated by isostatic re- bound and not by megaslumpings or outcrops of layered matter. 2. Circular faults ouside the original craters form in great number on icy bodies. In the future we will extend the analysis: 1. Relation between possible transient crater diameter and outer rings. 2. To make „evolutionary sequence" for giant craters with rebounded floors accourding to the reaction of the lithosphere and gravity [5,6], which can be useful in the analysis of ancient rheologic conditions in rocky bodies.

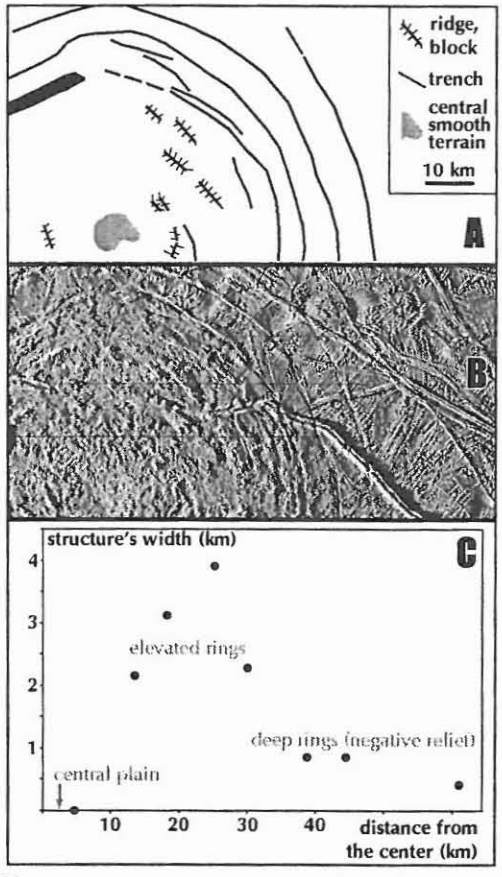

Fig. 2. Example structures

References: [1] Dence, M.R. et al. (1977) Terrestrial impact structures, Perrgamon Press, 1977. [2] Milton, D.J. et al. (1972) Displacement with impact craters, Proc. 24th Int. Geol. Congr. [3] Roddy, D.J. (1977), Large-scale impact and explosion craters, Pergamon Press, 1977. [5] Melosh H.J. (1989) Impact Cratering, Oxford Univ. Press. [6] Baldwin R.B. (1981) in Multiring Basins, LPI.

USING GEOCHEMICAL OBSERVATIONS TO CONSTRAIN PROJECTILE TYPES IN IMPACT CRATERING. Christian Koeberl, Institute of Geochemistry, University of Vienna, Althanstrasse 14, A-1090 Vienna, Austria (e-mail: christian.koeberl@univie.ac.at).

Introduction: Breccias and melt rocks found at possible meteorite impact structures on Earth may contain a minor extraterrestrial component. In the absence of evidence of shock metamorphic effects in such rocks, the unambiguous detection of an extraterrestrial component can be of diagnostic value regarding the impact origin of a geological structure. The verification of an extraterrestrial component in impact-derived melt rocks or breccias can be of diagnostic value to provide confirming evidence for an impact origin of a geological structure. Similar approaches are of great value in the investigation of distal ejecta layers (as we are taught by the case history of the Cretaceous-Tertiary boundary).

Qualitatively speaking, a small amount of the finely dispersed meteoritic melt or vapor is mixed during the impact event with a much larger quantity of target rock vapor and melt, and this mixture later forms impact melt rocks, melt breccias, or impact glass. In most cases, the contribution of meteoritic matter to these impactite lithologies is very small (<<1%), leading to only slight chemical changes in the resulting impactites. Geochemical methods can be used to determine the amount of such a meteoritic component (see below). However, there are plenty of open questions.

Methods: The detection of such small amounts of meteoritic matter within the normal upper crustal compositional signature of the target rocks is rather difficult. Only elements that have high abundances in meteorites, but low abundances in terrestrial crustal rocks (e.g., the siderophile elements) are useful. Another complication is the existence of a variety of meteorite groups and types, with widely varying siderophile element compositions. Distinctly higher siderophile element contents in impact melts, compared to target rock abundances, can be indicative of the presence of either a chondritic or an iron meteoritic component. Achondritic projectiles (stony meteorites that underwent magmatic differentiation) are much more difficult to discern, because they have significantly lower abundances of the key siderophile elements. Furthermore, in order to reliably constrain the target rock contribution of such elements, i.e., the so-called indigenous component, absolute certainty must be attained that all contributing terrestrial target rocks have been identified and their relative contributions to the melt mixture are reasonably well known.

Geochemical methods have been used to determine the presence of the traces of such an extraterrestrial component (see review [1]). Meteoritic components have been identified for just over 40 impact structures [1], out of the more than 160 impact structures that have so far been identified on Earth. The identification of a meteoritic component can be achieved by determining the concentrations and interelement ratios of siderophile elements, especially the platinum group elements (PGEs), which are several orders of magnitude more abundant in meteorites than in terrestrial upper crustal rocks. Iridium is most often determined as a proxy for all PGEs, because it can be measured with the best detection limit of all PGEs by neutron activation analysis (which was, for a long time, the only more or less routine method for Ir measurements at sub-ppb abundance levels in small samples).

The use of PGE abundances and ratios avoids some of the ambiguities that result if only moderately siderophile elements (e.g., Cr, Co, Ni) are used in an identification attempt. However, problems may arise if the target rocks have high abundances of siderophile elements or if the siderophile element concentrations in the impactites are very low. In such cases, the Os and Cr isotopic systems can be used to establish the presence of a meteoritic component in a number of impact melt rocks and breccias (e.g., [2]). In the past, PGE data were used to estimate the type or class of meteorite for the impactor, but these attempts were not always successful. It is difficult to distinguish among different chondrite types based on siderophile element (or even PGE) abundances, which has led to conflicting conclusions regarding the nature of the impactor at a number of structures (see [1]). Clearly, the identification of a meteoritic component in impactites is not a trivial problem.

Open Questions: Apart from analytical challenges, there is a whole suite of problems or questions associated with the identification of projectiles, which will be listed here in no particular order.

Some meteorite types do not have chemical compositions that are well enough separated from terrestrial rocks to allow a geochemical distinction in melt rocks. The chemical composition of specimens of the same meteorite type is not uniform, but shows a range of compositions. In addition, only a few samples of each type have been analyzed with enough detail to allow use of the data for mixing calculations. It is not yet possible to distinguish between comet and asteroid sources due to the lack of trace element data on a sufficient number of comet nuclei samples.

More peculiar, and possibly a point in which modeling calculations can be of use, is the very strange discrepancy between the interelement ratios of siderophile elements in impact glasses found at small impact craters and equivalent ratios in corresponding meteorite fragments found at the same craters (e.g., Meteor Crater, Wolfe Creek, Henbury, Wabar). No immediate physical explanation, or correlation with chemical and physical parameters, which could explain this fractionation, is available. In some other cases (e.g., Tswaing-Saltpan, Bosumtwi) there is a good fit for, e.g., Cr, Co, and Ni ratios and abundances between a particular meteorite type (e.g., chondrite), but the Ir abundances are about a factor of 2-10 too low for a chondritic projectile (which might otherwise also be confirmed by isotopic data). Why are some of the more refractory siderophile elements depleted? Is there some non-equilibrium process going on in the impact vapor plume?

Another interesting item are tektites. Tektites are natural glasses occurring on earth in four distinct strewn fields: Australasian, Ivory Coast, Central European, and North American. Ages of these strewn fields range from 0.78 to 35 million years. Geochemical arguments have shown that tektites have been derived by hypervelocity impact melting from terrestrial upper crustal rocks. Tektites are distal ejecta, which do not occur directly at a source crater, in contrast to impact glasses, which are found directly in or at the respective source crater. This has made the identification of the source crater somewhat difficult. Nevertheless, at least two of the four Cenozoic tektite strewn fields have been associated with known impact craters: the Ries crater in southern Germany and the Central European field, and the Bosumtwi crater in Ghana and the Ivory Coast field are rather firmly linked. In addition, the 85 km diameter Chesapeake Bay impact structure is a likely source crater for the North American tektites. This leaves the Australasian tektites as the only strewn field without a clear choice for a source crater.

Not much is known about the source meteorites (projectiles, meteorite types) for the four tektite fields. Attempts to determine of a meteoritic component in Australasian tektites has not yielded unambiguous results. Some Ni-Fe-rich spherules in philippinites, which were suggested to be a remnant of meteoritic matter, were later concluded to have formed by in-situ reduction from target material. Analyses of australites by radiochemical neutron activation analysis for a selection of volatile and siderophile element concentrations was not very conclusive either - only one of these samples showed a distinct enrichment in siderophile elements, while the other five do not indicate such an enrichment. On the other hand, Ir enrichments were found in several microtektite-bearing deep-sea sediment layers.

Regarding the Ivory Coast tektites, some researchers suggested an iron meteorite projectile (based on chemical data), others (more recently suggested a chondritic projectile). Os isotopic data clearly showed the presence of a meteoritic component in the tektites. Unfortunately, the Bosumtwi crater is in an area of known gold mineralization, which lead to high and irregular siderophile element contents in the target rocks.

Not much information is available regarding the Central European tektites, where an achondrite has been proposed for the Ries crater bolide. No information at all is available regarding the Chesapeake Bay crater/North American tektites. Thus, the question of projectile identification for tektites is still an open one.

In general, tektites are very poor in meteoritic matter, which led to the suggestion that they cannot form by jetting, as products formed by jetting should have high meteoritic components. On the other hand, tektites clearly formed from the rocks closest to the terrestrial surface – in some cases there is a soil component discernable. However, some recent data show that high-Mg microtektites do seem to have a significant (a few percent) meteoritic component. It seems that natural observations are still able to provide some puzzling constraints for future modeling calculations.

References: [1] Koeberl C. (1998) in: Meteorites: Flux with Time and Impact Effects, eds. M.M. Grady et al., Geological Society of London Special Publ. 140, pp. 133-152. [2] Koeberl C. et al. (2002) in: Geological Society of America Special Paper 356, pp. 607-617.

AMELIA CREEK, NORTHERN TERRITORY, AUSTRALIA: A 20 X 12 KM OBLIQUE IMPACT STRUCTURE WITH NO CENTRAL UPLIFT. F. A. Macdonald[1] and K. Mitchell[2], [1]Division of Geological and Planetary Sciences, Mail Code 170-25, California Institute of Technology, Pasadena, CA 91125, USA, francis@gps.caltech.edu, [2]Gerringong, NSW, Australia.

Introduction: The Amelia Creek Structure is located in the Davenport Ranges of the Northern Territory, Australia at lat. 20°55'S, long. 134°50E. Shock metamorphic features are developed on the southern, downrange side of the structure. No central uplift is developed and the dimensions of the impact structure are at least 20 X 12 km.

Geological Observations: Geologically, the Amelia Creek structure is situated within the Proterozoic sedimentary and volcanic rocks of the southern Tennant Creek Inlier. The structure is characterized by a central syncline flanked by a series of ramping, SSW trending thrust sheets. The canoe-shaped central trough (syncline) runs NNE-SSW and is ~1 km wide and 5 km long. Shatter cones, impact breccias and hydrothermal deposits were also discovered during detailed mapping of the central region in June of 2002.

Shatter cones at Amelia Creek are prolific in many quartzite beds on the southern side of the structure (fig. 1), and are invariably oriented upward, which in itself excludes the possibility that the impact occurred before the regional folding at ~1700 Ma [1]. The surface distribution of shatter cones forms a crescent-like shape approximately 1 X 3 kilometers on the southern side of the structure, extending at least 4 km south from the central syncline.

Allogenic breccias are developed along many of the major thrust faults within the structure. These breccias show evidence of baked margins and contain shocked clasts.

Discussion: Most impacts occur obliquely, not vertically as typically modeled [3]. In very oblique impacts, the initial transfer of energy into the target is less efficient and the resulting craters are smaller for a given impactor mass and velocity [2]; oblique impacts should produce much shallower deformation than their more vertical counterparts, and perhaps central uplifts do not develop even for large structures.

Paleozoic erosion rates estimate that a kilometer of rock is denuded from the surface of Australia every 100 Ma [4]. The presence of large breccia sheets indicates that the current level of exposure is less than a kilometer below the original crater floor, and thus the impact probably occurred sometime in the Phanerozoic. Some breccias in and around the structure were originally mapped as Cambrian and Tertiary breccias [1], but they may actually be impact breccias and impact ejecta; however, as deep canyons cut the structure and no impact melt has yet been identified it seems unlikely that the impact occurred in Tertiary times.

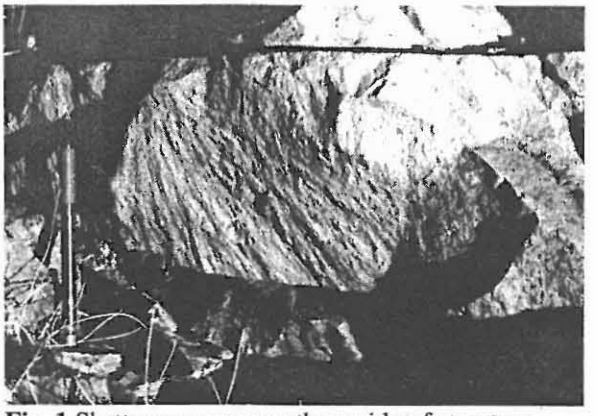

Fig. 1 Shatter cones on southern side of structure.

The rocks uprange of the structure also appear to be anomalously deformed, so there is a distinct possibility that Amelia Creek is part of a crater field or a ricochet structure. On geological maps, Aster and aeromagnetic images, the total area of anomalous deformation around Amelia Creek is strikingly similar in shape to the extremely oblique impact structures on Mars and the Moon [3].

Conclusion: We believe that the shock metamorphosed rocks at Amelia Creek are the relict of an extremely oblique impact event. Evidence for this includes the elongation of the deformed area, the SSW direction of movement of most of the structural elements, the presence of a central trough and syncline in place of a central uplift, and the distribution of shatter cones only on the downrange side of the structure.

The mechanics of large, very oblique impact cratering is poorly understood [2]. This is due in part to the fact that no exposed, extremely oblique terrestrial impact structures have been previously reported [5]. As such, there are very few field measurements to put constraints on theoretical models. The impact-deformed rocks in the Davenport Ranges are incredibly well exposed, and this structure promises to be the world's type locality for oblique impacting.

References:

[1] Stewart A. J. et al. (1984), Expl. Notes of the 1: 250,000 Bonney Well Sheet, BMR. [2] Melosh H. J. (1989) Impact Cratering: A Geologic Process. Oxford, 11. [3] Schultz P.H. and Gault D.D. (1990), GSA Spec. Pap. 247. [4] Koln et al., Aus. JES (2002), 49. [5] Spray J.G. (2002) Earth Impact Database http://www.unb.ca/passc/ImpactDatabase/CINameSort.html

GOLDILOCKS AND THE THREE COMPLEX CRATER SCALING LAWS. William B. McKinnon,[1] Paul M. Schenk[2], and Jeffrey M. Moore[3], [1]Dept. of Earth and Planetary Sciences and McDonnell Center for the Space Sciences, Washington University, Saint Louis, MO 63130, mckinnon@levee.wustl.edu; [2]Lunar and Planetary Institute, 3600 Bay Area Blvd, Houston, TX 77058, schenk@lpi.usra.edu, [3]NASA Ames Research Center, Moffett Field, CA 94035, jmoore@mail.arc.nasa.gov.

Introduction: Formed in the gravity regime, complex craters are larger than their simple crater equivalents, due to a combination of slumping and uplift. Just how much larger is a matter of great interest for, for example, age dating studies. We examine three empirical scaling laws for complex crater size [1-3], examining their strengths and weaknesses, as well as asking how well they accord with previously published and new data from lunar, terrestrial, and venusian craters.

Croft (1985): The most widely quoted complex crater scaling is due to the detailed study of S.K. Croft [1]. He gauged the upper and lower limits to the position of the transient crater rim provided, respectively, by the terrace sets and central peak complexes of lunar and terrestrial complex craters. Added to these were a range of crater enlargements based on theoretical and experimental evidence for the geometric similarity of ejecta blankets [4]. Finally, a geometric restoration model was used to get an independent estimate. Bracketed mainly by terrace sets for craters closer to the simple-to-complex transition and central peak complexes of very large lunar craters (a size range that could have included peak-ring basins), he determined that the transient diameter D_{tr} scaled as $D^{0.85 \pm 0.04}$, where D is the final diameter. Inverting, we get

$$D = D_c^{-0.18 \pm 0.05} D_{tr}^{1.18 \pm 0.06} , \quad (1)$$

where D_c is the diameter of the simple-to-complex transition. A little remarked on aspect of this scaling law is that it nearly restores the diameter (through not the volume) of complex craters to strength scaling (i.e., D is proportional to $a^{0.92}$, where a is the impactor radius).

McKinnon and Schenk (1985): We used a transient crater restoration model for the Moon, based on Pike's lunar crater morphometric data [5]. Crater rims were restored using a range of constant slope angles for the ejecta deposit, with the restoration criterion being that the transient apparent (ground-plane) crater had a depth/diameter of $1/2\sqrt{2}$ [6]. Remarkably, the derived depth/diameter ratios for the full transient crater were close to constant, which is self-consistent support for transient crater geometric similarity. In terms of fit to a power law, we found

$$D = k D_{tr}^{1.13} , \quad (2)$$

where k is a constant. For the Moon, our k implied that simple craters near the simple-to-complex transition (~11 km from depth/diameter statistics) are ~15-20% wider than their original transient craters. This amount agrees with the amount of widening calculated for Brent and Meteor Craters due to breccia lens formation [6]. At the time it was less appreciated that all simple craters in rock are probably shallowed and widened by breccia lens formation. Breccia lens formation is something that has not been observed in laboratory impact studies to our knowledge (certainly not in dry sand), so direct application of sand crater scaling laws, even to simple craters, should be done with caution.

As for eq. (2), it can be put in the same functional form as eq. (1) if k is proportional to $D_c^{-0.13}$, and we recommend $k = 1.17 D_c^{-0.13}$. Using such, [2] were able to show that the continuous ejecta blankets on the Moon and Mercury measured by [7] could be close to geometrically similar if compared in terms of transient crater diameter.

Holsapple (1993): Holsapple presented, in his review of crater scaling, a new model for complex crater scaling, also based on volume conserving geometric restoration, but using improved functional forms for the ejecta blankets of craters derived from laboratory experiments in sand [e.g., 4]. Although details were not given, the overall functional form is familiar:

$$D = 1.02 D_c^{-0.086} D_{tr}^{1.086} . \quad (3)$$

A slightly different form was given in terms of transient excavation radius, which presumably refers to the ground plane.

Comparisons: All three scaling laws have similar forms but clearly different exponential dependences. They cannot all be correct. Each scaling law uses a different definition or value for D_c on the Moon, as well, which complicates comparisons. In terms of an "equivalent simple crater," however, eqs. (1-3) predict, e.g., 70.7, 74.1, and 79.7 km, respectively, for the 93-km-diameter Copernicus. We will discuss which of the formulations give too much or too little crater enlargement, and which if any might be considered "just right."

References: [1] Croft S.K. (1985) *JGR, 90, suppl.*, C828–C842. [2] McKinnon W.B. and Schenk P.M. (1985) *LPSC XVI*, 544-545. [3] Holsapple K.A. (1993) *AREPS, 21*, 333–373. [4] Housen K.R. et al. (1983) *JGR, 88*, 2485–2499. [5] Pike R.J. (1977) in *Impact and Explosion Cratering*, Pergamon, 484-509. [6] Grieve R.A.F. and Garvin J.B. (1984) *JGR, 89*, 11,561–11,572. [7] Gault D.E. et al. (1975) *JGR, 80*, 2444–2460.

MODELING METEORITE IMPACTS: WHAT WE KNOW AND WHAT WE WOULD LIKE TO KNOW. H. J. Melosh (Lunar and Planetary Lab, University of Arizona, Tucson AZ 85721. jmelosh@lpl.arizona.edu).

Meteorite impacts can be studied by computer simulation: Large meteorite impacts are among those phenomena that are either too large or too dangerous to study experimentally. Although impacts have affected the formation and surfaces of nearly every body in the solar system, we are limited to observing the results of past events. Investigation of impact processes is thus divided into observational studies of the traces of past impacts, small-scale analogue laboratory experiments and, most recently, detailed computer modeling. Computer models offer the possibility of studying craters at all scales, provided we completely understand the physics of the process and possess enough computer power to simulate the features of interest [1].

But computer models cannot do everything! One of the most common disappointments of geologists not familiar with modeling is that computer simulations cannot answer all questions we might like to ask. Numerical simulations suffer two major shortcomings: One is that they cannot treat processes that are not included in the computer code. Thus, no computer code presently treats the chemical or isotopic interactions that occur during an impact. This does not mean that such processes are untreatable, just that the appropriate codes that embody the correct physics must be created. In some cases the physics is poorly known and research must be done to improve the basic foundations. The second shortcoming stems from resolution in both space and time. All digital computer simulations depend on dissecting time and space into discrete blocks. The number of such blocks is limited by the amount of time and physical memory available for the computation. These limits can be easily exceeded by even an apparently modest computation. Thus, if an investigator wants to know about the dynamics of meter-size ejecta blocks in a 10 km diameter impact crater, he or she may discover that the required resolution far exceeds the capacity of any existing computer (a 3-D computation must include at least 10^12 computational cells!). Models to "predict" the effects of the impacts of Shoemaker/Levy 9 fragments with Jupiter [2] were still running at the time of the impacts, more than a year after the comet was discovered! These limitations can be surmounted both by faster computers with more memory as well as by better solution algorithms, such as the recent adoption of SPH codes when both hydrodynamics and self-gravity are important in a simulation [3].

Before beginning any computer simulation it is important to ask whether the numerical computation is capable of answering the desired question. Are all of the relevant processes included in the code to be used? Can the problem be solved in reasonable time on the available hardware? Too often the answer is "no" and the potential modeler must look elsewhere for enlightenment. But there **are** plenty of open questions that are still ripe for computer solutions.

The three pillars of impact simulation: The physics needed to simulate large meteorite impacts lies squarely in the classical domain. The size scale is so large that quantum effects are not important (although quantum mechanics does determine the thermodynamic equation of state) and the velocities are well below the speed of light, so classical Newtonian mechanics, supplemented by classical thermodynamics, provides an adequate framework for modeling impacts. In addition, it has become clear that successful simulation of real impact craters often requires a detailed understanding of the response of real rocks to stress and heat.

Of these three supporting pillars, Newtonian mechanics is probably the least troublesome. All modern "hydrocodes" (a now obsolete term that reflects the historical development of computer codes that, at first, did not contain material strength) incorporate the standard F = ma foundation of mechanics, although this is often obscured by an impressive amount of bookkeeping to keep track of all the pieces. All codes incorporate some form of gravitational acceleration, although only a few employ self-gravitation (only important in planet- scale impacts). It is notable that there do not appear to be any talks at this conference on this aspect of computer modeling.

The next supporting pillar is thermodynamics, through the equation of state [4]. The equation of state for impact modeling is a little peculiar: Instead of the conventional thermodynamic relation relating pressure P to density ρ and temperature T, $P(\rho,T)$, hydrocodes require a relation between P, ρ and internal energy E. Equations of state for metals have been vigorously pursued by squadrons of physicists since the end of WWII, mainly to support the design and testing of nuclear weapons. However, few good equations of state exist for geologic materials, such as rock or ice. More research is needed to create these important relations.

Finally, in the late stages of an impact event material strength becomes important. Very little work has been done on good strength models for rock [5]. Porosity is also now recognized to play a key role for some impacts, especially on asteroids, which recent research has shown might be as much as 50% porous. Impact crater collapse and the morphology of large craters are controlled by strength, and observations suggest that a poorly understood mechanism must operate to greatly degrade the strength of rocks surrounding an impact site shortly after an impact event

[6].

What next? Our ability to numerically simulate impact events is currently being taxed by a number of difficult problems. We are concerned about the possibility of impacts causing future extinctions, as they did at the K/T boundary. Two and three-dimensional models have already been used to estimate the mass and type of environmentally active gases released by the impact [7], but the ultimate effects of these gases on climate is still largely unknown. Chemical reactions of material in hot vapor plumes may be important for both environmental effects as well as explaining the observed oxidation state and isotopic fractions observed in the ejecta. Several new craters with unusual morphologies such as the Silverpits crater in the North Sea [8] and the Chesapeake Bay crater [9] challenge our understanding of the response of the Earth's surface to large impacts. Crater morphologies on Europa [10] may be indicating the thickness of the ice shell beneath the surface, but we must understand the cratering process better before we can cite a numerical value for the thickness. An active question is whether damaging tsunami result from relatively small impacts in the Earth's ocean. Solving this problem requires a full understanding of interactions near the surface and the physics of wave breaking, a new challenge to existing computer codes.

We currently have a list of urgent needs for making our simulations more realistic. Much work is needed in the near term on equations of state and constitutive models for geologic materials. We will hear more about these needs in subsequent talks. Nevertheless, numerical modeling of impact processes has made important contributions to our understanding of impacts in the past and will surely continue to do so in the future.

References:

[1] Anderson, C.E. (1987) *Int. J. Impact Engineering* **5**, 33.
[2] Zahnle, K. & Mac Low, M.-M. (1994) *Icarus* **108**, 1.
[3] Benz, W. in *Numerical Modeling of Nonlinear Stellar Pulsation: Problems and Prospects* (eds. Buchler, J.R.) 269 (Kluwer Academic, Dortrecht, 1990).
[4] Melosh, H.J. *Impact Cratering: A Geologic Process* 1-245 (Oxford University Press, New York, 1989).
[5] Ivanov, B.A., Deniem, D. & Neukum, G. (1997) *Int. J. Impact Eng.* **20**, 411.
[6] Melosh, H.J. & Ivanov, B.A. (1999) *Ann. Rev. Earth Planet. Sci.* **27**, 385.
[7] Pierazzo, E., Kring, D.A. & Melosh, H.J. (1998) *J. Geophys. Res.* **103**, 28607.
[8] Stewart, S.A. & Allen, P.J. (2002) *Nature* **418**, 520.
[9] Poag, C.W. (1997) *Sed. Geol.* **108**, 45.
[10] Turtle, E.P. & Pierazzo, E. (2001) *Science* **294**, 1326.

LIMITS TO THE PRESENCE OF IMPACT-INDUCED HYDROTHERMAL ALTERATION IN SMALL IMPACT CRATERS ON THE EARTH: IMPLICATIONS FOR THE IMPORTANCE OF SMALL CRATERS ON MARS. H. E. Newsom and Hagerty J. J., University of New Mexico, Institute of Meteoritics, Dept. of Earth & Planetary Sciences, Albuquerque, NM 87131 U.S.A. Email: Newsom@unm.edu

Introduction: Impact craters on the earth contain evidence for hydrothermal activity. An important property of small craters is the limit to the amount of energy deposited during the impact that can lead to hydrothermal activity. Hydrothermal activity is potentially important for producing alteration minerals, trapping water, and transporting mobile elements to the martian surface. Hydrothermal systems in impact craters may also be important for astrobiological investigations in terms of providing environments for organic chemical processes to occur and as near-surface locations that could be easily investigated by surface exploration missions [1]. Another important reason for understanding the lower limit on thermal effects for small craters is in the use of small superimposed craters as probes of larger craters during surface missions. If hydrothermal material is found associated with superimposed craters it will be important to distinguish between hydrothermal events associated with the earlier versus the later crater. In the future, comparisons of our observations with numerical models for the formation of small craters can lead to a better understanding of the role of small craters on Mars.

Lonar Crater: The 50,000 year old, 1.8km diameter Lonar crater is located in Maharashtra, India (19°58'N, 76°31'E) [2]. This relatively small crater is of particular interest because of its unique morphological and mineralogical properties, which make it a valid analogue for similar craters on the surface of Mars [2, 3]. We show that even in this relatively small crater substantial hydrothermal alteration has occurred, probably due to the thermal effects of the impact event.

In addition to textural data from the SEM, microprobe and X-ray diffraction were used to determine the nature of alteration minerals in the Lonar samples. The microprobe results suggest that the majority of the clay materials in the Lonar samples are saponites and celadonites. Both saponite and celadonite are produced during the hydrothermal alteration of basalt, typically at temperatures of 130-200°C. The production of these "hydrothermal" clays at Lonar was further established through geochemical modeling of the alteration process, and by stable isotope analysis.

Limits to hydrothermal activity in terrestrial craters: The presence of hydrothermal alteration at the Lonar crater can be used to suggest that Lonar is near the lower heat limit for generating hydrothermal processes, thus establishing a new lower size limit of 1.8 km diameter for impact-induced hydrothermal activity. A hydrothermal system has been documented in the somewhat larger 4 km diameter Kärdla impact crater [4]. In contrast, no evidence of hydrothermal activity has been found in the smaller 1.13 km diameter Pretoria Saltpan (Tswaing) crater [5], or in the 1.2 km diameter Meteor Crater in Arizona [6]. This information can be used to imply that small martian craters greater than one or two kilometers in diameter may also have the potential to form hydrothermal systems, as long as water was present in some form.

Implications for Mars: Hydrothermal alteration is important for trapping fluids, such as water in the subsurface of Mars, and for releasing material to the surface. As a preliminary example, the amount of water that could be trapped due to alteration of craters in the size range from 2 to 11 km in diameter can be calculated. Assuming an average depth of alteration of 400 m, a degree of alteration of 3% based on the average of our SEM feature scan determinations, a volume of altered material equivalent to a global layer of 2.8 m will be formed over martian history. Assuming a water content of 10 wt% (e.g. similar to the amount in Lafayette martian meteorite iddingsite alteration material) this amount of material could trap an amount of water equivalent to a global layer of water 0.7 m deep. The one-meter value compares to estimates of the amount of water on Mars ranging up to a few hundred meters. In contrast Griffith and Shock [7] estimated that 8% alteration of 10% of the Martian crust could trap 30 m global equivalent of water.

References: [1] Newsom et al., (2001) *Astrobiology 1* 71. [2] Fredriksson, K. et al. (1973) *Science, 180,* 862. [3] Hagerty and Newsom (2003) *JGR* submitted. [4] Kirsmäe K. et al., (2002) *MAPS 37*, 449-457. [5] Brandt D. AND Reimold W.U. (1999) *Memoir 85* Council for Geoscience, Geological Survey of South Africa, 6-34. [6] Hörz F., et al (2002), *MAPS, 37*, 501-531. [7] Griffith L. L., and Shock E. L. (1997) *JGR 102*, 9135-9143.

SULFUR CHEMISTRY IN K/T-SIZED IMPACT VAPOR CLOUDS. S. Ohno[1], S. Sugita[1], T. Kadono[2], S. Hasegawa[3], G. Igarashi[4], [1]Dept. of Earth and Planetary Science, University of Tokyo (email: oono@space.eps.s.u-tokyo.ac.jp), [2] Institute for Frontier Research on Earth Evolution, Japan Marine Science and Technology Center, [3]The Institute of Space and Astronomical Science, [4]Laboratory for Earthquake Chemistry, University of Tokyo

Introduction: The geologic record indicates that the mass extinction at K/T boundary, 65 Myrs ago, was caused by a hypervelocity impact of an asteroid or a comet [1]. During the K/T impact event, a large amount of sulfur was degassed from the impact site [e.g., 2, 3, 4]. The degassed sulfur converts to sulfuric acid aerosol and stays in the stratosphere for a long time [3, 4]. This reduces the sunlight significantly and leads to a mass extinction. However, if the degassed sulfur is dominated by SO_3 not SO_2, then the conversion to sulfuric acid aerosol occurs very rapidly and the blockage of sunlight does not last for a long time [3, 4, 5]. The chemical reaction of sulfur-oxides in an impact vapor cloud, nevertheless, has not been studied in detail previously, and the SO_2/SO_3 ratio in a vapor cloud is yet highly uncertain. The purpose of this study is to estimate the SO_2/SO_3 ratio in the K/T impact vapor cloud. Here we discuss the results of calculation of chemical equilibrium and kinetics of sulfur-containing species in an impact vapor cloud as well as mass spectroscopic analysis of vapor plumes created by laser irradiation on anhydrite.

Chemical Equilibrium Calculation: We calculated equilibrium chemical composition in vapor clouds generated from calcium sulfate ($CaSO_4$). We assumed several different impact velocities and different types of projectiles for the K/T impact.

The result of the calculation indicates that $SO_2+1/2O_2$ is more stable at high temperatures and high pressures and that SO_3 is more stable at low temperatures and low pressures. Over the entire range of the impact conditions we assumed, the SO_2/SO_3 ratio dramatically changes in the range between 600K and 1000K. If the reaction SO_2+O to SO_3 quenches at a temperature higher than 1000K, most of impact-degassed sulfur is released to the environment as SO_2. However, if the reaction SO_2+O to SO_3 quenches at a temperature lower than 600K, SO_3 is dominant.

Kinetics of Redox Reaction of Sulfur Oxides: We estimate the SO_2/SO_3 ratio in vapor clouds at the quenching temperature using a theoretical evaluation of chemical reaction rate of the reaction SO_2+O+M to SO_3+M [6]. The result of the calculation indicates that the SO_2/SO_3 ratio is smaller for a vapor cloud with a larger mass and that the SO_2/SO_3 ratio in a K/T-size vapor cloud is approximately unity. Because the result of this kinetic model estimation is an upper limit of the SO_2/SO_3, the SO_2/SO_3 ratio in K/T-size impact vapor cloud may have been much smaller than unity.

Laser Irradiation Experiment: A YAG laser beam (1.06μm of wave length, 25-400 mJ of pulse energy, 0.5-2 mm of irradiation spot diameter) was irradiated to a sample of anhydrite in a vacuum chamber. Vapor degassed by laser irradiation was analyzed with a quadrupole mass spectrometer (QMS). The gas sample obtained in every laser irradiation experiment was dominated by SO_2, but SO_3 was also detected. The SO_2/SO_3 ratios measured in experiments were between 80 and 300, and decrease with the laser beam diameter. The dependence of the SO_2/SO_3 ratio on laser beam diameter is $SO_2/SO_3 = 120D^{-0.61}$.

The SO_2/SO_3 ratio in the experiment is about 10^{-3} time that in the kinetic model estimation for the size of vapor clouds produced in the laboratory. Our experimental results also show that the rate of decrease in the SO_2/SO_3 ratio obtained in the laser experiment as a function of vapor mass is higher than that predicted by the kinetic calculation. The power-low relation obtained in the laser experiments predicts that it will be 10^{-6} for a K/T-size impact vapor cloud. This strongly suggests the possibility that SO_3 was dominant in the degassed sulfur by the K/T impact.

Conclusion: Chemical equilibrium calculation indicates that SO_3 is more stable than $SO_2+1/2O_2$ at low temperatures and low pressures. Kinetic model calculation shows that the SO_2/SO_3 ratio in a K/T-size vapor cloud is lass than unity. The SO_2/SO_3 ratio estimated based on the laser-irradiation experiments is about 10^{-6} for a K/T-size vapor cloud. Three lines of evidence strongly suggests that the SO_2/SO_3 ratio in K/T impact vapor cloud may have been much smaller than 1. Then sulfuric acid aerosol may not have blocked the sunlight for a long time. Instead, there may have been an extremely intense global acid rain immediately after (<100 days) the K/T impact.

References: [1] Alvarez, L.W. et al. (1990) *Science, 208,* 1095-1108. [2] Sigurdsson, H. et al. (1992) *EPSL, 109,* 543-559. [3] Pope, K.O. et al. (1994) *EPSL., 128,* 719-725. [4] Pope, K.O. et al. (1997) *JGR, 102,* 21645-1664. [5] Ohno et al, (2002) *Earth Planet. Sci. Lett.,* Submitted. [6] Troe, J., (1978) *Ann. Rev. Phys. Chem., 29,* 223.

IMPACT INDUCED TARGET THERMO-MECHANICAL STATES AND PARTICLE MOTION HISTORIES, John D. O'Keefe,[1] and . Thomas J. Ahrens[1], Lindhurst Laboratory of Experimental Geophysics, California Institute of Technology, Pasadena, CA 91125, dinosr@aol.com

Objectives The first objective of this effort is to determine how the post impact measurable crater features relate to the processes that take place during impact and the second is to the determine from a given suite of measurements the uncertainty in estimating the impactor's parameters.

Approach. We have taken a numerical approach using the CTH code[1] to calculate the evolution of the near field impact process. This includes the details of the early time shock wave driven flow fields, the development and collapse of the transient cavity [2], and in a few limited cases the very late time thermal and stress histories. To quantify the impact process, we placed massless tracer particles in layers that simulate the target stratigraphy (Figs 1-4) and stored the motion and thermo-mechanical state histories (e.g. pressure, temperature, damage, peak stress/strain rate..) of these particles. We took this approach because the late time distributions are significantly different from the initial distributions. We used the ANEOS model for equation of state and a Mohr-Coulomb damage model for the strength degradation by shear strain fracture [2,3]. The key parameters for the impacts are a, the impactor radius, U, the impactor velocity, Yc, target cohesive strength, μ, internal friction, μd, damaged internal friction. We found that we could replicate the key features with values of target material parameters within the magnitudes found in laboratory measurements. We developed scaling laws for the key target metrics based upon the Mohr-Coulomb strength model. This provides a the link between the measureable features and the impactor parameters,. In addition it, bounds the effect of damage on the magnitude of the metrics.

Target Motion Histories and Thermo-mechanicl States..

Shown in Figs 1-4 are the particle motion histories and the melted and damaged (shear fractured) regions for three representative cases: 1) simple crater –strength dominated, 2) transition crater - between strength and gravity regimes, and a 3) basin forming impact represented by the Chixculub event[4].:

The geometry of the flow in the strength dominated case (Fig. 1) is very similar to that of all cases at the time of maximum penetration. The melt has two major zones. The melt layer and melt ejecta. The melt layer is underneath the impact point and is on top the damaged region, The trajectories of the melt particles are shown and labeled at the top of the computational grid.

We found that in the strength dominated region that that the depth of penetration decreases with the magnitude of the internal friction. This is due to the dynamic pressure increasing the local strength.

An example of a transition crater is shown in Fig. 2. In this case the low strength material flows over and covers part of the melt layer.

As an example of the motion histories and thermo-mechanical states in basin forming impacts, we simulated the Chicxulub event. The distribution and extent of the damaged region is critical to the crater flow and determines 1) transient cavity dimensions (e.g. depth of penetration), 2) ejecta lofting angles, 3) occurrence and number of terrace/slump faults and 4) distribution of melt. The radial extent of the damage region that replicates the Chicxulub morphology is ~ 100 km. (Fig. 4). At the time of maximum penetration, the transient cavity geometry is similar to Fig. 1. The transient cavity collapses and compresses the melt layer to a region near the center of the cavity and on top of the damaged material (e.g. Fig.3). After the transient peak collapses, the melt flows in a thin layer over the peak ring (Fig. 4), The peak ring is formed by the collision of the downward flowing transient peak with the nearly vertically launched transient cavity flow. Note that while the transient central peak is moving upward that the ejecta curtain is still impacting the surface and that slumping is occurring in front of the ejecta curtain (Fig. 3). In addition, an asymmetric fault (diameter = 150 km) is formed that bounds the terraced zone and extends downward to the Moho. This feature has been interpreted as the crater rim [4]. On the other hand, the radius of the overturned stratigraphy (Fig 4), which is a measure of the transient cavity size is probally a more accurate determinant of the energy of impact [5]. Further out, a 200 km diameter exterior ring is formed as a result of secondary impact of ejecta on the damaged region. The Mohr-Coulomb scaling accounts for basin forming impacts and shows the effect of internal friction on depth of penetration and quantifies the effect of overburden pressure.

References [1]McGlaun, J and S.L. Thomsen *Int. J. Impact Eng.*(1990)**10**,360-361,.[2] O'Keefe, J.D. and T.J. Ahrens (2001)*Int. J. Impact Eng.*,**36**,17.011-17,038. [3] Johnson, G.R. and T. J. Holmquist. (1994) High Pressure Science and Technology, 981-984 [4] Morgan , J., *et a.l* (1997)Nature, **370**, 472-476, [5] O'Keefe, J.D. and T.J. Ahrens (1999) *JGR* ,**10(E11)**27,091-27,1093

PARTICLE MOTION HISTORIES: J. D. O'Keefe and T.J. Ahrens

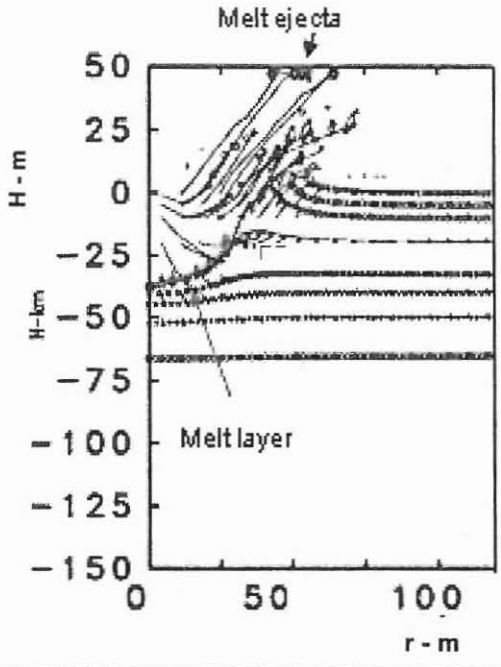

Fig. 1. **Strength dominated crater**. Particle motion histories and melted and fractured regions. Time = 0.15 s U=20 km/s, a = 5 m, Yc = 1.0e9, μ = 0.75, μd = 0.1, εf = 0.05., g = 0.0 m/s^2. Damage colors shown in Fig.3

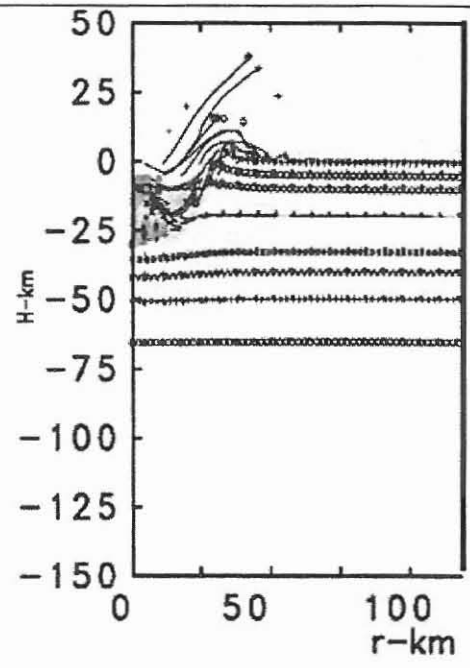

Fig. 2 **Transition crater**. Particle motion histories and - melted and fractured regions. Time = 39 s,. U=20 km/s, a = 5 km, Yc = 0.0, μ = 0.75, μd = 0.1, εf = 0.05, g = 9.8 m/s^2. Damage colors shown in Fig.3

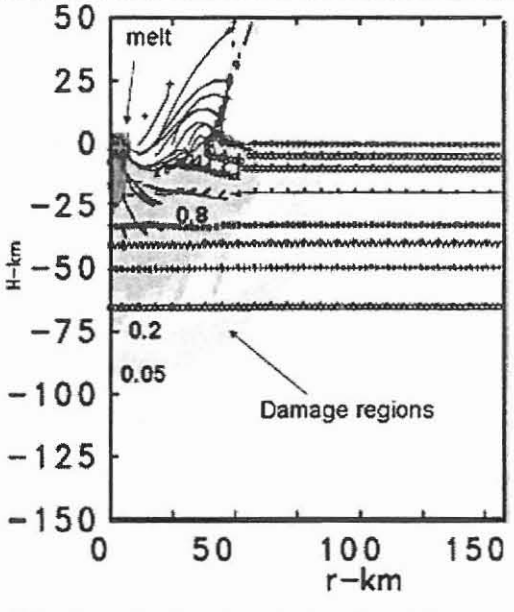

Fig. 3 Complex crater. Chicxulub. Time = 88 s.. U=20 km/s, a = 5.0 km, Yc = 2.4e9, μ = 0.75, μd = 0.1, εf = 0.05. g = 9.8 m/s^2. Note dips in damage region indicating faulting.

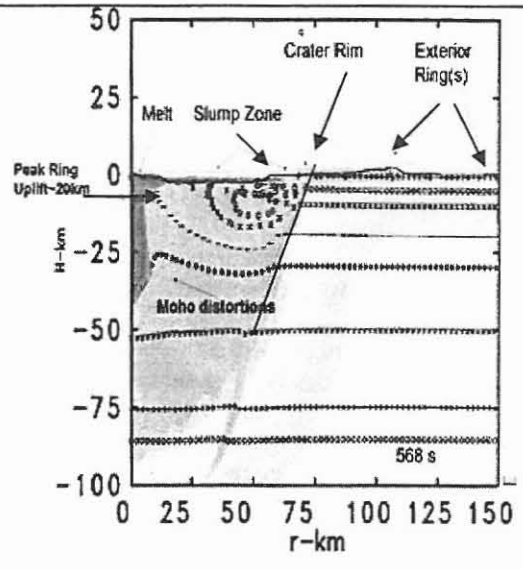

Fig. 4 3 Complex crater. Chicxulub. Time = 568 s. U=20 km/s, a =7. 5 km, Yc = 1.0e9, μ = 0.75, μd = 0.2, εf = 0.1, g = 9.8 m/s^2.Note dips in damage region indicating faulting. Damage colors shown in Fig.3.

Velocity Distributions of Fragments and its Time Dependence

N. Onose and A. Fujiwara, The Institute of Space and Astronautical Science, 3-1-1 Yoshinodai, Sagamihara, Kana-gawa, 229-8510, JAPAN, onose@planeta.sci.isas.ac.jp

Introduction: Oblique impact cratering experiments were done, and the fragment size and velocity were measured for fragments larger than 1mm in diameter, and slower than 200m/sec. A high speed CCD video camera was used to see the fragments in flight, and secondary collisions with a window of the target chamber. The purpose of this paper is to provide a database of fragments velocity, which is essential to deeper understanding of the surface evolution of small aster-oids.

Experimental Procedure: A two-stage light-gas gun was employed, and impact velocities are around 4km/sec. A high-speed CCD video camera of 4500frames/sec and 9000frames/sec enabled us to track fragments in flight, and to measure the locations and the times of the secondary collisions. A target box with a slit of15mm width was employed to limit the ejection in the plane including the trajectory of the projectile.

Results: An example of the time dependence of the ejection pattern is shown in figure 1. In this run a target box with a slit was employed. Ejection is divided into 4 stages according to the ejection pattern. The first stage (order of μsec) corresponds to ejection of very fine and fast fragments like jetting and the earliest conical ejecta cloud, and these particles could not be traced individually. Their typical size is less than 1mm in diameter, and velocity is over 1km/sec. The ejecta in the second stage (0-3msec) consists of 0.1 to 1mm fragments ejected conically at a few hundreds m/s, and at an ejection angle higher than about 60degree from the target surface. The 3D velocity derived from the secondary collisions also shows that the ejection at the second stage is conical. In the third stage (1-10msec), larger spall fragments, about 1cm in diameter, ejected in a cone narrower than that of the second stages. And a cluster of small and slow fragments (0.1-5mm in diameter and a few m/sec) ejected nearly perpendicular to the target surface characterizes the last stage (3msec-). 3/4 fragments are ejected normal to the target surface slower than 6m/s at this stage.

To discuss the size-velocity correlations, all results from the experiments of 7mm Nylon Sphere on Gypsum target at about 4km/sec, include the oblique impacts, are shown in figure 2. The line in figure 2 is from the spallation theory in Melosh (1989). The dotted line gives an apparent upper limit line drawn by assuming the same functional dependence on the size as in Melosh. It should be noted that great many small fragments exists in the velocity region much less than the upper limit velocity, and majority of particles have velocity of more than one order lower than the upper limit.

References: [1] Melosh, H. J. (1989) Impact Cratering.

Acknowledgements: We must thank Prof. Mizu-tani, Prof. Kato, and persons in ISAS who gave us important suggestions.

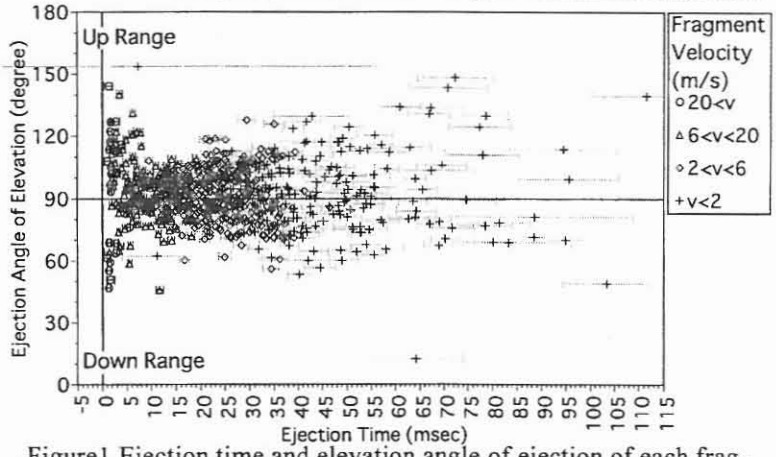

Figure1 Ejection time and elevation angle of ejection of each fragment in the impact at 0degree.

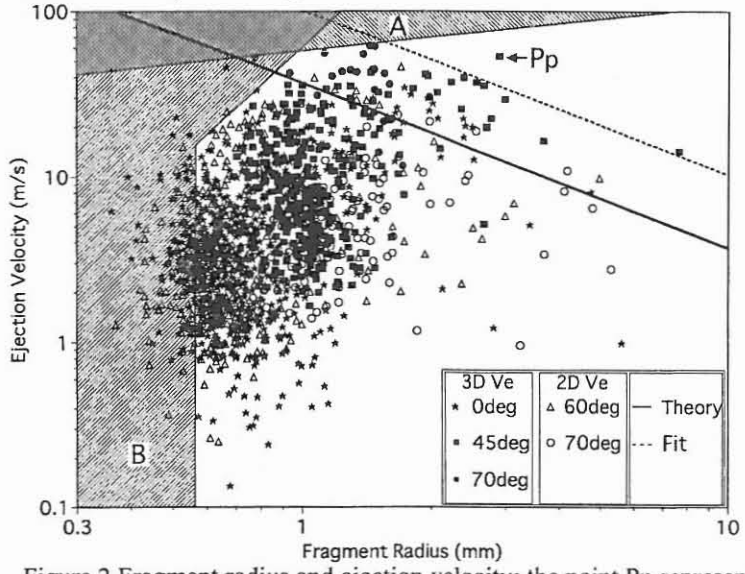

Figure 2 Fragment radius and ejection velocity: the point Pp represents a rebounded projectile. Area A and B represent the region which is difficult to measure because of too fast and too small, respectively.

Velocity Distributions of Fragments in Oblique Impact Cratering on Gypsum

N. Onose and A. Fujiwara, The Institute of Space and Astronautical Science, 3-1-1 Yoshinodai, Sagamihara, Kanagawa, 229-8510, JAPAN, onose@planeta.sci.isas.ac.jp

Introduction: In order to understand the behavior of the impact-induced fragments on the small asteroid, oblique impact cratering experiments were produced using gypsum targets, which were used as one of porous and low density materials. The fragment size and velocity were measured for fragments larger than 1mm in diameter, and slower than 200m/sec. A high speed CCD video camera was used to see the frag-ments in flight, and secondary collisions with a win-dow of the target chamber were also employed to measure fragment velocity. Especially, we focused to measure the behaviors of very low velocity fragments, which have special meaning for the ejecta on very small asteroids.

Experimental Procedure: We used almost the same experimental procedure as our other paper pre-sented in this meeting, Velocity Distributions of Frag-ments and its Time Dependence. Since in this series of oblique impact, we shot the target surface inclined downward, the extremely slow fragments could come out from the crater cavity.

Results: In the paper cited above, it is shown that the impact ejection is divided into 4 stages according to the ejection pattern. In the second stage (0-3msec), the elevation angle of ejection decreases slightly, and the data are more scattered compared with the case of verti-cal impact, in the impact at 45degree. In the impact at 70 degree, the secondary collision on the window only was identified in the down range direction, and that was also consistent with the result of the run using witness papers.

Figure 1 indicates the ejected time and the elevation angle of ejection of the each tracked fragments also mentioned in the other paper for the vertical impact one. In the impact at 0degree, and 45degree, a target box with a slit was installed to get the 3D velocity of the fragments, and there is few fragments were ejected target surface normal in the second stage. The large number of small and slow fragments ejected later, consists the last stage (3msec-). The average direction of the flow composed by a cluster of small and slow fragments slightly deviate from the surface normal in the oblique impact.

Acknowledgements: We must thank Prof. Mizu-tani, Prof. Kato, and persons in ISAS who gave us important suggestions.

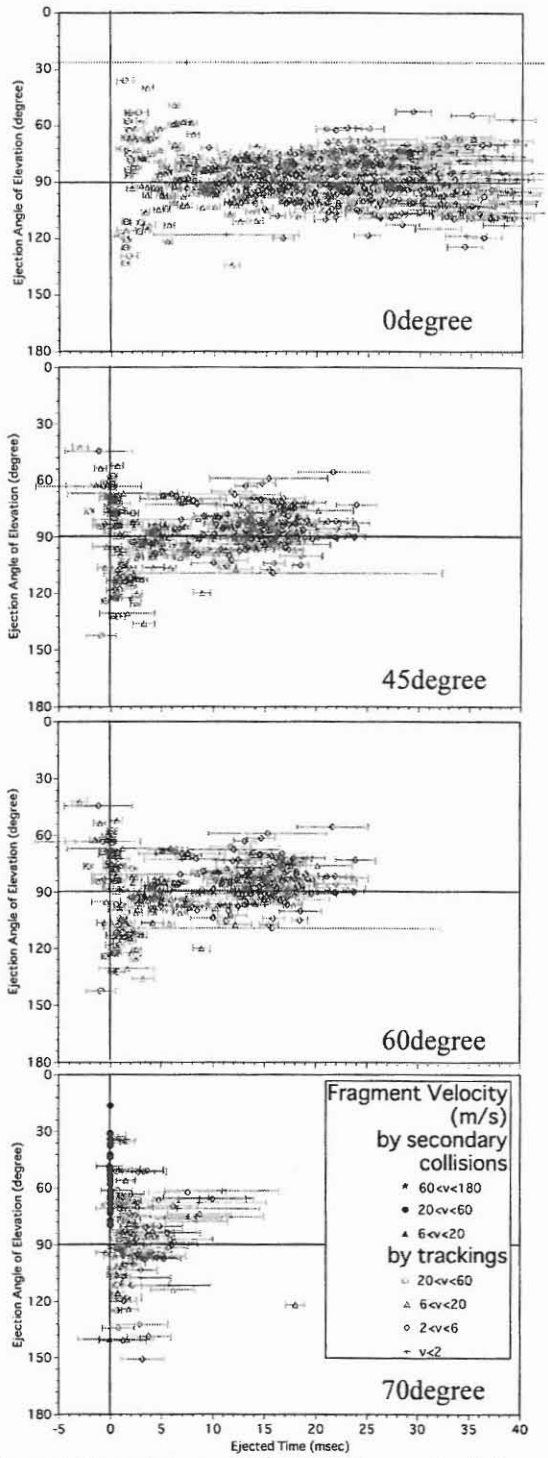

Figure 1 Ejected time and the elevation angle of ejection in the oblique impacts: the later half of the film in the impact at 70degree was lost by an accident.

NEXT STEP IN MARINE IMPACT STUDIES: COMBINING GEOLOGICAL DATA WITH NUMERICAL SIMULATIONS FOR APPLICATIONS IN PLANETARY RESEARCH. J.Ormö[1] [1]Centro de Astrobiologia (CAB), Instituto Nacional de Técnica Aeroespacial, Ctra de Torrejón a Ajalvir, km 4, 28850 Torrejón de Ardoz, Madrid, Spain. (ormo@inta.es)

Introduction: Baltoscandia is favourable for geological studies of marine-target (M-T) craters. One reason is the relatively dense population of craters of different diameters, of approximately the same age, and with different target water depths. This allows comparative studies of the effects of a target water layer on the lithologies and morphologies of the resulting craters [1]. Baltoscandian craters like Kärdla [2] and Lockne [3] are well documented. Today, a considerable number of the documented craters and impact sites on Earth are known to have formed at sea. All but one, the Eltanin impact site west of Chile, have formed in epicontinental seas. This circumstance is mainly a result of higher probability of both formation and preservation in such areas [1]. Famous craters as Chicxulub, Chesapeake Bay, and Mjölnir were also formed at sea [e.g. 4, 5, 6]. Marine impact cratering is an important topic within impact research. The fact that our planet is mostly covered by water must be taken into consideration when evaluating consequences and hazards from impact events. In addition, M-T craters may have applications in the exploration of our Solar System.

Definition: An M-T crater forms from an impact into a target with an upper layer of water. In its transient stage, an M-T crater consists of a water cavity and, in some cases, a seafloor crater. Only the latter may be preserved. How much of the crater that develops in the seafloor depends on the amount of expended energy in relation to the depth of the sea. This relation has been analysed both experimentally [7] and numerically [8]. Studies by Ormö and Lindström [1] show a strong link between the water depth and the geology of the seafloor crater. At relatively shallow water depth the crater resembles a "land-target" crater, although sometimes with stronger collapse of the rim. At deeper water the crater is concentric with a deep crater in the basement surrounded by an outer crater, apparently formed by a shallow excavation flow in connection with the development of a wide water cavity [1, 8, 9]. The outer crater may in these cases be cut by gullies eroded by the resurge of debris-loaded water.

The potential of numerical simulation: Geological studies of the Lockne crater have improved our understanding of water related features to such an extent that they can be used as constrains not only for a rough simulation of the impact, but for modeling specific parameters. The codes have likewise developed so that they now better can simulate the complex process of an impact into a layered target. This development led to an attempt to make a detailed numerical modeling of the 455 Ma Lockne crater [9]. The aim was primarily to find the target water depth, which was an unknown variable, but also to better understand the processes behind some of the special features of the crater (e.g. the development of a wide overturned flap). The model also gave the opportunity to test the code on a full-scale impact in a layered target. Main geological constraints in the Lockne modeling were (1) the occurrence of a 7.5 km wide inner crater in the crystalline basement with a slightly elevated rim, (2) a shallow outer crater with no obvious rim, (3) an about 3 km wide, overturned flap of basement rock outside the basement crater rim, (4) strong stripping of an initially 80 m thick sedimentary cover prior to the deposition of the flap, and (5) evidence for a forceful resurge. The simulations were done at various water depths of the likely depth interval (200-1000 m). Impactor size, mass, and velocity were also varied. It was concluded that for a 400 m radius asteroid striking at 20 km/s, the target water depth was slightly less than 1000 m. The study is continued with more sophisticated software (3D) to analyse the effects of impact angle and ejecta/water interactions [10].

Perspectives: Knowledge of M-T craters can be used when analysing planetary paleoenvironments and surface properties where remote sensing may provide the only information. Ormö and Muinonen [11] propose that Martian M-T craters could reveal paleo-water depths and, hence, the climatic evolution of the planet. Any low-strength material in the upper part of a layered target may respond as a water layer. Craters from impacts into hydrocarbon and nitrogen seas have indeed been suggested to exist on Titan [12]. Cassini radar data may reveal their features. Future studies of M-T craters should focus on the mechanics of the concentricity, and the influence of obliquity on the ejecta distribution, resurge flow, and how they affect tsunami formation. This is currently pursued by the new impact research group at CAB by combining experiments, fieldwork, planetary research, and numerical modeling.

References: [1] Ormö J. and Lindström M. (2000) *Geol.Mag*, 137, 67-80. [2] Puura V. and Suuroja K. (1992) *Tectonophysics*, 216, 143-156. [3] Sturkell E. (1998) *Geol. Rundsch.*, 87, 253-267. [4] Morgan J. et al. (1997) *Nature*, 398, 472-476. [5] Poag C.W. (1997) *Sed. Geol.*, 108, 45-90. [6] Gudlaugsson S.T. (1993) *Geology*, 21, 291-294. [7] Gault D.E. and Sonett C.P. (1982) *Geol. Soc. Am. Spec. Paper*, 190, 69-92. [8] Shuvalov V.V. and Artemieva N.A. (2001) *LPS XXXII*, Abstract #1122. [9] Ormö, J. et al. (2002) *JGR-Planets*, in press. [10] Shuvalov V.V. et al. (2002) *Advances in Impact Studies*, submitted. [11] Ormö J. and Muinonen P. (2000) *LPS XXI*, Abstract #1266. [12] Lorenz R.D. (1997) *Planet. Space Sci.*, 45, 1009-1019.

TRANSIENT CRATER FORMATION AND COLLAPSE: OBSERVATIONS AT THE HAUGHTON IMPACT STRUCTURE, ARCTIC CANADA. G. R. Osinski, J. G. Spray, Planetary and Space Science Centre, University of New Brunswick, 2 Bailey Drive, Fredericton, NB E3B 5A3, Canada. (osinski@lycos.com).

Introduction: It is generally believed that the processes involved in the formation of an initial transient crater and its subsequent excavation, are common for all craters, regardless of their size. A critical assumption is that the depth/diameter ratio of a transient crater remains constant for any given crater size [1,2]. The morphological diversity of impact structures is, therefore, attributed to the modification or collapse of an initial simple hemispherical transient crater [e.g., 2]. The mechanisms of impact crater collapse remain one of the least understood stages in the impact cratering process. Indeed, standard strength models used in conventional hydrocode modeling techniques are not successful in describing crater collapse [2]. Numerical models have also rarely been constrained by field data from terrestrial impact structures. This is, however, a catch-22 situation because very few detailed field investigations of the tectonics of complex impact structures have been made.

Here, we present new constraints on the formation of complex impact craters based on detailed field studies of the Haughton impact structure, Arctic Canada.

Geological setting: The 23 Ma, 24 km diameter Haughton impact structure has been the focus of detailed field investigations over the course of 4 field seasons (1999-2002) as part of the PhD thesis of GRO. Haughton is superbly exposed due to the prevailing polar desert environment. The target rocks consist of 1750 m of almost flat lying sedimentary rocks overlying Precambrian metamorphic basement. Key stratigraphic horizons provide evidence for the depth of excavation and amount of structural uplift and deformation.

Reconstruction of the transient crater: Detailed mapping carried out as part of this study indicates that the transient crater at Haughton had a diameter of 12-12.5 km. This supports a previous estimate of 12 km based on seismic reflection data [3]. The presence of basement gneisses in the crater-fill melt rocks indicates a depth of excavation (H_{exc}) between 1750 m and ~2200 m. It is generally considered that the depth of the transient crater (H_{tc}) is ~2-3 times greater than H_{exc} [4]. This would yield a H_{tc} of ~4-6 km for Haughton. However, this is incompatible with our field studies and previous seismic investigations [3] that do not indicate significant deformation and displacement of the Precambrian basement (depth to upper surface: 1750 m).

Modification of the transient crater: Our work has revealed that the tectonic modification of the early-formed Haughton crater involved the complex interaction of a series of interconnected concentric and radial faults.

Radial faults. Radial faults record predominantly oblique strike-slip movements. There is generally little (<10 m) or no displacement of marker beds across radial faults. This is despite the fact that substantial volumes of fault breccia (>8 m) are typically present. Importantly, these radially orientated faults are cut and offset by later concentric faults.

Concentric faults. It is noticeable that the intensity and style of concentric faulting changes around the periphery of the crater. They are predominantly listric extensional faults with rotation of beds in the hanging-wall up to ~75°. The outermost concentric faults generally dip in towards the centre of the crater. We suggest that these faults were initiated during the inward collapse of the crater walls. The innermost faults, however, tend to dip away from the crater centre and may represent the outward collapse of the central uplift. The outermost concentric faults typically display two episodes of deformation: (1) early major dip-slip extensional movement; (2) later minor oblique strike-slip movement resulting in the offset of radial faults. A zone of (sub-) vertical faults and bedding occurs along the edge of the central uplift (~6 km radius). This suggests complex interactions between the outward collapsing central uplift material and the inward collapsing crater walls.

Comparison with models: It appears that the transient crater at Haughton was significantly shallower than current models for the cratering process predict. This may suggest a decrease in the depth/diameter ratio of transient craters with increasing crater size. This will have important implications for estimating the size of deeply eroded large impact craters (e.g., Vredefort).

Field studies at Haughton indicate that deformation during the modification stage of complex impact crater formation was brittle and localized along discrete fault planes. We find no evidence to support the hypothesis of 'acoustic fluidization' throughout the whole crater. The presence of little offset along radial faults, despite the large thicknesses of fault breccia, may suggest limited block oscillation along discrete fault surfaces as proposed by Ivanov et al. [5]. However, the scale seen in the field at Haughton is greater than in the models [5].

Acknowledgments: This work represents part of the PhD thesis of GRO and was funded by the Natural Sciences and Engineering Research Council of Canada (NSERC) through research grants to JGS.

References: [1] Grieve R. A. F. et al. (1981) *LPS XII*, 37-57. [2] Melosh H. J. and Ivanov B. A. (1999) *Annu. Rev. Earth Planet. Sci., 27*, 385-415. [3] Scott D. and Hajnal Z. (1988) *Meteoritics & Planet. Sci., 23*, 239-247. [4] Melosh H. J. (1989) Impact Cratering: A geologic process. Oxford University Press, 245 pp. [5] Ivanov, B. A. et al. (1996) *LPS XXVII*, 589-590.

IMPACT MELTING IN SEDIMENTARY TARGET ROCKS? G. R. Osinski[1], J. G. Spray [1] and R. A. F. Grieve[2], [1]Planetary and Space Science Centre, University of New Brunswick, 2 Bailey Drive, Fredericton, NB E3B 5A3, Canada. [2]Earth Sciences Sector, Natural Resources Canada, Ottawa, ON K1A OE8, Canada (osinski@lycos.com).

Introduction: Sedimentary rocks are present in the target sequence of ~70% of the world's known impact structures [1]. One of the outstanding questions in impact cratering studies is: do sedimentary rocks undergo impact melting? This question cannot be addressed through experimentation in the laboratory, which is limited to impact velocities generally below that required for wholesale melting [2]. Numerical and computer-based modeling may offer some important information, however, as Pierazzo et al. [3] note, "there is no good model for melt production from impact craters in sedimentary targets". Studies of naturally shocked rocks, therefore, offer the only true ground-truth data on the response of sedimentary rocks to impact. We have carried out detailed field and analytical studies of naturally shocked sedimentary rocks that will hopefully provide constraints for future modeling.

Physics of impact melt generation: Theoretical considerations of the impact process reveal some important results regarding the generation of impact melt [4]: (i) the volume of target material shocked to pressures sufficient for melting *are not* significantly different in sedimentary or crystalline rocks; (ii) Hugoniot curves indicate that *more* melt should be produced upon impact into sedimentary targets as compared to crystalline targets. Impacts into sedimentary targets should, therefore, produce as much, or even greater volumes of, melt as do impacts into crystalline targets [4].

Where have all the melts gone? It is generally considered that the high volatile content of sedimentary rocks results in the "unusually wide dispersion" of impact melt [4]. However, it is becoming increasingly clear that such lithologies can undergo shock-melting and are preserved in significant quantities in some impact craters.

Haughton impact structure: The target rocks at the 24 km diameter, 23 Ma Haughton structure comprised a ~1750 m thick series of sedimentary rocks (predominantly carbonates, with minor evaporites, sandstones and shales), overlying Precambrian metamorphic basement. Osinski and Spray [5] have recently interpreted the crater-fill deposits at the Haughton impact structure as carbonatitic impact melt rocks. Importantly, the volume of these crater-fill deposits (>12 km^3) is roughly equal to the observed impact melt volumes for comparably sized craters developed in crystalline targets (e.g., >11 km^3 melt at Bolytsh (diameter 24 km) [6]).

Ries impact structure: The 24 km diameter, 15 Ma Ries impact structure comprised a target sequence of ~850 m sedimentary rocks (limestone in upper parts, predominantly sandstones in lower parts), overlying Hercynian granites and gneisses. Carbonate melts have been documented at the Ries impact structure by Graup [7] and Osinski [8]. In addition, Osinski [8] has also recognized the presence of SiO_2-rich impact glasses that were clearly derived from sandstones in the lowermost part of the sedimentary sequence.

Implications: Based on our studies of the Haughton and Ries structures, we suggest that sedimentary rocks can undergo shock-melting during impact events. Thus, it should NOT be assumed that all sedimentary rocks and minerals completely degas and disperse at pressures sufficient for melting. This will have implications for the way in which we model the cratering process.

Modeling: The Ries impact event has recently been the focus of numerical modeling studies and 3D hydrocode simulations [9]. These models suggest substantial melt generation from sandstones in the sedimentary sequence, seemingly at odds to the general held view that these lithologies were not shock-melted [e.g., 10]. Recent studies by Osinski [8] have shown that sandstone-derived melts are present. This is an instance where modeling and field studies clearly agree. This is not the case when carbonates are considered. All models to date have considered that carbonates are completely degassed above a certain pressure threshold (e.g., >55 GPa in [9]). This is despite the fact that carbonate melts are known to occur in the Ries and other structures. We suggest that the melting of carbonates should be included in any future modeling studies.

Acknowledgments: This work represents part of the PhD thesis of GRO and was funded by NSERC through research grants to JGS. Financial support for fieldwork at the Ries impact structure came from the Eugene Shoemaker Impact Cratering Award presented to GRO.

References: [1] Earth impact database (2002) http://www.unb.ca/passc/ImpactDatabase/index.htm. [2] Grieve R. A. F. and Cintala, M. J. (1992) *Meteoritics & Planet. Sci., 27*, 526-538. [3] Pierazzo et al. (1997) *Icarus, 127*, 408-423. [4] Kieffer, S. W. and Simonds, C. H. (1980) *Rev. Geophys. Space Phys., 18*, 143-181. [5] Osinski G. R. and Spray J. G. (2001) *EPSL, 194*, 17-29. [6] Gurov, E. P. and Gurova, E. P. (1985) *LPSC XXII*, 310-311. [7] Graup G. (1999) *Meteoritics & Planet. Sci., 34*, 425-438. [8] Osinski, G. R. (2002) *Meteoritics & Planet. Sci.*, (in review). [9] Stöffler et al. (2002) *Meteoritics & Planet. Sci.*, (in press). [10] Englehardt et al. (1995) *Meteoritics & Planet. Sci., 30*, 279-293.

APPLICATION OF GRAVITY DATA TO UNDERSTANDING IMPACT MECHANICS. J. B. Plescia, U. S. Geological Survey, 2255 N. Gemini Drive, Flagstaff AZ 86001, jplescia@usgs.gov..

Introduction: Gravity data provide important constraints on morphometry of impact structures and on the crustal response to the impact process [1-3]. Such data can provide insight that may not be obtainable from surface geologic mapping and may not be quickly or cheaply obtained by other geophysical means. The gravity data can be used to constrain the dimensions of a completely to partly buried structure (e.g., diameter, central uplift, etc.) and can provide information on the subsurface character of both exposed and buried structures. Gravity data can also be used to reject some structures as being of impact origin.

Morphometry: The most direct use of gravity data is establish morphometric properties of partly to completely buried structures. Gravity data have been used at several structures in Australia to establish the nature of these impacts. Mulkarra was proposed [4] to be a 9 km diameter simple crater in a sedimentary section. Gravity data [5], however, reveal positive and negative anomalies that indicate the structure is actually an 18-20 km complex structure with an 8 km central peak or peak ring. At Kelly West [6], gravity data have been used to study the central uplift area. Those data (a low surrounded by a high associated with the central uplift) suggest the central uplift is a small central peak-ring filled with breccia rather than a solid central peak. At the Manson impact [7] gravity data show that the central uplift is probably an incipient peak ring and that the zone of low density material (breccia) extends to a depth of 3 km.

Deep Crustal Effects: Gravity data can be used to provide constraints on the depth of crustal deformation. Impacts produce shock effects which reduce the effective density of rocks at depths greater than the transient cavity filled with the breccia lens. At Meteor Crater the breccia lens is 220 m thick, yet the zone of low density persists to a depth of 800 m [8]. Shock waves from the impact event had sufficient energy to significantly fracture the basement for distances of 500-600 m below the crater floor, thus providing a constraint on the energy decay rate. The breccia and the shattered basement contribute to the total 0.6 mGal anomaly [9].

Upheaval Dome is a deeply eroded complex crater in Utah [10], although apparently not everyone agrees with this interpretation [11]. Detailed geologic mapping show that the normal faults that are exposed around the margin of the structure and which cut the Navajo, Kayenta and Wingate units flatten at depth. From the attitudes of the exposed faults, the faults probably flatten into a decollement within the deeper Cutler Group. Such a geometry would imply that the deformation was restricted to levels above the Culter. Gravity data collected over the structure show that there is no gravity anomaly. The absence of an anomaly is explained in that at the current structural level deformation is entirely associated with slip along faults translating different sandstone blocks. Simple translation does not produce a density contrast. Erosion is at such a level that the breccia lens has been removed. These data indicate the shock did not have substantial influence below the level of the decollement.

The gravity data for an impact structure can also be used to model the nature of the central uplift. The Connolly structure in Australia [12] is a 9 km diameter complex crater. Gravity data reveal the presence of a high over the central uplift surrounded by an annular lower amplitude high over the crater interior. The central gravity high is due to uplift of deeper sandstones from a depth of ~1 km. These sandstone are of higher density than the surrounding rock and have shed relatively high density material into the crater interior causing the annular high.

Summary: These examples serve to illustrate that gravity can provide information on the deep structure of impacts. Such data place constraints on the cratering process by providing insight into how the crust responds to the impact: how deep the effects of the shock extend, how much structural uplift occurs, the shape of the central uplift with depth, etc.

References: [1] Grieve, R. A. F., and Pilkington, M. (1996) AGSO J., 16, 399-420. [2] Pilkington, M. and Grieve, R. A. F. (1992) Rev. Geophys., 30, 161-181. [3] Plado, J. et al. (1999) GSA Special Paper 229-239. [4] Flynn, M. (1989) The Cooper and Eromanga Basins Australia, 431-439. [5] Plescia, J. B. (1999) *Berichte zur Polarforschung, 343*, 74-78. [6] Shoemaker, E. M. and Shoemaker, C. S. (1996) *AGSO J.*, 16, 379-398. [7] Plescia, J. B. (1996) *GSA Special Paper 302*, 89-104. [8] Ackerman, H. D., et al. (1975) *JGR, 80*, 765-775. [9] Regan, R. D. and Hinze, W. J. (1975) *JGR, 80*, 776-788. [10] Kriens B. J. et al. (1999) *JGR, 104*, 18867-18887. [11] Jackson, M. P. A. et al. (1998) *GSA Bull., 110*, 1547-1573. [12] Shoemaker, E. M. et al. (1989) LPSC 20th, 1010-1011.

IMPORTANCE OF TARGET PROPERTIES ON PLANETARY IMPACT CRATERS, BOTH SIMPLE AND COMPLEX. P.M. Schenk, Lunar and Planetary Institute, Houston TX 77058 (schenk@lpi.usra.edu)

Introduction: For 20 years, the issue of whether surface gravity or target properties control the shape of planetary craters has continued unabated. Periodic revisions to and questions about quality control of the planetary crater database have vexed the debate. Here I review the current status of the observations and our understanding of the results. The observational data fall into two related categories: crater depths, and morphologic transitions from one landform to another. As it turns out there is more than one way to measure these transitions. It would appear that both target gravity and properties are important.

Silicate Planets: Pike [1] made one of the first attempts to compare crater morphology on the silicate terrestrial planets, using data from the Moon, Mars and Mercury. The effort to sort out the relative importance of surface gravity and target properties (i.e., crustal strength) is complicated by the small number of such bodies for which we have data (5) and the influence of other forces. Three of these bodies (Earth, Venus, and Mars) have substantial atmospheres, which may couple to the ejecta curtain and alter landforms [2]. Earth and Mars have been subject to substantial surface erosion and modification, and crater data for Earth, which together with Venus represent the high-gravity end of the spectrum, is wholly unreliable. Magellan stereo allows depth measurements to be made [3] but the dense atmosphere prevents the formation of simple craters (by assuming lunar-like simple crater morphology, an estimate of transition diameters can be made).

Although there is clearly a general inverse trend of transition diameters with gravity from the Moon to the other higher-gravity bodies, the result of these competing forces is something akin to confusion. There appear to be major differences in morphology on Mercury and Mars, where surface gravity is otherwise similar. Pike [1] reports significant differences in the depths and transition diameters of craters on the lunar mare and on the highlands. This points to an important role for material properties, with the regolith rich highlands have a different strength than the less heavily cratered basaltic mare. Additional evidence for or against the influence of layering or rock type will be reviewed, including the latest MGS results.

Icy Satellites: The icy satellites of the outer planets are a different ball of ice. There are at least a dozen such moons for which we have data and which have complex craters. They are also of sufficiently different size that a large gravity range can be examined. Chapman and McKinnon [4] and Schenk [5] made the first satellites comparisons, suggesting that in fact there was a strong dependence of complex crater depths and transition diameters on surface gravity, but also, that these were significantly smaller than would be expected from comparison with silicate-rich planets. These observations were based on Voyager data, but subsequent Galileo data has shown that the Ganymede data was partially compromised by resolution insufficient to resolve simple craters. Callisto and Europa have also been added. The updated transitions and depths [6] clearly show that the icy satellites all fall on a g^{-1} trend. The only exceptions are Enceladus and Mimas. Enceladus craters are very irregular even by icy satellite standards and it is likely that these craters have been modified, possibly by volcanism [7]. Mimas remains to be explained, but unusually low internal porosity conditions may or may not be involved.

The unusual complex crater landforms on the larger icy satellites, especially Europa, may point to the importance of thin lithospheres and possibly liquid layers at shallow depths [6,8]. These morphologies and their dimensions provide key constraints that can be used to model icy satellite interiors [9].

Future Shock: On silicate bodies, additional data at the low end of the gravity spectrum is needed. All asteroids observed to date are too small to allow complex crater formation. The Dawn mission to Vesta and Ceres will be important for adding rocky bodies of low to moderate gravity to the data set, and indeed I will venture a prediction as to transition diameters on these bodies. Until then, the case of the silicate planets remains uncertain. For the icy satellites, a better understanding of the internal structure of Mimas is required. We might see something unexpected on two-faced Iapetus. There is also some scatter in the small saturnian satellite data which could use clearing up. Mapping of crater morphology on Titan, similar in size to Ganymede and Callisto, will be useful for comparison, although the atmosphere there may cloud the issue. Cassini beginning in 2004 should address these needs. It is curious that we do not see substantial differences between those satellites believed to be mostly water ice, and those with more exotic (and lower strength) ices such as ammonia, carbon dioxide and nitrogen (e.g., Ariel, Miranda and Triton). Pluto and other Kuiper Belt objects may be much richer in these ices and could behave differently. We have only a decade to wait (hopefully)!

References: [1] Pike, R., *Icarus*, 43, 1 (1980). [2] Schultz, P., *J. Geophys. Res.*, 97, 16183 (1992). [3] Herrick, R., & B. Sharpton, *J. Geophys. Res.*, 105, 20245 (2000). [4] Chapman, C., & W. McKinnon, in *Satellites*, U.of A. Press (1986). [5] Schenk, P., *J. Geophys. Res.*, 96, 15635 (1991). [6] Schenk, P., Nature, 417, 419 (2002). [7] Schenk, P., & J. Moore. *J. Geophys. Res.*, 100,19009 (1995). [8] Moore,J., et al., *Icarus*, 135, 127 (1998). [9] Turtle, E., & B. Ivanov, LPSC XXXIII, (abst. 1431, 2002).

IMPACT CRATER MORPHOLOGY AS A GUIDE TO REGOLITH STRUCTURE AT TAURUS-LITTROW. H. H. Schmitt[1], [1]University of Wisconsin-Madison, P.O. Box 90730, Albuquerque, NM 87199, schmitt@engr.wisc.edu.

Introduction: Mapping of variables in primary crater morphology relative to crater size can be used as an initial guide to factors that will affect mining and processing of that material for lunar resources such as helium-3, hydrogen, oxygen and water. Although time did not permit the systematic mapping of craters during the Apollo 17 exploration of the Valley of Taurus Littrow, the writer was able to provide descriptions of the variety of crater morphologies present (1).

About 3.5 b.y. ago (2), the Valley of Taurus-Littrow and its surroundings had been blanketed with a dark, pyroclastic mantle (3,4). Orange and black varieties of this mantle were specifically sampled at Station 4, Shorty Crater (5) as well as being a significant component of most samples of the regolith (4). All of the craters investigated, observed, and described are younger than the period of pyroclastic mantling. Every later impact, however, re-mobilized the fine pyroclastic material as well as the developing regolith, partially mantling all nearby younger materials.

Crater Age: The primary process that visibly ages impact craters on the Moon is the impact of small and micro-meteors over time (6) and the associated deposition of nanophase iron on all particle surfaces (7). Micro-meteor impacts generally keep the surfaces of boulders clear of this debris.

Small-scale impact processing of the upper few centimeters of the lunar surface gradually degrades and/or buries the primary features of larger impact craters and their ejecta. Crater age Category One (C1) are ubiquitous in Taurus-Littrow [<1 m.y.?]. They consist of the youngest and statistically the smallest craters and are characterized by bright halos and irregular but coherent pools of impact glass on their floors and regolith breccia fragments scattered on their walls, rims and ejecta blankets. Category Two (C2) craters include several observed on the traverse from Challenger to Station 2 and Van Serg Crater at Station 9 [1.5-3.7 m.y. (8,9)]. Relative to C1 craters, the bright halo has faded in C2 craters. Category Three (C3) craters, such as Ballet Crater [2-5 m.y. (8,10)], the coherent masses of impact glass have disappeared but fragments of regolith breccia have been retained. Category Four (C4) craters, including Shorty Crater at Station 4 [10-19 m.y. (4,11)], are marked by the full degradation of visible regolith breccia fragments. If a C4 crater is large enough to have penetrated to bedrock, it will have visible bedrock fragments on their floors and in their walls and ejecta blankets.

Additional age categories can be defined for craters large enough to expose bedrock in their floors and/or have bedrock as part of their ejecta blankets. Category Five (C5) craters have no visible bedrock on their floors even though bedrock fragments are exposed in the walls and in their ejecta blankets. Examples of C5 craters are Camelot Crater at Station 5 [70-95 m.y. (4)], Emory Crater at Station 1 [~100 m.y. (12)]. Category Six (C6) craters, such as Horatio Crater, have bedrock fragments exposed only in their walls.

Regolith Depth: Fresh craters that penetrate the regolith have fragments of the underlying bedrock on their rims as well as exposing that bedrock on their floors. They can be used to map variations in the depth of the regolith.

Regolith Layering: Craters with continuous interior benches in their walls give an indication of a significant discontinuity in the physical properties of the regolith with depth. Generally, as apparently is the case with Van Serg Crater, a bench indicates a sharp increase in compaction or strength with depth. An extreme version of a bench crater, given the field name of "pit bottomed crater," may indicate a sharp decrease in compaction or strength with depth. Pit bottomed craters were only observed on the light mantle and may indicate better compaction near the top of the light mantle than lower down as might be expected in a fluidized avalanche deposit (5).

Buried Boulder Concentrations: Craters of insufficient size to penetrate the regolith to bedrock, but which have boulders in their ejecta blankets are indicative of a concentration of buried boulders, presumably ejecta from a larger crater. Radar scans, including look-ahead radar from a mining-processing machine, might be employed to fully map a buried boulder field.

References: (1) Schmitt, H. H., (1972) in E. Jones, (2002) Apollo Lunar Surface Journal: http://www.hq. nasa.gov/office/pao/History/alsj/ frame.html; (2) Tera, F., and G. J. Wasserberg (1976) Lun. Sci. VII Absts., LSI, 858-860; (3) Lucchitta, B. K. (1973) Lun. Sci. Conf. 4, **1**, Geochim. Cosmochim. Acta, Supp. 6, 149-162; (4) Wolfe, E. W., et al. (1981) The Geologic Investigation of the Taurus-Littrow Valley: Apollo 17 Landing Site, Geol. Sur. Prof. Paper 1080, 96-98; (5) Schmitt, H. H. (1973) Science, **182**, 687-688; (6) Shoemaker, E.M. (1968) Surveyor Project Final Rept., Part II, JPL Tech. Rept. 32-1265, NASA SP-146, 21-136; (7) Taylor, L. A. et al. (2001) J. Geophys. Res. (Paper 2000JE0011402), 27,985-27,999; (8) Yokoyama, Y., et al. (1976) Lun. Sci. Conf. 7 Absts., LSI, 956-958; (9) Bhandari, N., et al. (1976) Lur. Sci. Conf. 7 Absts., LSI, 49-51; (10) Corzaz, G., et al, (1974) Lun. Sci. Conf. 5, Geochim. et Cosmochim. Acta, Supp. 5, 2475-2499; (11) Eugster, O., (1977) Lun. Sci. Conf. 3 Absts., LSI, 3059-3082; (12) Arvidson, R., (1976) Lun. Sci. Conf. 7, **3**, Geochim. Cosmochim. Acta, Supp. 7, 2817-2832

ATMOSPHERIC EFFECTS AND OBLIQUE IMPACTS: COMPARING LABORATORY EXPERIMENTS WITH PLANETARY OBSERVATIONS. Peter H. Schultz, Brown University, Department of Geological Sciences, P. O. Box 1846, Providence, RI 02912, peter_schultz@brown.edu

Introduction: Without direct observations of a major impact, one of the few ways to study the impact process is by assessing the effects of its environment (gravity, atmosphere) or conditions of impact (e.g., impact angle). The purpose of this contribution is to review selected consequences of both the atmosphere and impact angle as witnessed in laboratory experiments or revealed by large-scale craters preserved on different planets.

Atmospheric Effects: The lunar impact cratering record is an invaluable template for interpreting the pristine cratering record on other planets. In addition to its lower gravity, the absence of an atmosphere simplifies the cratering process. While it is often assumed that the tenuous atmosphere of Mars is overwhelmed by both the initial blast and the later advancing ejecta curtain, this assumption can be shown to be unwarranted. The atmosphere does play a significant role in modifying the late-stage ejecta emplacement but this role changes as a function of target, scale, and atmospheric pressure/density. The challenge is to identify meaningful tests to isolate this effect from other processes whether through statistical studies of the planetary cratering record or by case studies.

Laboratory impact experiments provide fundamental clues for assessing atmospheric effects since the process is complex and evolving. Such experiments are not just one-to-one comparisons between results in the laboratory and examples on the planets. Rather they should be designed to isolate variables in order to enable appropriate extrapolations. For example, performing an impact experiment at 100 bars to reproduce conditions on Venus or 6mbars to simulate conditions on Mars would only produce a crater of that particular size, in that specific target. Such laboratory observations combined with theory have yielded important predictions that can be tested by the planetary impact record. Applications to Mars and Venus illustrate this strategy which elevate the discussion beyond "look-alike" comparisons.

The distinctive ejecta facies surrounding craters on Mars have generated a range of interpretations. The fluidized appearance has commonly been used to interpret the presence of buried water (1, 2). Although popular ("follow the water" theme), this could be the planetary equivalent of a mirage. It is valid to assume explicitly that fluidized ejecta represents the presence of water and then explore the implications of this extrapolation; it is not valid, however, to simply state that fluidized ejecta deposits provide evidence for water. The problem is more ambiguous....and much more interesting.

Extensive laboratory impact experiments demonstrated that the response of the atmosphere to the crater formation is as important as the effect of the atmosphere on the ejecta. Early studies noted that the atmospheric drag acting on individual ejecta should be profound, even on Mars (3). For a given crater size (hence ejection velocity at the same stage of crater growth), atmospheric drag arrests the ballistic range over a relatively narrow size range of the ejecta (factor of 10) when scaled to the ambient atmospheric density. Conversely, for a given atmospheric density and ejecta size, the effect of drag increases with increasing crater size. If blindly applied, such considerations predict that ejecta would never get out of the crater for very fine-grained ejecta (25 microns in laboratory experiments and centimeter sizes for 10 km-diameter crater on Mars). But both experiments and the existence of excavated craters on Mars (not to mention Venus) demonstrate that craters do form. The paradox was resolved by recognizing that kinematic flow created by the outward moving ejecta curtain set up intense vortices that entrain sufficiently small decelerated ejecta (4, 5). Moreover, the presence of even a small fraction (10% by weight) of such a fine-grained component can change ballistically ejected material into a vortex with tornadic velocities. Then by isolating the controlling variables, later studies were able to compare models of the kinematic flow field with simplified experiments using controlled conditions in a wind tunnel (6, 7).

Such comparisons between models and observations both in the laboratory and on planetary surfaces led to specific predictions for ejecta deposits on Mars (4, 5, 8). First, onset for fluidized ejecta should depend on crater size due to the combination of increased ejection velocities and decreased ejecta sizes (comminution). Second, run-out distances scaled to crater radius should be proportional to crater size on Mars due to increasing ejecta entrainment (but decrease on Venus). Third, increased run-out distances with increasing latitude reflect an increased fraction of fine-grained sediments. Fourth, rampart-terminated ejecta facies represent coarser grained fractions that were mobilized but not fully entrained; hence, "rampart craters" should characterize the mare-like ridged plains rather than water-filled substrates. Fifth, radial facies indicate enhanced explosive expansion and hence the most (rather than the least) volatile-rich targets (or have been extensively modified). Sixth, anomalously long ejecta run-out distances can be created by autosuspension that feeds the vortex or flow with energy or gas (e.g., near-surface volatiles entrained by basal ejecta flow). Ninth, the development of late-stage ejecta-entrained vortices will not be significantly affected by the surrounding disturbed atmosphere (heated) since such blast effects rapidly equilibrate in the tenuous Martian atmosphere and do not drastically affect the results (8).

The above list of predictions and observations challenge some models of ejecta emplacement imposing only water. Nevertheless, the presence of volatiles can be recognized, whether in post-emplacement flow of water-lubricated near-rim ejecta or in enhanced run-out through autosuspension. Ironically, the critical importance of fine-grained lithologies may reflect enhanced weathering conditions (including fluvially transported sediments) during the Noachian and Hesperian and the role of climate-controlled processes (e.g., polar sinks for dust, obliquity changes, and polar wandering). Such considerations will not resolve the debate about Martian cratering. It simply challenges interpretations and assumptions to look further than the translating the term "fluid-

ized" into "water-entrained".

Oblique Impacts: Until relatively recently, full three-dimensional models of hypervelocity impacts have not been possible. As a result, important clues about the impact process have been gleaned from laboratory experiments compared with the planetary cratering record. Advances in computing power now has not only allowed more widespread use of 3-D codes (e.g., 9) but also enabled new diagnostics in the laboratory. These parallel advances will permit unprecedented opportunities to validate the codes and to test extrapolations to large scales, whether directly from laboratory experiments or comparisons with the codes. The oblique impact process represents one of the most challenging of these tests.

Oblique impacts map time into space. During vertical impacts, rapid changes in the transfer of energy and momentum from impactor to target are generally lost or overprinted by each successive stage of formation. Oblique impacts, however, expose this transfer along the initial trajectory. Laboratory experiments have long documented the overall change in crater dimensions and ejecta distributions (10), but new studies are providing other possible strategies for identifying the initial trajectory. First, direct measurements of far-field pressures reveal that oblique impacts cannot be simply modeled using point-source assumption (11). These measurements are clearly captured in asymmetries, timing, and nature of failure in three dimensions. Such laboratory measurements are also captured in recent computational models (9). Second, three dimensional particle image velocimetry (3D-PIV) is capturing the evolving flow field expressed by ejecta leaving the crater (12, 13). The enigmatic oblong crater shape perpendicular to the trajectory for modestly oblique impacts is now recognized in the ejecta flow field in addition to failure patterns in strength-controlled craters. Third, high-speed imaging and novel experimental designs are capturing the contact and failure pattern of the projectile.

Applying such laboratory experiments to planetary-scale phenomena and processes cannot be made without analytical or computational modeling. For example, the crater/projectile dimension ratio for cratering in sand for hypervelocity experiments is 50:1. But this ratio for large-scale (100 km) craters approach 15:1. Because oblique impacts reduce the peak pressure in the target, this ratio decreases still further to 8:1. Consequently, large-scale cratering more closely resembles strength-controlled laboratory impacts in terms of the relative dimensions of the crater and impactor. This also means that the transition from the region controlled by the transfer of momentum and energy becomes a significant fraction of the crater at large scales. Hence, observational evidence of the trajectory becomes more evident as well.

Observational evidence for impact trajectory (e.g., 15, 16) includes asymmetries in shock effects expressed by erasure/survival of pre-impact structural control, crater shape in plain view (whether oblong perpendicular to or along the trajectory), uprange offset of the central peak, breached central ring downrange, and downrange ricochet effects. Not all craters will exhibit such features. In addition to changes in expression with scale, impactor density and velocity also will play a role. For example, very high-velocity oblique impacts (>40km/s) will increase the crater/projectile ratio and partition more energy to melting and vaporization. Target topography (relative to the scale of the impactor) also can be shown to radically modify early-stage coupling processes. Consequently, statistical studies of crater morphologies may not reveal the key signatures. Such an approach is similar to including a failed experiment in laboratory impacts.

References: [1] Barlow, N., (1994) *JGR 99,* 10,927-10,935. [2] Head, J. W. III *et al.* (1999) Science 286, 2134-2137. [3] Schultz, P. H. (1979) *JGR 84,* 7669-7687. [4] Schultz, P. H. (1992) *JGR 97,* 11,623-11,662. [5] Barnouin-Jha, O. and Schultz, P. H. (1996) *JGR 101,* 21,099-21,115. [6] Barnouin-Jha, O. and Schultz, P. H. (1999) *JGR 104,* 27,105-27,116. [7] Barnouin-Jha, O. and Schultz, P. H. (1999) *JGR 104,* 27,117-27,132. [8] Barnouin-Jha, O. and Schultz, P. H. (1998) *JGR 104,* 27,105-27,116. [9] Pierazzo, E. and Melosh, H. J. (1999) *Earth Planet. Sci. Letts. 165,* 163-176. [10] Gault, D. E. and Wedekind, J. (1978) *Proc. Lunar Planet. Sci. 3rd,* 3843-3875. [11] Dahl, J. and Schultz, P. H. (2001) *Int. Jrnl. Impact Eng. 26,* 145-155. [12] Schultz, P. H., Heineck, J. T., and Anderson, J. L. B. (2000) *Lunar and Planet. Sci. XXXI,* Abst. #1902. [13] Anderson, J. A., Schultz, P. H., and Heineck, J. T. (2000) *Lunar and Planet. Sci. XXXI,* Abst. #1749. [14] Anderson, J. A.., Schultz, P. H. and Heineck, J. T. (2002, this volume). [15] Schultz, P. H. and Anderson, R. A. (1996) *Geol. Soc. Sp. Paper 302,* 397-417. [16] Sugita, S. and Schultz, P. H. (2002) *Icarus 155,* 265-284.

EXCAVATION FLOW AND CENTRAL PEAK RINGS: IS THERE A CONNECTION? V. L. Sharpton[1] and B. O. Dressler[2], [1]Geophysical Institute, University of Alaska Fairbanks, 903 Koyukuk Drive, Fairbanks, AK 99775 (buck.sharpton@gi.alaska.edu); 2 Lunar and Planetary Institute, 3600 Bay Area Blvd, Houston, TX 77058.

Introduction: To approximate the conditions associated with the excavation stage of the impact process, many numerical simulations rely on some form of the Z-model [1-5], where the radial velocity of particles below the ground surface is given by:

$$u_R = \alpha(t)/R^Z$$

and R is the radial distance from the flow origin, α is a strength parameter, and Z determines the velocity change with radial distance. While inherited from studies of explosion cratering [1-3], the Z-model has been shown to provide a first order approximation of excavation flow in simple craters as long as some appropriate effective depth of Z-model flow (EDOZ) is provided. EDOZ is usually assumed to be equivalent to one projectile diameter [e.g., 1,2,4]. The most-often applied form of this model is the steady-flow version where α, Z (~3) and EDOZ are assumed to be time constants [e.g. 1,2,5,6]. This practice, however, seems to be based on convenience rather than on sound theoretical grounds as (1) the steady flow assumption allows the flow field to be explicitly evaluated at all times [2] but (2) violates conservation of energy [1]. Furthermore, studies of laboratory-scale impacts [4,5] indicate a time-dependence to the Z-model parameters. Despite these limitations, the Z-model's ability to provide qualitative insights into the dominant spatial features of the early-time impact flow field has been emphasized [1-3]. While this may be true for laboratory scale craters and even simple craters on planetary surfaces, observations from a well-studied terrestrial complex crater indicate that neither excavation flow nor the shape of the excavation cavity are well approximated by the Z-model.

Haughton Crater. The ~24 km diameter Haughton impact crater is located at 75° 22´ N; 89° 41´ W on the western portion of Devon Island in the Canadian Arctic [7,8]. The geological map shown in Fig. 1 is derived from previous studies [9,10] with modifications resulting from our 1997 field expedition. These observations, combined with the results of reflection seismic studies [11] provide useful constraints on the target and how it was affected by the impact event. Here, we use these data to evaluate models of the size and shape of the excavation cavity generated during the formation of Haughton crater and show that these characteristics cannot be reconciled with the constant-flow Z-model. Our analysis suggests that the poorly organized peak ring at this crater reflects radial inflections in the original excavation crater prior to its uplift during late-stage modification.

The target is a nearly flat-lying sequence of Paleo-

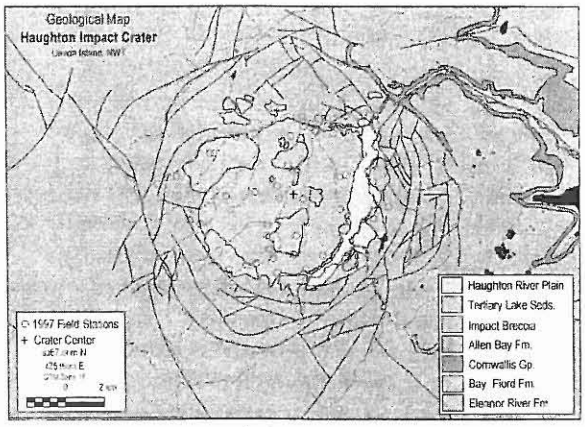

Figure 1

zoic platform rocks, ~1.8 km thick, overlying high-grade crystalline basement. The platform sequence consists of the following units [9]: **1**. The Allen Bay Fm. (OSA) limestone and dolomites, ~450 m thick. This unit forms the present surface around the crater and is found to within ~4.5 km of the center. **2**. The Cornwallis Group (OCTI) shales and carbonates with a combined thickness of ~110 m. OCTI crops out along the walls of steep valleys to the northeast of the crater. **3**. The Bay Fiord Fm. (OCB) carbonates and gypsum, ~330 m thick. Large exposures of OCB occur within 5-7 km of the crater center, as well as in valley floors as close as 8 km east of the crater center. **4**. The Eleanor River Fm. (OE) chert-bearing carbonates, ~400 m thick. Inliers of OE, representing the central uplift, occur between 0.7 and 4.8 km from crater center. The closest authochthonous OE outcrops occur ~16.5 km from the crater center. **5**. Undifferentiated Lower Ordovician-Cambrian (OCU) shale, sandstone, dolomite, and conglomerates, ~420 m thick. No parautochthonous units of OCU have been discovered within the

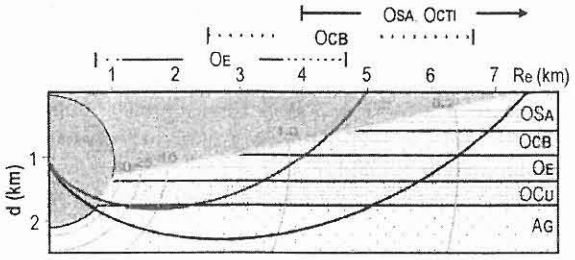

Figure 2. OCTI (not shown) is located between OSA and OCB. Shock pressures after [12].

crater; however, near the center abundant highly shocked blocks of sandstone probably represent the OCu Blanley Bay Fm. Authochthonous exposures have been mapped 32 km east of crater center.

Excavation Depth and Central Uplift. Filling the shallow central basin (radius of ~5 km), the allogenic impact breccia forms a nearly continuous unit that ranges from ~10 m to over 100 m in thickness. Breccia outliers also exist beyond this deposit, with the farthest mapped deposit located ~7.8 km southeast of center. The matrix and clasts of this breccia were derived primarily from the platform rocks; however, clasts of partially melted, highly shocked, and weakly shocked clasts of Archaean high-grade metamorphic rocks (AG, Fig. 2) prove that the excavation cavity penetrated into the subjacent crystalline basement. Modal analysis [9] indicates ~10-15% of the breccia clasts are derived from the crystalline basement. Extending ~1 km from the crater center are large and extensively shatter-coned outcrops of OE (with minor OCB; Figs. 1 and 2) that form a discontinuous ring of uplifted but otherwise coherent target rocks. As their structural heights exceed the basal height of the Tertiary lake beds that filled the crater shortly after it formed, these OE exposures represent a true topographic, albeit incipient, peak ring.

Reconstructing the Excavation Crater. The excavated diameter De=2Re has been estimated at 10 km based on the incoherent zone in reflection seismic data [11]. Redeker and Stöffler [10] prefer De=15 km, based on shock isobar constraints from the Kieffer and Simonds [12] model and the need to excavate crystalline rocks. Fig. 2 shows the half-space shape of the Z=2.71 model for both the 10-km *(red line)* and 15-km *(blue line)* excavation craters predicted for Haughton crater.

Discussion. When assessed against the geological constraints provided by outcrops of parautochthonous target rocks, substantial problems with these models become evident: **1**. The Re=5 model predicts excavation completely through OE to a distance of ~3.3 km; Re=7.5 removes OE to a distance of nearly 6 km. Both therefore fail to account for the central uplift (OE derived from beneath the excavation crater) that is observed within 1.2 km of the center. **2**. Similarly, the models predict that OCB would be completely removed within 4 km (Re=5) or 6.8 km (Re=7.5) yet outcrops occur within 3 km of center and are abundant within a radius of 5 km. **3**. The Re=5 model does not account for the proportion of crystalline rock clasts observed in the allogenic breccia [10].

Conclusions. The geological constraints at Haughton crater are not compatible with a constant Z excavation flow field regardless of the choice of Re. Observations presented here constrain the zone of deep excavation to be less than 1 km from center. The *yellow line*, Fig. 2 indicates the maximum depth to the excavation crater boundary permitted by geological constraints. The resulting shape is characterized by a localized near-center zone of deep excavation – from which the crystalline rocks originate – flanked by a broad zone of shallow excavation at least 4-5 times the width of the central zone. Off-axis, deep excavation, and thus a Z-model-type of excavation flow are not incompatible with the Haughton crater observations *if and only if* Z is a strong function of time. High-Z flow (deep, near-center excavation, steep ejection angles) would occur during the earliest excavation stage and as ejection proceeded, Z, excavation depth, and ejection angle would decay.

At Haughton, the uplifted outcrops form the cusp separating two distinct sub-domains in the excavation crater: the broad outer zone of shallow excavation and the narrow, centrally located zone of deep excavation. Consequently this peak ring seems to represent a fundamental structural inflection in the base of the excavation crater that was subsequently uplifted during late-stage modification.

It is not clear whether the excavation-crater model for peak ring formation can be extended to all central peak rings, or even to those in other craters formed in layered targets. Similar excavation geometries, however, have been reported at several other complex craters with central rings [e.g. 13,14] in layered targets where such reconstructions are possible.

References: [1] Maxwell, D. E. (1977) *Impact and Explosion Cratering*, 1003-1008. [2] Croft, S. K. (1985) *Proc. Lunar Planet. Sci. Conf.* 11th, 2347-2378. [3] Orphal et al., (1977) *Impact and Explosion Cratering*, 907-917. [4] Austin et al. (1981) *Multi-ring Basins*, 197-205. [5] Austin *et al.* (1980) *Proc. Lunar Planet. Sci. Conf. 11th*, 2325-2345. [6] Collins, G. S. (2002) *Icarus 157*, 24-33. [7] Asphaug, E. and Melosh, H. J. (1993) *Icarus 101*, 144-164. [7] Frisch, T. and Thorsteinsson, R. (1978) *Artic Institute Journal* **31**, 108-124. [8] Robertson, P. B. and Mason, G. D. (1975) *Nature 255*, 393-394. [9] Thorsteinsson, R. and Mayr, U. (1987) *Geol. Survey Can. Mem. 411*, 182 pp. [10] Redeker H.-J. and Stöffler, D. (1988) *Meteoritics 23*, 185-196. [11] Bischoff, L. and Oskierski, W. (1988) *Meteoritics 23*, 209-220. [12] Kieffer, S. W. and Simonds, C. H. (1980) *Reviews of Geophysics and Space Physics* 18, 143-181. [13] Brennan, R. L. *et al.* (1975) *WY Geol Assoc. Earth Sci. Bull. 8*, 41 pp. [14] Milton, D. J. *et al.* (1972) *Science 175*, 1199-1207.

MECHANISMS OF IN SITU ROCK DISPLACEMENT DURING HYPERVELOCITY IMPACT: FIELD AND MICROSCOPIC OBSERVATIONS J.G. Spray, Planetary and Space Science Centre, University of New Brunswick, Fredericton, NB E3B 5A3, Canada. jgs@unb.ca

Introduction: The nature of rock deformation due to hypervelocity impact is discussed, especially with regard to the larger terrestrial structures (e.g., Sudbury, Vredefort, Manicouagan). Based on field observations and thin section microscopy, evidence is presented for two end-members of rock response to extreme strain rates: (1) bulk deformation, due to pervasive fracture generation and ensuing micro-displacement with melting; (2) localized large-displacement faulting, accompanied by friction melt generation (pseudotachylytes). There is no evidence for bulk "fluidization" at the thin section scale, except where bulk melting has occurred during impact melt sheet generation, wherein truly fluid (igneous) rocks are formed.

S- and E-type fracture-fault systems: Bulk deformation in footwall rocks beneath the Sudbury Igneous Complex (melt sheet) is limited to a zone some 10-15 km beyond the contact with overlying melt. Fracture-microfault systems are typically a few mm thick and are akin to shock veins in meteorites. These have been referred to as S-type pseudotachylytes [1]. They may contain high-pressure polymorphs. Melting is probably due to a combination of shock and microslip. In this proximal footwall zone at Sudbury, there are 10-20 pervasive S-type veins per cubic meter, with the frequency decreasing progressively away from the melt sheet.

Localized, large-displacement faulting can be related to concentric and radial structures that appear to be formed during the modification stage of the cratering process. These post-date the shock wave and are primarily driven by gravitational forces and possible rebound effects. Movement on the concentric systems commonly occurs after movement on the radials. Movement on the concentric faults is typically significantly greater than that realized on the radial fracture-fault systems. Large displacement, single slip faults have been referred to as superfaults when displacement is >100 m in one event [2]. Under superfaulting conditions, thick (1-1000 m) friction melt (pseudotachylyte) bodies may result. These may be responsible for the rings seen in multiring impact basins on the moon and other planets. The thickest pseudotachylytes are formed when these faults undergo displacements of several kilometers in one slip event. Superfaults generate terraces in the larger impact structures. This class of pseudotachylyte has been referred to as E-type [1]. E-type pseudotachylytes are formed in the same way as endogenic fault-related pseudotachylytes, though displacements due to impact can be many orders of magnitude greater than those realized during regular faulting (the latter typically resulting in cm-wide pseudotachylyte veins).

Central uplifts: While S- and E-type pseudotachylytes have been documented with regard to melt sheet footwall occurrences, there are very few references made to them with regard to the internal structure of central uplifts. Central uplift mechanics remains poorly understood. How is it possible for vast volumes of rock to move, supposedly downwards (during compression) many kilometres, and then back up many kilometres (on decompression), and probably within seconds or minutes? In fact, there is little hard evidence that transient cavities are pushed downwards during compression and excavation (i.e., in a gross plastic/elastic manner). In so, cannot rebound be attributed merely to pressure release at a free surface? The internal structure of central uplifts has not been studied in any real systematic detail in the field. Work on smaller impact structures, such as Decaturville [3] reveals a crude concentric piston-like form, with the deepest level rocks being exposed in the centre of the uplift and successively higher level rocks being exposed around this core. The uplift is thus not chaotic, although each concentric zone appears to comprise blocks of coherent rock in a fragmental matrix (breccia) that has been well mixed. Preliminary work thus indicates that some uplifts are similar to telescopic hydraulic rams in their cylinder-within-cylinder structure. Whether the contacts between "cylinders" are sharp (i.e., fault bounded) or gradual (fluid like), is not yet clear.

References: [1] Spray, J.G. (1998) *Spec. Pub. Geol. Soc. London* 140, 195-204. [2] Spray, J.G. (1997). *Geology* 25, 579-582. [3] Nickerson, G.A.J. (2002) Unpublished MSc thesis, University of New Brunswick, Canada, 127 p.

TOWARD A COMPLETE MEASUREMENT OF THE THERMODYNAMIC STATE OF AN IMPACT-INDUCED VAPOR CLOUD. Seiji Sugita[1], Keiko Hamano[1], Toshihiko Kadono[2], Peter H. Schultz[3], and Takafumi Matsui[1], [1]University of Tokyo (7-3-1 Hongo, Bunkyo-ku, Tokyo, JAPAN, sugita@eps.s.u-tokyo.ac.jp), [2]IFREE, JAMSTEC (2-15 Natushima-cho, Yokosuka, Kanagawa, JAPAN), [3]Brown University (Providence, RI 02912, USA).

Introduction: Vaporization phenomena induced by hypervelocity impacts play an important role in the origin and evolution of Earth and other planets. There have been extensive research efforts made for understanding this process. However, the equation of state (EOS) and chemical reaction within high-pressure and high-temperature conditions of impact vapor are yet highly uncertain [e.g., 1, 2]. This is primarily owing to the lack of experimental data on impact vapor cloud. Here we discuss newly developed spectroscopic methods to determine the thermodynamic state of impact-induced vapor very accurately.

Thermodynamic State of Impact Vapor: Among the four fundamental thermodynamic quantities (temperature T, pressure p, entropy s, and density ρ), two of them are necessary to designate the thermodynamic state of an equilibrium system. If the system has a multiple components and is ionized, both chemical composition x and ionization ratio ϕ are also needed to describe the system. The spectroscopic methods we have developed can obtain sufficient thermodynamic quantities to designate uniquely the thermodynamic state of a system.

Spectroscopic Method: The emission spectra of rapidly evolving impact vapor clouds have to be taken with high resolution in both time and wavelength. This had been extremely difficult until an intensified charge-coupled device (ICCD) arrays were introduced. They are capable of taking a thousand of different wavelengths of light at once with an extremely short exposure time (up to ~10 ns). This permits obtaining high-quality emission spectra of impact vapor clouds.

Temperature T. When a high-resolution spectrum is obtained, the intensities of emission lines are measured to generate a Boltzmann diagram (Fig.1), which shows the logarithm of emission intensities I normalized by transition probability A, statistical weight g, and photonic energy $h\nu$ as a function of the upper energy level E of the transition divided by Boltzmann constant. The inverse of the slope in a Boltzmann diagram gives the temperature T of the measured vapor [e.g., 3,4,5].

Chemical Composition x. Once a Boltzmann diagram is made, one can also obtain the chemical composition. The vertical intercept of a fit line gives the logarithm of the number of ground state atoms, which is approximately the total number of atoms in vapor clouds generated in a laboratory [3,4,5]. Then the difference in the intercepts of two different atoms (Cu and Ca in Fig.1) in a Boltzmann diagram gives the ratio of the two atoms: atomic composition x.

Ionization ratio ϕ. Some atoms exhibit very strong ion emission lines. When these ion lines are treated as a different atom and a Boltzmann diagram is made, the number ratio of ionized to neutral atoms is obtained. This gives the ionization ratio ϕ [3,4].

Density ρ. The density of high-temperature plasma can be estimated by spectral line profile of emission lines. Some atoms such as hydrogen exhibit a large line width due to Lorentz broadening, which is proportional to 2/3rd power of electron density [3]. Laboratory experiments show that such Lorentz broadening can be observed with high enough accuracy to obtain a reliable value of electron density. The electron density can be converted to the bulk vapor density ρ using ionization ratio ϕ and chemical composition x [6].

Application to Planetary-Scale Impacts: The above methods have a wide variety of application in hypervelocity impact study. An immediate application is to determine the EOS of highly compressed impact vapor, which may be highly different from an ideal gas. When the thermodynamic state of an impact vapor cloud is determined, the chemical reaction processes within the vapor cloud can be estimated much more easily. Such knowledge will help understand the problem of sulfur oxides in the K/T impact vapor cloud [7]. Furthermore, a quantitative comparison between impact- and laser-induced vapor clouds can be done with these methods. It will widen the range of the application of laser-simulated "impact vapor clouds" greatly [2,8]

References: [1] Stevenson, D.J. (1987) *Ann. Rev. Earth Planet. Sci., 15*, 271. [2] Muhkin et al. (1989) *Nature, 340*, 46 [3] Griem, H.R. (1964) *Plasma Spectroscopy.* [4] Sugita S. et al. (1998) *JGR, 103*, 19,427. [5] Sugita S. et al., *JGR, 104*, 30,825. [6] Hamano et al. (2002) *Proc. 35th Lunar Planet. Symp.* 174. [7] Ohno, S. et al. (2002) *EPSL*, submitted. [8] Kadono et al. (2002) *GRL*, in press.

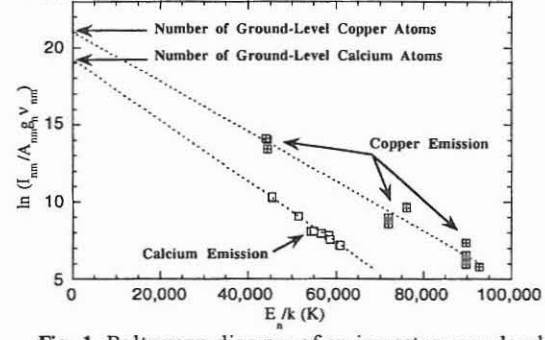

Fig. 1. Boltzmann diagram of an impact vapor cloud. The vapor cloud is induced by copper projectile impacting dolomite target. The copper and calcium emissions represent the projectile and target components, respectively.

COOLING OF THE KÄRDLA IMPACT CRATER: I. THE MINERAL PARASEQUENCE OBSERVATIONS. E. Versh[1], A. Jõeleht[2], K. Kirsimäe[3] and J. Plado[4], [1,2,3,4]Institute of Geology, University of Tartu, Vanemuise 46, Tartu 51014, Estonia ([1]desty@ut.ee, [2]ajoeleht@ut.ee, [3]arps@ut.ee, [4]jplado@ut.ee).

Introduction: Kinetic energy released to the target by a meteorite impact results in the heating-to-melting and vaporization of the projectile and target rocks, which then start to cool to the ambient conditions. In dry environments (e.g. Moon) the heat loss occurs mainly by conduction and radiation transfer. If the water is present at the crater site as on Earth and supposedly on Mars, then the cooling can include also convective heat transfer by hydrothermal circulation systems. Evidences of impact-induced hydrothermal activity have been found at many terrestrial craters [1], and it is suggested for extraterrestrial craters as well [2]. Cooling and development of such impact-induced hydrothermal systems can be recognized by the means of (1) mineralogical/fluid inclusion studies, and (2) by impact and geothermal modeling.

In this and following paper (see Jõeleht et al., in this volume) we report a complex geological observation and modeling study of post-impact cooling of a medium-to-small scale impact crater of Kärdla, Hiiumaa Island, Estonia. The Kärdla crater is 4 km in diameter and ~540 m deep with a central uplift exceeding 100 m height above crater floor. It formed in a shallow (<100 m deep) epicontinental Ordovician sea ~455 Ma ago into a target composed of thin siliciclastic and carbonate sedimentary sequence covering crystalline basement [3]. In this first part of our contribution we present the results of mineralogical, fluid inclusion and stable isotope studies.

Mineral parasequence: The crater-fill sequence at Kärdla crater hosts up to 400 m thick allochthonous and autochthonous breccias that have undergone water-rock interaction. A complex clay-feldspar-carbonate(Fe-oxyhydrate) assemblage characterizes the post-impact hydrothermal mineralization. The most intensive alteration is found in breccias and shattered basement around and above the central uplift. The results of homogenization temperature measurements of quartz fluid inclusions in allochthonous breccia encompass a wide range from 110 to 440°C, with the maximum between 150 and 300°C [4] (Fig). This temperature range is in agreement with the chloritic minerals formation temperatures of 150-325°C. However, the mineral paragenesis suggests that the main phase of chloritization was preceded by earlier cryptocrystalline K-feldspar formation, whereas the second generation of euhedral K-feldspar inside fractures and voids precipitated after the chlorite, probably at temperatures of 200-100°C. Dolomite-calcite and sulfides/Fe-oxyhydrates (hematite and goethite) reflect the final stages of cooling when temperature reached ambient conditions. Calculated fluid equilibrium temperatures for carbonates indicate that those fluid temperatures were below 100°C (in the range of 75-35°C).

Initial temperatures: Studies of hydrothermal mineral assemblages and fluid inclusions provide information about the post-impact temperatures and enables the mapping of thermal aureole. However, studies of mineral parageneses lack in information on the life times of these hydrothermal systems and the cooling time is not assessed by this approach. Heat and fluid transfer simulations can resolve that question. However, this needs the initial post-impact temperature distribution to be known. Mineral geothermometry results suggest maximum initial temperatures at least 150-300°C in the central part of the Kärdla crater. The same is suggested by PDF studies in shocked quartz, which refer to the maximum shock pressures during the impact event in a range of 20-35 GPa [5]. The distribution of the most frequent fluid inclusion homogenization temperatures suggests also approximately the same range (Fig). However, the high temperature inclusions on homogenization temperature graph suggest trapping temperatures as high as 350-450°C.

Comparison with the preliminary results of the hydrocode modeling of impact (Jõeleht et al., in this volume) shows that the initial temperatures remaining in the rocks estimated by geothermometry are significantly higher than the model predictions using Tillotson equation of state, but are in general agreement when ANEOS is used. The details of modeling problems are discussed in part II by Jõeleht et al. (see this volume).

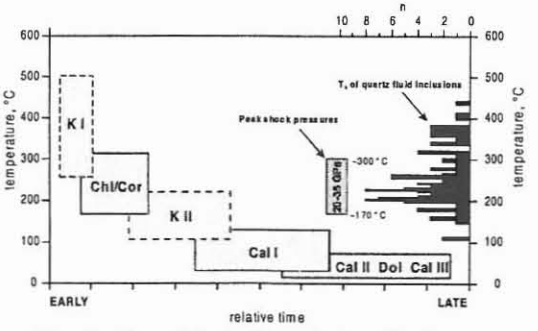

Fig. Post-impact hydrothermal mineralization parasequence at Kärdla crater. Shock pressures (20-35 GPa) from [5] and histogram of aqueous (H2O-NaCl) quartz fluid-inclusion homogenization temperatures (T_h) from [4] are shown at the RH side. K - K-feldspar, Chl/Cor - chlorite/corrensite, Cal - calcite, Dol - dolomite; I, II, III - 1st, 2nd and 3rd generation. Formation temperatures for chlorite-corrensite and carbonate minerals are estimated form geothermometry and stable isotope composition, respectively. Positions of K-feldspar I and II fields are tentatively assumed from paragenetic relationships with chloritic and carbonate minerals.

References: [1] Naumov M.V. (2002) *Impacts in Precambrian Shields*, pp. 117-171. [2] Newsom H.E. (1980) *Icarus*, 44, 207-216. [3] Puura V. and Suuroja K. (1992) *Tectonophysics*, 216, pp. 143-156. [4] Kirsimäe K. et al. (2002) *Meteoritics & Planet. Sci.*, 37, 449-457. [5] Puura et al. (submitted) *Meteoritics & Planet. Sci.*